Interrogating the Structural Landscape of Malaria Biomarkers with Epitope Targeted Peptide Capture Agents

Thesis by

JingXin Liang

In Partial Fulfillment of the Requirements for the

degree of

Doctor of Philosophy

CALIFORNIA INSTITUTE OF TECHNOLOGY

Pasadena, California

2018

(Defended March 22, 2018)

JingXin Liang

ORCID: 0000-0001-6600-8409

Acknowledgements

There's a famous proverb that says, "It takes a village to raise a child." In my opinion, it takes no less than that – in actuality, even more – to teach, nurture, and grow a scientist. The journey towards becoming a scientist is an arduous one, filled with twists and turns, experimentation, learning on the fly, and displaying tenacity in the face of adversity. Completing a doctoral program is as much an intellectual feat as it is an exercise of persistence. As my doctoral advisor would say, "You can't do science in a vacuum," and he is absolutely right. There are people, both within and outside of the scientific community, who have helped me, shaped me, and contributed along my journey.

Voilà! Here is my village.

First and foremost, I thank my parents, H.X. Liang and C.W. Leung, as well as my brother, J.Y. Leung. We are a family of first-generation immigrants to America. My parents are the most selfless and brave people I know – it is through their sacrifices that their children had better lives, educations, and opportunities. I cannot even begin to fathom the amount of strength, persistence, and courage it took for them to create new lives on foreign shores, to build something from nearly nothing. From humble beginnings, they created possibilities for their children and our family. When I struggle, I think of the bravery they displayed to overcome even greater obstacles, and it gives me the perspective to push on and persevere. I would not be here without my family. My deepest gratitude and love goes out to them.

I thank my advisor, Professor James R. Heath, for his mentorship, insight, and optimism for the past five years. I have always admired his unique scientific view of the world, his intellect, and his ability to think of creative solutions to problems that span

multiple disciplines. When I am at a scientific crossroads, I tend to think, "What would Jim do?" I appreciate his dedication to science, his willingness to help when I had a scientific problem, his insight and constructive criticism that helped me grow the independence to captain my own ship. I am privileged to have had the opportunity to learn from him and grow under his mentorship.

I also express gratitude for the team of scientists who are my committee members: my chair, Professor Douglas C. Rees; my secondary advisor, Professor William A. Goddard, III; and Professor Shu-ou Shan. They provided time, questions, and valuable insight during meetings and exams. I thank Professor Mitchio Okumura and Agnes Tong (Caltech Y) for the meaningful contributions they made during my first year at Caltech. I must acknowledge and thank Professor Spiridoula Matsika, who was most formative in my nascent years of scientific research at Temple University.

Thank you to all the members of Heath lab team whom have inhabited the basement of Noyes with me. I want to acknowledge my team of colleagues who provided knowledge, leadership, good times, and help when I needed it. Here we go: Samir Das, Arundhati Nag, Jessica Pfeilsticker, Jun Wang, Blake Farrow, Sung A Hong, Jongchan Choi, JC Hyun, Byung Jun Kim, Mary Beth Yu, Aiko Umeda, David Bunck, Yapeng Su, Sharareh Gholamin, Alice Hsu, William Chour, Amy McCarthy, Heather Agnew, and Bert Lai. In later years, the basement of Noyes has been graced with new, wonderful colleagues and inhabitants: Alphonsus Ng, Min Xue, Anvita Mishra, John Heath, Fan Liu, Yue Lu, Matthew Idso, Songming Peng, Dazy Johnson, Alex Xu, and William Denman. I also thank Katrine Museth, Elyse Garlock, and Rena Beccara-Rasti, for all they do to make our lives easier, as well as Kevin Kan, who lets me have first dibs on all the snacks.

I thank my partner, Mark Nesbit, for his love, companionship, patience, and support. Thank you for enriching my life, for being the kind of partner with whom I can be comfortable around all the time, and a steady ship. We all have to sail through rough seas from time to time – the journey is infinitely more pleasant with you on board. I love you and I'm so proud of you. Through Mark, I've also had the blessing of growing my family: Dorothy and Skip, who have always treated me like their own; Katherine, my marine biologist sister; Veronica, my warrior sister. I love you all.

I am grateful for friendships that have enriched my life and demonstrated that wealth is not always accumulated through capitol: Regina Baglia, *mi hermana de otra madre* and first mate, for a decade of friendship, sleepovers, and study dates – words cannot encompass the last ten years, but eating our fill of cheese samples from Di Bruno Bros is a good start to the story. I'm so excited to meet Èlia! Roberta Poceviciute, for wonderful company, showing me the European way of life, honesty, and always opening her home to me. Tahmineh Khazaei and Betty Wong, for encouragement, kindness, and supporting artistic endeavors. Anastasia Pagán, a warm, generous soul who brings light and shows me new horizons. Kaycie Deyle, for five years of support and meaningful conversations, even from Switzerland. Ellen Casavant, who taught me how to grow friendships over great distances. Nicole LaBerge and Marcus Drover, who are two of my favorite Canadian expats and wonderful friends. Elizabeth O' Brien, for all we've experience together in the journey of graduate school. In no particular order, all the people who've been part of good times: Paul Walton, Jenna Bush, Matt Mayers, Leanne Chen, Siobhán MacArdle, and Nikolas Malafek. From my Temple University days, I thank Mark Fennimore, Christopher

Kozak, Professor Zhen Lu, Professor Kurt A. Kistler, and Catherine Triandafillou, who all played significant parts leading up to today.

And now, onwards!

"A smooth sea never made a skilled sailor."

- *Franklin D. Roosevelt*

Good timber does not grow with ease:

The stronger wind, the stronger trees;

The further sky, the greater length;

The more the storm, the more the strength.

By sun and cold, by rain and snow,

In trees and men good timbers grow.

- *Douglas Malloch, "Good Timber"*

Abstract

Antibodies have conventionally been used as molecular recognition agents against epitopes, or antigenic regions, for protein capture and detection. The ability of monoclonal and polyclonal antibodies to selectively bind their targets with high affinities makes them excellent agents for specific protein recognition. However, as large proteins themselves (~150 kDa), antibodies are susceptible to changes in pH, temperature, and biochemical environment, particularly proteolytic cleavage. Additionally, epitope binding on antibodies is reliant on their rigid tertiary structure to position key functional groups that facilitation antigen recognition. Retaining the integrity of the protein structure creates rigid limitations against chemical modifications of antibodies to suit unique needs.

Protein-catalyzed capture agents (PCCs) developed within the Heath group at Caltech address the limitation of antibodies as affinity agents. Using epitope-targeted *in situ* click screening methodology, the Heath group has developed peptidomimetic molecules that offer an alternative solution to antibodies. These PCCs exhibit high affinity and selectivity for their protein targets. As peptide-based molecules, PCCs can be engineered to be biochemically stable and resistant to changes in their chemical environment. Their peptide-based structures are readily amenable to chemical modifications and allow for adaptation to a range of applications.

This thesis describes the development of PCCs against unique protein biomarkers for the detection of the most lethal species of malaria infection, *Plasmodium falciparum*. Malaria is a global health epidemic and its eradication is reliant on rapid and accurate diagnostics for prompt treatment. We targeted the *P. falciparum* specific biomarkers lactate dehydrogenase (LDH) and Histidine-rich protein 2 (HRP2), both of which present

unique challenges for protein capture. The LDH biomarker is homologous across malaria species, whereas HRP2 is highly polymorphic and lacks distinct secondary structure. The variation in sensitivity of HRP2 detection by antibody-based tests has been attributed to the genetic polymorphism of the biomarker.

In Chapter 1, we describe the development of high affinity PCCs that bind selectively to the LDH biomarker. We targeted an epitope that was highly homologous across LDH species. This chapter also details the expansion of mono-valent PCC agents into bivalent ligands using the protein architecture to select secondary ligands for binding improvement. For the HRP2 biomarker, we developed a multiple epitope targeting strategy to address protein polymorphism. We targeted for epitopes in HRP2 and developed PCCs that bind in the range of monoclonal antibodies.

Chapter 2 details the expansion of PCC agents developed against HRP2 into multivalent molecules for improved binding. The development of bivalent ligands from combinatorial screening of linker libraries is presented. The optimal linker lengths determined by the screens are described.

In Chapter 3, a general strategy for targeting the protein landscape to inhibit formation of a protein and biomolecule complex with PCCs against HRP2 is demonstrated. Specifically, the inhibition of heme sequestration by HRP2 is shown. A bivalent ligand that targets two epitopes on HRP2 is shown to have enhanced inhibitory potency over any single or cocktail combination of PCCs.

Altogether, the studies herein demonstrate the utility of peptidomimetic molecules as agents for protein capture and detection as well as a generalizable strategy of functional inhibition through epitope-targeting.

Published Content and Contributions

1. *S. Das, *A. Nag, **J.X. Liang**, D.N. Bunck, A. Umeda, B. Farrow, M.B. Coppock, D.A. Sarkes, A.S. Finch, H.D. Agnew, S. Pitram, B. Lai, M.B. Yu, A.K. Museth, K.M. Deyle, B. Lepe, F.P. Rodriguez-Rivera, A. McCarthy, B. Alvarez-Villalonga, A. Chen, J. Heath, D.N. Stratis-Cullum, J.R. Heath *Angewandte Chemie International Edition*, **2015**, *54(45)*, 13219-13224. DOI: 10.1002/anie.201505243

- J.X. Liang conceived of the strategy, executed, and tested capture agents developed against *Pf*HRP2. J.X. Liang also participated in the screening, synthesis, and validation of capture agents and epitopes for affinity agents against *Pf*LDH.

2. J. R. Heath, H. Agnew, B. Farrow, D. Bunck, **J.X. Liang**, A. Nag, S. Das, B.T. Lai, S.M. Pitram "Il-17f-specific capture agents, compositions, and methods of using and making" US15211759, Patent Pending, Published February 23, 2017.

- J.X. Liang innovated a bivalent capture agent against *Pf*HRP2 that demonstrated inhibition of protein function.

3. **J.X. Liang**, D.N. Bunck, A. Mishra, M. Idso, J.R. Heath, "Inhibition of heme sequestration of Histidine-Rich Protein 2 using multiple epitope-targeted peptides" *Submitted 2018*

- J.X. Liang conceived of, designed, and executed all heme-binding experiments.

Table of Contents

List of Figures and Tables

Chapter 1

Chapter 2

Chapter 3

Chapter 4

Chapter 5

Abbrevations

Aib (aminoisobutyric acid)

AP (alkaline phosphatase)

Az4 (Fmoc-Lys(N_3)-OH, azide click handle)

BCIP/NBT (5-bromo-4-chloro-3'-indolyphosphate, nitro-blue tetrazolium)

BSA (bovine serum albumin)

CuACC (Copper(I)-catalyzed azide-alkyne cycloaddition)

cy (denotes triazole cyclization, prefix*)

DCM (dichloromethane)

DIEA (N,N-Diisoproprylethylamine)

DMSO (dimethylsulfoxide)

EC_{50} (half-maximal effective concentration)

ELISA (enzyme linked immunoassay)

FPLC (fast protein liquid chromatography)

GST (glutathione S-transferase)

HATU (2-(7-Aza-1H-benzotriazole-1-yl)-1,1,3,3-tetramethylammonium hexafluorophosphate)

HPLC (high-performance liquid chromatography)

HRP (horseradish peroxidase)

K_D (dissociation constant)

MALDI-TOF (matrix assisted laser desorption ionization-time-of-flight)

NMP (N-methylpyrrolidone)

OBOC (one-bead-one-compound)

PCC (protein-catalyzed capture agent)

PEG (polyethylene glycol)

Pra (Fmoc-L-propargylglycine-OH, alkyne click handle)

***Pf*HRP2** (*Plasmodium falciparum* histidine-rich protein 2)

Pf*LDH (Plasmodium falciparum* lactate dehydrogenase)

***Pv*LDH** (*Plasmodium vivax* lactate dehydrogenase)

RCM (ring-closing metathesis)

RDT (rapid diagnostic test)

SynEp (synthetic epitope)

TBS (tris buffered saline)

TES (triethylsilane)

TFA (trifluoroacetic acid)

Chapter 1

An Introduction to Protein-Catalyzed Capture Agents

1.1 Peptidomimetics as Antibody Alternatives in RDTs

Conventional methods of protein capture and detection rely on the use of antibodies as agents of molecular recognition.[1] Monoclonal and polyclonal antibodies are large proteins on the scale of ~150 kDa which exhibit high affinity and selectivity for their targets. One application of antibodies for molecular recognition is the antibody-based rapid diagnostic test (RDT), which is essentially a sandwich immunoassay employed as a fast screening platform for myriad health conditions. A typical antibody-based RDT is a lateral flow device, or dipstick, that is used to measure biomarkers in samples such as urine and blood (Figure 1-1A).[2] A capture antibody is immobilized on the surface, which is typically nitrocellulose, that pulls down the target protein out of the biological sample by recognizing a particular region on the antigen. A second antibody binds to an orthogonal region of the antigen and is typically tethered to a colored particle that provides a colorimetric readout to indicate a positive or negative confirmation. RDTs require no trained personal and can provide a diagnostic answer in the time frame of minutes. They are easy to use, require no trained personal or external resources such facilities, and can be easily transported and distributed.[3] As such, antibody-based RDTs have utility for disease detection where diagnoses of large populations are required, such as global infections like malaria.[2,4,5]

However, while RDTs provide a means for rapid disease detection, there are drawbacks to these antibody-based platforms. Antibodies are expensive to produce, exhibit batch-to-batch variability, and like all proteins, require storage and use in controlled pH, temperature, and chemical environments. They are susceptible to biochemical processes such as proteolytic cleavage and their sensitivity to abrupt changes in their environments limitss their widespread use outside of laboratory settings. The ideal affinity agent would be one that is cost-effective, easy to synthesize, and stable against biochemical fluctuations.

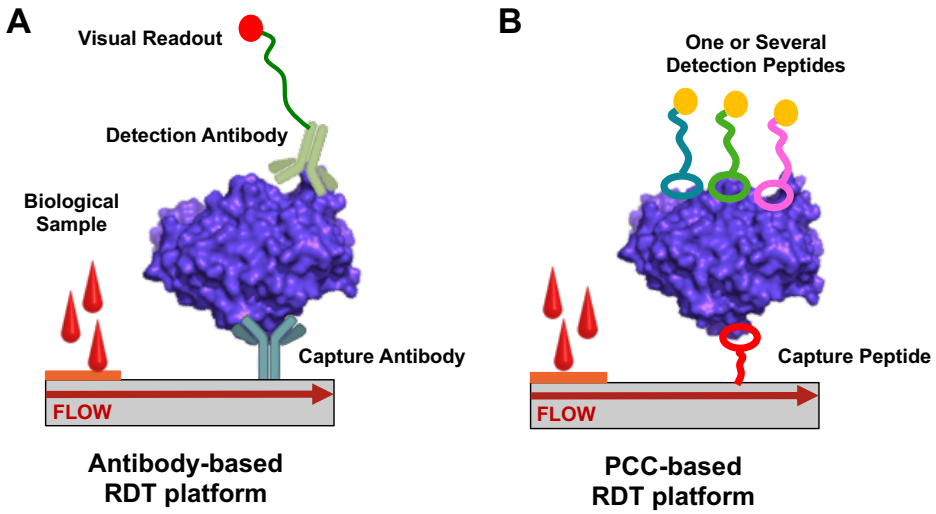

Figure 1-1. A typical rapid diagnostic test (RDT) is a lateral flow assay. (A) An antibody-based RDT relies on proteins to capture and detect the antigen. (B) An alternative RDT where the antibodies are replaced by PCCs.

Protein-catalyzed capture agents (PCCs), developed in collaboration between Heath and Sharpless labs, offers an alternative to antibodies as agents of molecular recognition.[36–9,9,10] These synthetic PCCs are developed from high throughput screening of peptide-based one-bead-one-compound (OBOC) libraries. The goal of PCC development for diagnostics is to create pairs of molecular recognition agents that can replace antibodies in a lateral flow assay (Figure 1-1B). Using high throughput screening

methodology allows for the rapid discovery of new ligands with precision targeting and engineering of affinities. Like antibodies, PCCs developed within the Heath group are built from amino acid chains (peptides), but these peptidomimetic molecules have multiple advantages over their protein counterparts (Figure 1-2).

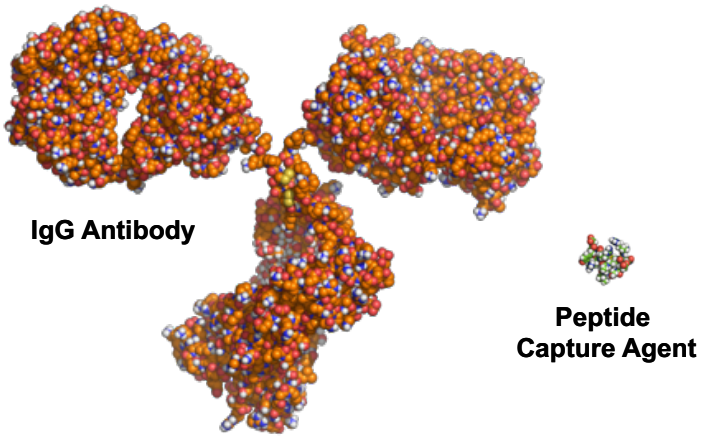

Structure	~160 kDa Rigid Scaffold Required	~2 kDa Modular, Adaptable
Stability	Temperature, pH, Buffer, Protease Sensitive	Thermostable Protease Resistant
Selectivity	High to variable	High
Affinity	High to variable	High pM to Low nM

Figure 1-2. A comparison of antibodies to peptide-based affinity agents (PCCs) for protein capture and detection. (PDB: 1IGT)

First, PCCs have high affinity and selectivity for their protein targets, similar to antibodies, but are developed synthetically. Peptides are cost-effective to produce relative to antibodies and display excellent thermostability against high temperatures.[11] Second, the synthesis of small peptidomimetic molecules from amino acid building blocks allows for increased chemical flexibility in design that cannot be accomplished with antibodies. For example, unnatural D-amino acid buildings blocks can be used to generate PCCs that

are resistant to proteases.[9] Cyclization of the peptide backbone increases stability against degradation and allows for chemical flexibility of affinity agent architectures. In addition, the synthesis of PCCs on solid support allows for modular and adaptable synthesis of the peptidomimetic scaffold. The synthetic flexibility of PCCs allows for the generation of molecules ranging from ~1 to ~5kDa. The synthesis of PCCs on large scale can be accomplished via automated techniques, which makes their production cost effective, and the simplicity of their structures relative to antibodies significantly reduces batch-to-batch variability.

1.2 PCCs as Antibody-Alternatives in Malaria Diagnostics

This thesis describes the development of PCCs as alternatives to antibodies in lateral flow assays for malaria diagnostics. Malaria, a mosquito-borne infectious disease caused by the protozoan *Plasmodium*, persists in subtropical and tropical regions of the world. Despite widespread measures to treat and prevent the disease, malaria persists as a global health epidemic. The disease infects over 200 million people annually and claims over 600,000 lives.[12] The most lethal species of the disease is caused by *Plasmodium falciparum*, which contributes to the majority of malarial deaths. The gold standard of disease detection is through blood smear microscopy, but its widespread use is hindered by the need for dedicated facilities and personnel. In malaria endemic regions, RDTs are the most cost-effective and efficient means to rapidly diagnose infection in large populations.

Currently, malaria RDTs exist that detect the antigens *P. falciparum* lactate dehydrogenase (*Pf*LDH) and histidine-rich protein II (*Pf*HRP2) for the diagnosis of lethal malarial infection.[5,13] The utility of RDTs are limited by their variability in sensitivity of

detection in instances where parasitemia, or parasite load, is low (<200 parasites/μL). This variation in sensitivity is especially a concern for tests that detect *Pf*HRP2, which is highly polymorphic.[4,14] The inaccuracy of diagnoses can lead to false negatives, which contributes to untreated infections and potential death. Thus, an ideal RDT must reliably detect antigens that are unique to *P. falciparum* and have the sensitivity to capture biomarkers at low concentrations.

There are several factors that make the diagnosis of malaria infection through traditional antibody-based RDTs problematic. First, antibodies are sensitive to heat and humidity, which are less than ideal for the climates in which malaria persists. Second, *Pf*HRP2 antigen detection tests have been shown to exhibit variable performance, which has been attributed to the genetic variations of the protein across regions of the world.[4,14–16] In total, over 400 isolates of *Pf*HRP2 exist globally.[4] These isolates have variations in repeat sequences of the proteins or deleted sections,[94,14] making antigen detection problematic if monoclonal antibodies in RDTs are targeted against such regions. Another issue is the existence of *P. falciparum* isolates lacking the pfhrp2 or pfhrp3 genes which encode for *Pf*HRP2 and its homolog, *Pf*HRP3.[17] The complete absence of *Pf*HRP2 antigen would result in false positives, which underscores the importance of RDTs that reliably detect *Pf*LDH protein. However, *Pf*LDH antigen tests also exhibit issues of their own which include low specificity.[13] The variability in detection of malaria infection results in under- and over-diagnosis of the disease. Poorly implemented treatment programs that result from misdiagnosis can contribute to antimalarial drug resistance, which also increases malaria-related fatalities.[18,19] In order to treat and eradicate malaria, the development of rapid and accurate RDTs is imperative for individual patient case

management, disease surveillance, and properly implemented drug treatment programs. In this thesis, we leverage and expand upon existent technology in the Heath group to innovate PCCs that address the shortcomings on antibodies with applications towards future RDTs for malaria.

1.3 Engineering PCCs with High Affinity and Target Selectivity

Within the Heath group, PCCs have been developed through combinatorial screening of combinatorial OBOC peptide libraries of varying architectures (Figure 1-3). Earlier screening methodology utilized randomized 5-mer linear peptide libraries.[7,9,10,20] These libraries were synthesized on bead via split-and-mix synthesis using amino acids of L- or D-stereochemistry and yielded affinity agents that bound in micromolar to nanomolar affinities (Figure 1-3A).[7,9,20] Later PCC methodology utilized libraries that were cyclized through clicking between azide and alkyne or ring closing metathesis, the latter of which afforded a larger, more flexible ring structure (Figure 1-3B). Cyclization of the 5-mer libraries restricts the numbers of conformations accessible to PCCS. Since linear PCCs sample more conformations than cyclic PCCs, they exhibit lower binding affinities. Conformational restriction through cyclization drastically limits the conformation accessible through bond rotation, which can be thought of as prepaying the entropic cost of PCC:target binding. In later work within the Heath group, cyclic PCCs have demonstrated affinities in the picomolar regime.[7,21] The OBOC libraries are comprehensive in 18 of naturally occurring amino acid side chains with cysteine and methionine eliminated for chemical stability which yields 18^5, or roughly 2 million, diverse elements.[7] After synthesis of the 5-mer region, the libraries are cyclized and appended

with an azide or alkyne click handle, also denoted as Az4 or Pra, respectively. Linear libraries require no cyclization and are immediately appended with a handle. The libraries are validated for confirmation of cyclization and successful synthesis by sequencing on an Edman instrument.

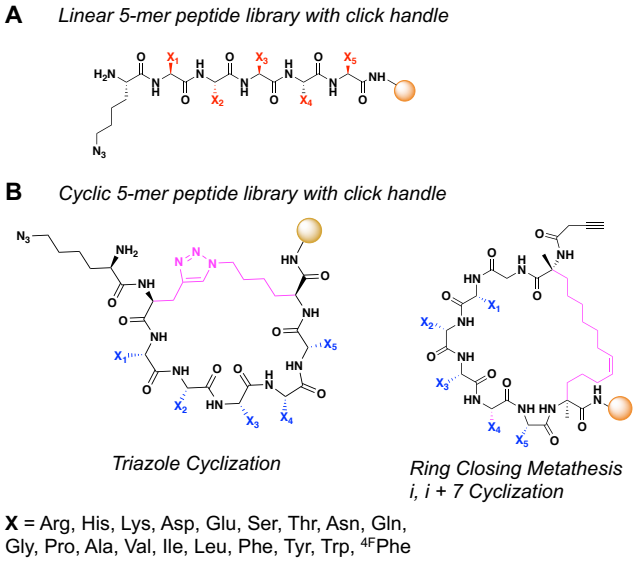

Figure 1-3. Architectures of OBOC libraries used for high throughput screening. The libraries are comprehensive in 18 amino acids, can be constructed with L- or D-stereocenters, and bear alkyne/Pra or azide/Az4 click handles.

Standard development of PCCs within the Heath group first begins with epitope targeting.[7,8,11,20,21] Epitopes are antigenic determinants, also known as amino acid sequences which are recognized by antibodies. After identification of the antigen, one or several epitopes are selected after inspection of the primary protein sequence. Ideally, this epitope is a minimum of ~10 amino acids in length, and is unique to the target, thus engineering selectivity into the final PCC. It is also beneficial to select an epitope that is accessible to an affinity agent, i.e., not buried within the protein core, and that has some secondary structure that might be maintained in a synthetic peptide. However, defined

secondary structure is not a necessarily a prerequisite for generating high-binding hits in screens. Following selection, the synthetic epitope (SynEp) is constructed via standard solid phase peptide synthesis, fitted with an azide or alkyne click handle that is complementary to the one on the OBOC library, and appended with a biotin tag for detection. (Figure 1-4).

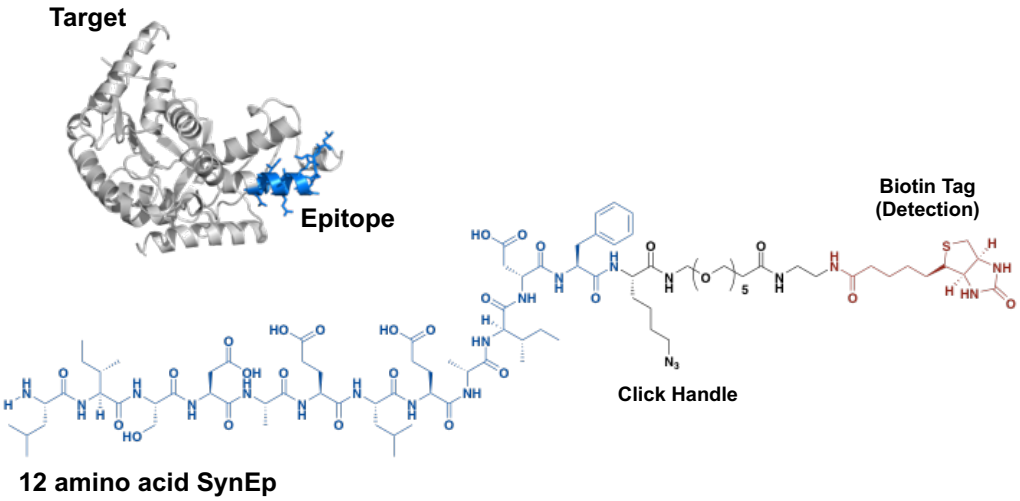

Figure 1-4. A targeted peptide sequence (epitope) is selected from a protein and synthesized (SynEp). The SynEp is affixed with an azide/Az4 (shown) or alkyne/Pra click handle and appended with a biotin tag for detection by an antibody. (PDB: 1LDG)

A general protocol of pre-clearing followed by screening of the OBOC library is followed (Figure 1-5) which includes non-specific binding to detection antibodies, such as anti-biotin or streptavidin, and human serum to yield a focused library. For increased selectivity in the final PCC, the library can be pre-screened against SynEps from off-target proteins to weed out binding to homologous biomolecules or even adjacent sites on the target. This focused library is then incubated with the SynEp from the target of interest.[7] Library elements that bind strongly to the SynEp position the complementary alkyne and azide click handles together to form a covalent triazole product.

The classic Copper(I)-catalyzed azide-alkyne cycloaddition (CuACC) reaction forms a covalent heterocyclic triazole product.[22] The Copper(I) catalyst increases the rate of reaction between azide and alkyne with complete conversion. In the absence of the Copper(I) catalyst in our screens, the triazole click product is low-yielding. Covalent linkage is entirely dependent on the molecular recognition between the SynEp and the library elements to hold the azide and alkyne fragments in close enough proximity to facilitate triazole formation.[6] Thus, it is largely the strength, or affinity, of binding between the SynEp and library elements that promote the click product in the absence of Copper(I). The affinity-driven catalysis of the click reaction allows for the development of PCC agents with nanomolar affinities in a single-generation screen.[7]

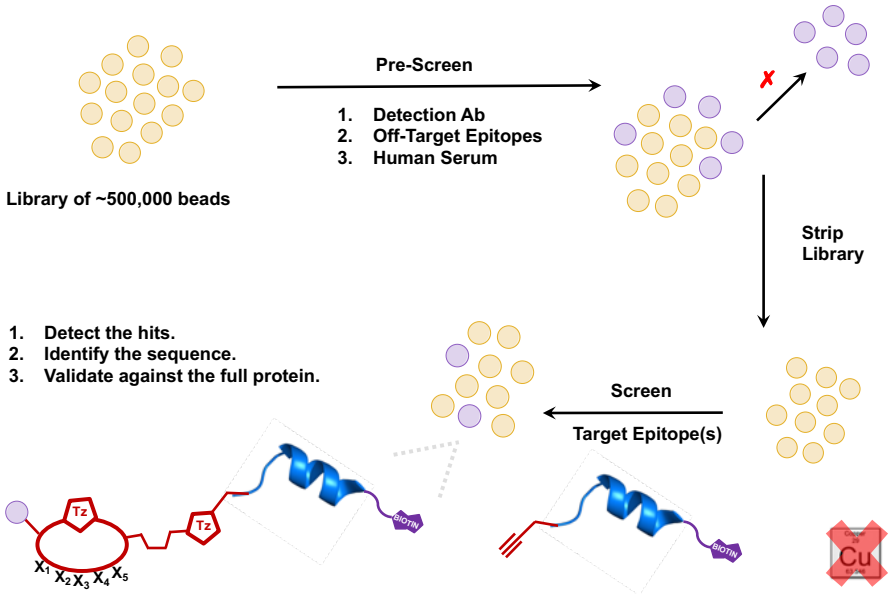

Figure 1-5. Schematic of a high throughout screen using epitope targeting, *in situ* click chemistry, and OBOC library methodologies. False-positives such as binders to detection antibodies, off-target epitopes, and human serum are removed from the OBOC library in a pre-clear. The pre-cleared library is incubated with the SynEp that bears a click handle complementary to the one on bead. Strong library binders promote formation of the covalent click product.

1.4 Chapter Summaries

This thesis presents the application of the aforementioned PCC technology for the development of peptidomimetics in malaria RDTs that detect lethal *P. falciparum* infection. In Chapter 2, the development of monovalent and bivalent ligands against the *Pf*LDH and Pan-*Plasmodium* LDH antigens is described. The use of cyclic OBOC libraries over linear libraries demonstrates the superiority of conformational restriction in generating peptide binders with nanomolar affinities. The expansion of PCCs into bivalent ligands through secondary ligand screens with the target antigen is also described within this chapter. In the instance of a linear peptide, we find that expansion into a bivalent structure can increase affinity.

Chapter 3 describes the development of cocktail combination of PCCs to bind the *Pf*HRP2 antigen. Unlike *Pf*LDH, *Pf*HRP2 is a highly patterned and polymorphic protein that lacks defined secondary structure. The primary amino acid sequence of this antigen differs across *P. falciparum* isolates and has been suggested to contribute to the variations in sensitivity observed in RDTs that detect *Pf*HRP2.[4,14–16] To address *Pf*HRP2 polymorphism, we devised a strategy where we target four unique epitopes within the protein. By developing a cocktail of affinity agents that target conserved and variant regions of *Pf*HRP2, we can account for variations or deletions in repeats through simultaneously binding multiple regions in a single protein for built in sensitivity amplification. In total, four regions of the *Pf*HRP2 antigen are targeted.

Chapter 4 describes the expansion of *Pf*HRP2 monovalent ligands into bivalent ligands through OBOC linker screens. A small library of peptide-based linkers was constructed for screening between different PCCs of the *Pf*HRP2 cocktail described in

Chapter 3. Even without defined secondary structure in the target antigen, we found that the linker screens selected for a defined ligation length though the hits generated were nonspecific. Knowledge obtained from this work was applied towards development of a bivalent ligand that demonstrated inhibitory properties against *Pf*HRP2 function as described in Chapter 5.

In addition to its diagnostic utility, *Pf*HRP2 has long been implicated as a target for the sequestration of cytotoxic free heme in the malaria parasite. In Chapter 5, the PCCs developed in Chapter 3 are demonstrated to inhibit the sequestration of *Pf*HRP2 binding to heme through targeting heme-binding epitope motifs. Through ligation of two PCCs that target internal regions of *Pf*HRP2, we find that inhibition of heme sequestration is significant and improved over using monovalent peptides.

Altogether, this thesis describes the interrogation of the structural landscape of two malarial proteins with unique diagnostic and scientific challenges. Firstly, PCCs were developed against *Pf*LDH, a highly homologous biomarker with a defined protein architecture for the generation of mono- and bivalent affinity agents. Secondly, PCCs were developed that could simultaneously target multiple regions in a single and unstructured biomarker with the added ability to inhibit protein function. Through the use of epitope targeting and *in situ* chemistry, PCCs were developed that bind to their *P. falciparum* targets with high affinity and selectivity. In addition, we demonstrate that the PCCs have utility outside of diagnostics and can inhibit protein and biomolecule interactions, showing potential as therapeutics through disruption of protein function through precision targeting.

References

(1) Borrebaeck, C. A. . Antibodies in Diagnostics – from Immunoassays to Protein Chips. *Immunol. Today* **2000**, *21* (8), 379–382.

(2) Koczula, K. M.; Gallotta, A. Lateral Flow Assays. *Essays Biochem.* **2016**, *60* (1), 111–120.

(3) Mouatcho, J. C.; Goldring, J. P. D. Malaria Rapid Diagnostic Tests: Challenges and Prospects. *J. Med. Microbiol.* **2013**, *62* (10), 1491–1505.

(4) Baker, J.; Ho, M.-F.; Pelecanos, A.; Gatton, M.; Chen, N.; Abdullah, S.; Albertini, A.; Ariey, F.; Barnwell, J.; Bell, D.; et al. Global Sequence Variation in the Histidine-Rich Proteins 2 and 3 of Plasmodium Falciparum: Implications for the Performance of Malaria Rapid Diagnostic Tests. *Malar. J.* **2010**, *9* (1), 129.

(5) Birku, Y.; Welday, D.; Ayele, D.; Shepherd, A. Rapid Diagnosis of Severe Malaria Based on the Detection of PfHRP-2 Antigen. *Ethiop Med J* **1999**, *37*.

(6) Agnew, H. D.; Rohde, R. D.; Millward, S. W.; Nag, A.; Yeo, W.-S.; Hein, J. E.; Pitram, S. M.; Tariq, A. A.; Burns, V. M.; Krom, R. J.; et al. Iterative In Situ Click Chemistry Creates Antibody-like Protein-Capture Agents. *Angew. Chem. Int. Ed Engl.* **2009**, *48* (27), 4944–4948.

(7) Das, S.; Nag, A.; Liang, J.; Bunck, D. N.; Umeda, A.; Farrow, B.; Coppock, M. B.; Sarkes, D. A.; Finch, A. S.; Agnew, H. D.; et al. A General Synthetic Approach for Designing Epitope Targeted Macrocyclic Peptide Ligands. *Angew. Chem. Int. Ed Engl.* **2015**, *54* (45), 13219–13224.

(8) Lai, B. T.; Wilson, J. A.; Malette Loredo, J.; Pitram, S. M.; LaBerge, N. A.; Heath, J. R.; Agnew, H. Epitope Targeted Macrocyclic Peptide Ligand with Picomolar Cooperative Binding to Interleukin-17F. *Chem. – Eur. J.* n/a-n/a.

(9) Deyle, K. M.; Farrow, B.; Qiao Hee, Y.; Work, J.; Wong, M.; Lai, B.; Umeda, A.; Millward, S. W.; Nag, A.; Das, S.; et al. A Protein-Targeting Strategy Used to Develop a Selective Inhibitor of the E17K Point Mutation in the PH Domain of Akt1. **2015**, *7*, 455.

(10) Millward, S. W.; Henning, R. K.; Kwong, G. A.; Pitram, S.; Agnew, H. D.; Deyle, K. M.; Nag, A.; Hein, J.; Lee, S. S.; Lim, J.; et al. Iterative in Situ Click Chemistry Assembles a Branched Capture Agent and Allosteric Inhibitor for Akt1. *J. Am. Chem. Soc.* **2011**, *133* (45), 18280–18288.

(11) Pfeilsticker, J. A.; Umeda, A.; Farrow, B.; Hsueh, C. L.; Deyle, K. M.; Kim, J. T.; Lai, B. T.; Heath, J. R. A Cocktail of Thermally Stable, Chemically Synthesized Capture Agents for the Efficient Detection of Anti-Gp41 Antibodies from Human Sera. *PLOS ONE* **2013**, *8* (10), e76224.

(12) WHO. World Malaria Report 2016. World Health Organization December 2016.

(13) Houzé, S.; Boly, M. D.; Le Bras, J.; Deloron, P.; Faucher, J.-F. PfHRP2 and PfLDH Antigen Detection for Monitoring the Efficacy of Artemisinin-Based Combination Therapy (ACT) in the Treatment of Uncomplicated Falciparum Malaria. *Malar. J.* **2009**, *8*, 211–211.

(14) Baker, J.; McCarthy, J.; Gatton, M.; Kyle, D. E.; Belizario, V.; Luchavez, J.; Bell, D.; Cheng, Q. Genetic Diversity of Plasmodium Falciparum Histidine Rich Protein

2 (PfHRP2) and Its Effect on the Performance of PfHRP2-Based Rapid Diagnostic Tests. *J Infect Dis* **2005**, *192*.

(15) Lee, N.; Baker, J.; Andrews, K. T.; Gatton, M. L.; Bell, D.; Cheng, Q.; McCarthy, J. Effect of Sequence Variation in Plasmodium Falciparum Histidine Rich Protein 2 on Binding of Specific Monoclonal Antibodies: Implications for Rapid Diagnostic Tests for Malaria. *J Clin Microbiol* **2006**, *44*.

(16) Kumar, N.; Singh, J. P.; Pande, V.; Mishra, N.; Srivastava, B.; Kapoor, R.; Valecha, N.; Anvikar, A. R. Genetic Variation in Histidine Rich Proteins among Indian Plasmodium Falciparum Population: Possible Cause of Variable Sensitivity of Malaria Rapid Diagnostic Tests. *Malar. J.* **2012**, *11*, 298–298.

(17) Menegon, M.; L'Episcopia, M.; Nurahmed, A. M.; Talha, A. A.; Nour, B. Y. M.; Severini, C. Identification of Plasmodium Falciparum Isolates Lacking Histidine-Rich Protein 2 and 3 in Eritrea. *Infect. Genet. Evol.* **2017**, *55*, 131–134.

(18) Le Bras, J.; Durand, R. The Mechanisms of Resistance to Antimalarial Drugs in Plasmodium Falciparum. *Fundam. Clin. Pharmacol.* **2003**, *17* (2), 147–153.

(19) White, N. J. Antimalarial Drug Resistance. *J. Clin. Invest.* **2004**, *113* (8), 1084–1092.

(20) Nag, A.; Das, S.; Yu, M. B.; Deyle, K. M.; Millward, S. W.; Heath, J. R. A Chemical Epitope-Targeting Strategy for Protein Capture Agents: The Serine 474 Epitope of the Kinase Akt2. *Angew. Chem. Int. Ed.* **2013**, *52* (52), 13975–13979.

(21) Farrow, B.; Wong, M.; Malette, J.; Lai, B.; Deyle, K. M.; Das, S.; Nag, A.; Agnew, H. D.; Heath, J. R. Epitope Targeting of Tertiary Protein Structure Enables Target-

Guided Synthesis of a Potent In-Cell Inhibitor of Botulinum Neurotoxin. *Angew. Chem. Int. Ed.* **2015**, *54* (24), 7114–7119.

(22) Kolb, H. C.; Sharpless, K. B. The Growing Impact of Click Chemistry on Drug Discovery. *Drug Discov. Today* **2003**, *8* (24), 1128–1137.

Chapter 2

Rapid Discovery of Capture and Detection Agents for *Plasmodium falciparum* Lactate Dehydrogenase

Reproduced in part with permission from:

*S. Das, *A. Nag, **J.X. Liang**, D.N. Bunck, A. Umeda, B. Farrow, M.B. Coppock, D.A. Sarkes, A.S. Finch, H.D. Agnew, S. Pitram, B. Lai, M.B. Yu, A.K. Museth, K.M. Deyle, B. Lepe, F.P. Rodriguez-Rivera, A. McCarthy, B. Alvarez-Villalonga, A. Chen, J. Heath, D.N. Stratis-Cullum, J.R. Heath

Angewandte Chemie International Edition, **2015**, *54(45)*, 13219-13224.

DOI: 10.1002/anie.201505243

2.1 Introduction

The mosquito-borne disease malaria is caused by the protozoan parasite, *Plasmodium*, and infects over 200 million human hosts annually in tropical and subtropical regions of the world.[1] The *P. falciparum* species is the most lethal and contributes to nearly all malaria related deaths. Eradication of this global epidemic requires the rapid and accurate diagnosis of the large human populations affected. Lateral flow immunochromatographic assays, also known as rapid diagnostic tests (RDTs), provide a means of rapidly diagnosing large populations with results in minutes, which allows for prompt treatment.[2–6] As described in Chapter 1 (Figure 1-1), RDTs are antibody-based

sandwich assays where a protein bioarker is captured by one antibody and detected by a second antibody, and the colorimetric readouts provide a positive or negative result.[7] Though the gold standard of malarial disease detection is microscopy,[4,5] RDTs are advantageous because they do not require dedicated facilities or personnel for examination of patient samples. Relative to other techniques, RDTs are relatively low-cost and provide results within 5 to 15 minutes.

There are commercially available RDTs for the *P. falciparum* histidine-rich protein 2 (*Pf*HRP2) and lactate dehydrogenase (*Pf*LDH) biomarkers, the latter of which is the focus of this chapter.[2,3,6] *Pf*LDH is key enzyme utilized by the parasite for glycolysis and energy production and interconverts lactate and pyruvate while simultaneously converting NADH/NAD+.[8] The LDH enzymes exists in other malarial species such as *P. vivax*, with which it is nearly 75% genetically identical with 90% residue similarity.[9,10] Since *P. falciparum* infection is so severe, it is imperative that malarial LDHs can be differentially detected in a single test. In addition to diagnostics, the selective detection of *Pf*LDH antigen by RDT is useful for assessing parasite burden. Unlike another *P. falciparum*-specific antigen, histidine-rich protein 2 (*Pf*HRP2), which is detected in malaria RDTS and persists even after treatment, the *P*LDH antigen clears from the blood within 24 hours after infection clearance, which holds prognostic utility.[11–14] The rapid clearance of the antigen is imperative for patient case management, determining the success of drug treatments such as artemisinin combination therapy, and for identifying recurrent malaria infections.[11,15]

Currently, *P*LDH RDTs are available that can detect *P. falciparum*-specific or pan-*Plasmodiu*m LDH antigens that allow for the diagnosis of specific or mixed infections

(schematic provided in Figure 2-1).[5] However, whilst malaria RDTs provide a means of rapidly diagnosing patients infected with *P. falciparum* for the administration of drug treatments, they have limitations. At high parasitemia, or high parasite densities, greater than 90% of sensitivities are achieved for *P. falciparum* specific RDTs. However, at low parasitemia where parasite density varies from 100 – 500 parasites/μL, sensitivities of these antibody-based RDTs can drop below 80%.[15] Antibody-based RDTS, particularly for *Pf*LDH detection, have been shown to be sensitive to temperature fluctuations and generate false negatives under heat.[2] The degradation in performance at higher temperatures is especially problematic for diagnostics in the tropical and subtropical climates in which malaria is prevalent.[2] *P*LDH-based RDTs are also less sensitive than their *Pf*HRP assay counterparts and cannot always detect clinical infection.[12]

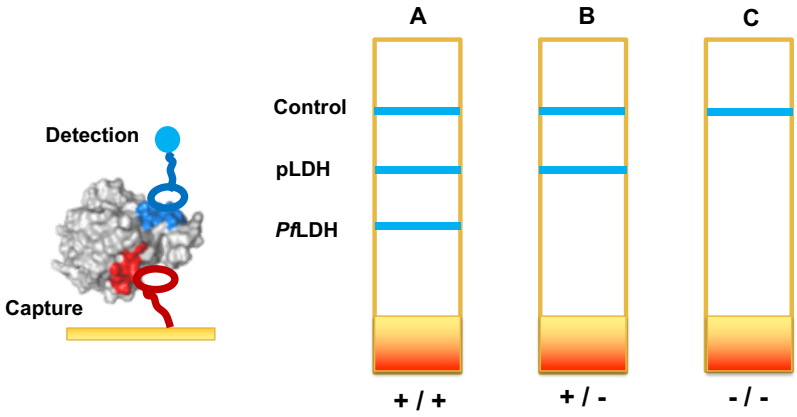

Figure 2-1. Schematic of an RDT for *P. falciparum*-specific and pan-*Plasmodium* infection. Representative results for (A) *P. falciparum* and possible mixed infection, (B) non-*P. falciparum*-specific infection, and (C) a negative result for malarial infection are shown. Figure adapted from the literature.[5]

This chapter focuses on the development of reagents that address the limitations of targeting *Pf*LDH antigen in antibody-based RDTs.[2,5,14] An ideal RDT (schematic provided

in Figure 2-1) for malaria should be able to distinguish between species infection, generate true positive/negative results, withstand temperature fluctuations for use in endemic regions of the world, be cost-effective, and be sensitive in low to high parasitemia. For prompt treatment of lethal malaria, it is especially important to distinguish *P. falciparum* from other *Plasmodiu*m species from an RDT.

In this chapter, we describe the development of peptidomimetic protein-catalyzed capture agents (PCCs) as synthetic, easily synthesizable, and cost-effective antibody alternatives for *Pf*LDH RDTs. We use epitope-targeted *in situ* click chemistry screening methodology,[16–18,18–20] which allows for the rapid discovery of peptide-based ligands from high throughput screening of one-bead-one-compound (OBOC) to develop affinity agents against *Pf*LDH. We use an epitope targeting strategy to engineer PCCs with specificity for *Pf*LDH over *Pv*LDH and other off-target proteins. A comparison of PCCs developed from linear and cyclic OBOC libraries is provided that demonstrates the superior utility of entropy restricted structures for affinity agents. We also explore using the structured landscape of *Pf*LDH antigen to screen for secondary ligands to develop bivalent PCCs.

2.2 Materials and Methods

Materials. Epitope and peptide syntheses were accomplished using standard Fmoc amino acids with acid-labile side chain protecting groups, which were purchased from Anaspec, Chempep, Chem-Impex International, and Aapptec. Specialty amino acids such as Fmoc-NH-Peg_n-$CH_2CH_2CO_2H$, (S)-N-Fmoc-2-(4'-pentenyl)alanine, and (R)-N-Fmoc-2-(7'-octenyl)alanine were purchased from Chempep and Sigma Aldrich, respectively. Grubbs CatalystTM 1st Generation and anhydrous 1,2-Dichloroethane was purchased from Sigma

Aldrich. All peptide syntheses were completed on solid support with standard methodology using Biotin NovaTag™ resin (Millipore Sigma) for biotinylated peptides or Rink Amide MBHA resin (Aapptec). The reagents N-Methyl-2-pyrrolidone (NMP, BDH Chemicals), N,N-Diisoproprylethylamine (DIEA, Sigma Aldrich), 2-(7-Aza-1H-benzotriazole-1-yl)-1,1,3,3-tetramethylammonium hexafluorophosphate (HATU, Chempep), and piperidine (Alfa Aesar) were used in synthesis. Trifluoroacetic acid (TFA, Chem-Impex International) and 2.5% triethylsilane (TES, Sigma Aldrich) were used for removal of peptides from solid support. TentaGel S-NH_2 resin (Rapp Polymere) was used for OBOC library synthesis. Copper (I) iodine (CuI) and L-Ascorbic Acid were purchased from Sigma Aldrich. Sodium diethyldithiocarbamate was purchased from Chem-Impex International. Dimethyl sulfoxide (DMSO) was purchased from EMD Millipore.

Recombinant *Pf*LDH and *Pf*HRP2 antigens were purchased from CTK Biotech. Human LDH was obtained form Abnova. Anti-biotin alkaline phosphatase antibody was purchased from Sigma-Aldrich. Anti-GST antibody conjugated to HRP was purchased from Abcam. For screening, 5-bromo-4-chloro-3'-indolylphosphate p-toludine salt/nitro-blue tetrazolium chloride (BCIP/NBT Color Development Substrate) was purchased from Promega.

General Preparation of OBOC Libraries. Linear OBOC libraries were synthesized on 90 μm TentaGel resin using standard split-and-mix synthesis on a 5g scale to generate a combinatorial mixture of pentameric peptides. The 18 standard L-amino acids, Fmoc-X-OH, where X= Ala, Val, Leu, Ile, Pro, Phe, Trp(Boc), Gly, Ser(tBu), Thr(tBu), Tyr(tBu), Asn(Trt), Gln(Trt), Asp(OtBu), Glu(OtBu), Lys(Boc), Arg(Pbf), and His(Trt), were used

with methionine and cysteine omitted for chemical stability. D-libraries were generated using the enantiomers of the standard amino acids. All syntheses were accomplished using standard solid phase techniques from the C- to N-terminus on a Titan 357 Peptide Synthesizer (Aapptec) with 0.2 M amino acid, 0.2 M HATU, 2 M DIEA solutions, and 20% piperidine/NMP solutions. An azide or alkyne click handle was appended to the N-termini of each library after synthesis of the pentameric region. Cyclic OBOC libraries were generated in the same manner with the addition of azide and alkyne amino acids (alkyne-$X_1X_2X_3X_4X_5$-azide). The libraries were cyclized overnight by treatement with 2 equivalents of CuI and 5 equivalents of ascorbic acid in 20% piperidine/NMP. The copper was removed by washing with 2% sodium diethyldithiocarbamate (w/v) and 2% DIEA (v/v) in NMP. An azide of alkyne click handle was then appended to the N-termini of the cyclized libraries. The side chain protecting groups were removed by treatment with 95% TFA, 2.5% TES, and 2.5% deionized water for 2 hours. The libraries were validated for cyclization and completion by sequencing via Edman degradation on a 494 CLC Procise Sequencer (Life Technologies). All reactions were performed at ambient temperature.

General Peptide Synthesis. All resin was preswelled in NMP for a minimum of 2 hours prior to synthesis. Fmoc groups were removed by treatment of 2 x 20 minutes in 20% piperidine/NMP. Couplings were accomplished using excesses of 4 equivalents of amino acid, 4 equivalents of HATU, and 12 equivalents of DIEA in NMP. Washes were performed between all steps with NMP. Peptides were cleaved off the resin by treatment with 95% TFA, 2.5% TES, and 2.5% deionized water for 2 hours with agitation. The cleavage solution was precipitated into diethyl ether. The precipitate was pelleted by

centrifugation and resuspended in minimal DMSO for purification. All reactions were performed at ambient temperature.

Protocols for Cyclization. For click cyclization, peptides bearing the azide and alkyne handles were subjected to 2 equivalents of CuI and 5 equivalents of ascorbic acid overnight at ambient temperature. Following the overnight reaction, the peptides were washed with 2% sodium diethyldithiocarbamate (w/v) and 2% DIEA (v/v) in NMP, followed by rigorous rinsing with NMP. Peptides cyclized by ring closing metathesis (RCM) had the specialty peptides, (S)-N-Fmoc-2-(4'-pentenyl)alanine, and (R)-N-Fmoc-2-(7'-octenyl)alanine, in place of the azide and alkyne click handles. The resin was dried down in DCM before resuspension in anhydrous DCE. The resin was placed under inert atmosphere and subjected to 8 mM Grubbs catalyst prepared in anhydrous DCE. The reaction was allowed to stir under argon for 6 hours, at which time all solution was drained from the flask, and fresh 8mM Grubbs catalyst solution was added. The reaction was allowed to proceed overnight under inert atmosphere at room temperature. Following the RCM procedure, the resin was washed rigorously with 10% sodium diethyldithiocarbamate (w/v) and 5% DIEA (v/v) in dimethyl formamide (DMF). Synthesis, cleavage, and characterization were accomplished as described.

Purification and Characterization. Synthetic epitopes and peptide hits were purified via reversed phase high-performance liquid chromatography on either a Beckman Coulter HPLC instrument with a Luna 10 μm C18(2) 100A column. Gradients were composed of 18 MegaOhm distilled water and HPLC grade acetonitrile with 0.1% TFA in both.

Peptides were characterized after purification by matrix assisted laser desorption ionization time-of-flight (MALDI-TOF) mass spectrometry. Product fractions were collected, lyophilized, and reconstituted for quantification prior to assays. Peptides were quantified by determination of extinction coefficients and measurement of absorbance at 280 nm on a ThermoFisher Nanodrop 2000c UV-Vis spectrophotometer.

Screening Protocols. All screening protocols were conducted using binding buffer (20 mM Tris, 150 mM NaCl, 0.1% bovine serum albumin, 0.05% Tween 20, pH 7.5) unless otherwise denoted. High salt buffer (25 mM Tris, 750 mM NaCl, 10 mM $MgCl_2$, pH 7.5) and BCIP buffer (100 mM Tris, 10 mM NaCl, 1 mM $MgCl_2$, pH 9) were also used. All steps were performed at ambient temperature unless otherwise denoted. All screens were conducted on 300 to 500 mg of library beads bearing the combinatorial pentamers.

General Library Preclear and Epitope Antiscreen. *Step 1*: The library beads were swelled in buffer with 0.05% TWEEN20 for 6 hours at 4°C. *Step 2*: The library was incubated with 7.5 μM of scrambled epitope (where applicable) for 6 hrs. After incubation, the library beads were washed for 3 x 5 minutes buffer, 3 x 5 minutes in TBST (TBS + 0.05% TWEEN20), and 3 x 5 minutes in TBS (standard wash). Non-covalent binders were removed by a 2 hour wash with guanidinium HCl solution (pH 2). *Step 3*: The library was treated with anti-biotin alkaline phosphatase at 1/10000 dilution and developed with BCIP/NBT for 15 to 25 minutes. The blue/purple beads (nonspecific hits) were discarded and the clear beads were retained for subsequent screens. *Step 4*: The clear beads were decolorized by agitation in NMP for 2 hours. The beads were washed and dried in DCM.

They were then agitated in guanidine hydrochloride for 3 hours followed by 10 x 5 minutes washes in deionized water.

General Human Antiscreen. *Step 1*: Library beads were swelled in binding buffer until homogenous. *Step 2*: Beads were blocked in 5% milk in buffer overnight. *Step 3*: The beads were washed 3 x 5 minutes in buffer followed by incubation with 1% filtered human serum in 0.5% milk for 1 hour. *Step 4*: The beads were washed 3 x 5 minutes in buffered followed by incubation with 1/10000 rabbit anti-whole human serum polyclonal antibody in 0.5% milk in buffer for 1 hour. *Step 5*: The beads were washed 3 x 5 minutes in buffer before incubation with 1/10000 goat anti-rabbit IgG polyclonal antibody in 0.5% milk in TBS for 1 hour. *Step 6*: The beads were washed 3 x 5 minutes in high salt TBS followed with an additional 1 hour wash. The beads were washed with BCIP buffer, pH 9. *Step 7*: The beads were developed with BCIP/NBT as described above.

General Product Screen (Single Ligand). *Step 1*: The beads retained from the antiscreen/preclear were swelled as described followed by incubation with 5 to 10 μM of target SynEP. *Step 2*: Beads were washed 3 x 5 minutes with buffer. Non-covalent binders were removed by washing in guanidinium hydrochloride for 2.5 hours. The beads were washed 10 x 5 minutes with deionized water. *Step 3*: The beads were swelled in buffered and blocked in 5% milk overnight at 4°C. *Step 4*: The beads were incubated with streptavidin or anti-biotin AP (1/10000) for 1 hour. The beads were washed for 3 x 5 minutes in buffer, followed by 3 x 5 minutes in TBST. *Step 5*: The beads were then washed

in BCIP buffer and developed as described above. *Step 6*: The colored/hit beads were isolated, decolorized, and retained for sequencing via Edman degradation.

Secondary Ligand Antiscreen and Preclear (Applicable to PfLDH Only for alkyne bearing library). *Step 1*: The library beads were swelled in buffer. A solution of 100 μM of the best anchor peptide hit with a C-terminal azide click handle, 200 mM human LDH, and 500 nM of GST was incubated for 30 minutes. The solution was subsequently incubated with the library for 90 minutes followed by 3 x 5 minutes washes in buffer. Step 2: The library beads were incubated with anti-biotin AP (1/10000) for 1 hour, washed in 3 x 5 minutes in buffer, and washed again in BCIP buffer. Step 3: The library was developed with BCIP/NBT. Hits (binders to the anchor ligand, hLDH, GST, and the detection antibody) were detected and removed. The library was stripped and prepped as usual for the next screening step.

Secondary Ligand Target Screen (PfLDH – screen for noncovalent binding). *Step 1*: Following the antiscreen/preclear, the library beads were swelled in buffer overnight at 4°C. *Step 2*: A solution of 90 μM of anchor ligand with an N-terminal azide click handle was incubated with 200 nM of *Pf*LDH-GSTfor 30 minutes. The anchor + protein solution was then incubated with the library for 90 minutes. *Step 3*: The library beads were washed 3 x 5 minutes in buffer and incubated with anti-GST (1/2000) antibody conjugated for 1 hour. *Step 4*: The library was then washed in BCIP buffer and developed with BCIP/NBT. Purple/hit beads were collected, decolorized, and stripped of protein for the product screen.

Secondary Ligand Product Screen. *Step 1*: The library beads retained from the target screen were incubated for 1 hour with anti-biotin AP antibody in TBST at 4°C. *Step 2*: The colored hit beads were washed for 5 minutes in BCIP buffer and developed with BCIP only. The darkest beads were isolated, stripped of protein, decolorized, and washed vigorously with water. The hit peptide sequences were identified by Edman degradation.

General Enzyme-Linked Immunosorbent Assay (ELISA) Protocols. The solution conditions of ELISAs were designed to mimic those in the screens. The same TBS binding buffer was used for all assays in general unless otherwise specified. All sandwich ELISAs were performed on NeutrAvidin or Streptavidin Coated Microtiter Plates (Pierce). All assay steps were performed at ambient temperature unless otherwise specified.

General Sandwich ELISA Protocol. *Step 1*: The plate was washed 3X with buffer, 200 μL per well at RT. The plate was then incubated with blanks or biotinylated ligands at 1 – 2 μM solutions for 2 hours. Lower concentrations can be used to reduce surface coverage for binding assays. *Step 2:* The plate was washed 3X and blocked with 3% BSA or 5% milk in TBST for two hours at RT or longer at 4°C. *Step 3:* The plate was washed 3X and incubated with either a single protein concentration or a dilution series when constructing a binding curve. The incubations were performed at ambient temperature if incubation time was less than 3 hours or at 4°C for longer times. *Step 4:* The plate was washed 3X and incubated with anti-GST-HRP (Abcam) antibody at 1:2000 dilution for 1 hour. *Step 5:* The place was then washed 3X with buffer, 1X with TBS, and developed with TMB Substrate/Peroxidase (ThermoScientific or KPL, 2-Step Kit). The development was

allowed to proceed for no longer than 10 minutes, at which time the reaction was quenched with 1M sulfuric acid. Absorbance measurements were taken at 450 nm on a plate reader. The data was worked up with blanks or control ligands removed as necessary for background subtraction. Measurements were taken in duplicate to triplicate, contigent on reagent availability.

2.3 Results and Discussion

2.3.1 Epitope Selection for Targeting *Plasmodium* LDH

The development of a sandwich pair of PCCs to target *Pf*HRP2 in an RDT requires two orthogonal epitopes for capture and detection (see Figure 1-1). A selective capture agent must be able to target *Pf*LDH over its homologs which are ~75% identical. [9,10] In line with a general sandwich assay, we targeted two orthogonal regions in *Pf*LDH so that affinity agents would not cross-react during simultaneous binding events. To engineer a capture PCC specific to *Pf*LDH, we targeted an epitope specific to the antigen. With the rational in mind that the capture PCC would solely pull down *Pf*LDH and thus eliminate concerns of cross-reactivity, we targeted a second epitope that is common to all P*lasmodium* LDH antigens for detection.

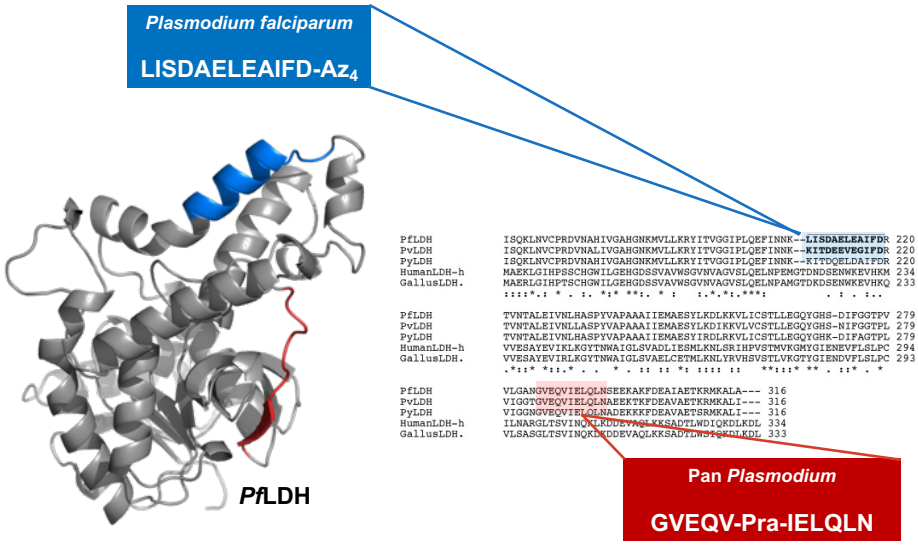

Figure 2-2. An epitope (blue) that is specific to *Pf*LDH was targeted for capture and fitted with an azide (Az4) click handle. A pan-species epitope (red) was selected for detection and fixed with an alkyne (Pra) click handle. The general schematic of the capture and detection PCC pair in a sandwich assay format is shown in the upper left-hand corner. (PDB: 1LDG, figure partially adapted.[8])

For capture of *Pf*LDH, the amino acid sequence from 208-219, LISDAELEAIFD, was selected for epitope synthesis as illustrated in Figure 2-2. It is important to note the high homology of the LISDAELEAIFD epitope to the homogolous epitopes in other malaria species which requires that the final PCC be able to distinguish between small changes in sequence identity. For example, amino acids 208-219 differ only by four amino acids between *P. falciparum* and *P. vivax* LDH antigens.[14] For the PCC screening process, the LISDAELEAIFD epitope was synthesized with an alkyne click handle, on the C-terminus to yield LISDAELEAIFD-Az4.[18] A scrambled version of this epitope, DDIAILIEEFALS-Az4, was also synthesized for prescreening. Inclusion of a scrambled epitope in a prescreen helps to eliminate hits that might generate false positives from lack of sequence specificity.[18] A pan-species epitope was selected for the development of a

detection PCC. The amino acids 297-308 of LDH, GVEQVIELQLN, are common to at least *P. falciparum*, *P. vivax*, and *P. yoeli* species of malaria.[14] The SynEp for *Px*LDH detection was synthesized with a Pra in the center to yield GVEQV-Pra-VIELQLN.[18]

2.3.2 Discovery of Capture and Detection PCCs Against *Pf*LDH

The primary detection PCC agent against GVEQVIELQLN was developed using older screening methodology from the Heath group that utilized *in situ* click screening with OBOC linear peptide libraries.[16,16] The screen was conducted against a OBOC D-stereochemistry library fitted with an Az4 click handle that was prescreened to remove false-positives. This screen yielded a linear 5-mer D-peptide with the sequence **hevwh**.[18] The use of D-amino acids in a linear library is to provide increased proteolytic stability in the final peptide sequences. The EC_{50} of **hevwh** as determined by enzyme-linked immunosorbent assay (ELISA) was found to be 1.7 μM (Figure 2-3).[18] The EC_{50} value offers an upper limit to the true binding affinity, or K_D, of a ligand to substrate, and the affinity of this PCC is considered modest. Further work detailed in this chapter will describe the expansion of this primary ligand into a bivalent molecule for increased target binding.

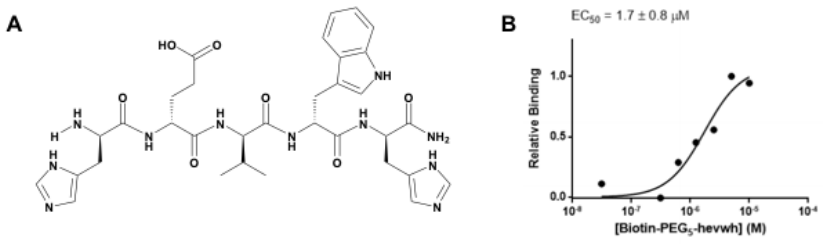

Figure 2-3. (A) Structure of **hevwh**. (B) Sandwich ELISA of the binding affinity of **hevwh** (EC_50 = 1.7 μM).

The development of the capture PCC for *Pf*LDH was accomplished with a OBOC click cyclized L-peptide library appended with Az4 as shown in Figure 1-3. Non-specific binding to the detection antibody and the scrambled epitope, DDIAILIEEFALS-Az4, were removed in the prescreening process. After removal of false positives, the OBOC cyclized library was subjected to *in situ* click screening with the LISDAELEAIFD-Az4 SynEp. In the absence of Copper(I) catalyst, the click reaction between the azide and alkyne moieties is low yielding. Typical screens are initiated with ~10^6 beads, which are focused through elimination of false positives and nonspecific interactions. The product screen against LISDAELEAIFD-Az4 SynEp yielded just 7 covalent click products as hits. This is anticipated.[18] The hit beads were sequenced via Edman degradation for identification of the 5-mer peptides that bind to the SynEp (Table 2-1).

X_1	X_2	X_3	X_4	X_5
K	K	I	H	L
I	L	Y	W	K
P	L	K	G	G
L	K	Q/T	H	Q/T
H	W	S	A	N
Y	W	Q	W	--
R	G	G	I	L

Table 2-1. Hit peptides for *Pf*LDH capture PCCs as determined by Edman degradation presented in single amino acid letter code.

The *Pf*LDH hits were synthesized and accessed for binding performance in single point ELISAs. Briefly, the hits in Table 2-1 were synthesized with a biotin tag on the C-terminus end that was separated from the macrocycle by a Peg5 linker. The hits were also cyclized using Cu(I) catalyzed click to reproduce the structures present on the library beads during screening. In the initial validation of hit binding to the target epitopes, the *Pf*LDH

capture SynEp was appended with a 3-unit polyethylene glycol (Peg3) linker and conjugated to bovine serum albumin to yield LISDAELEAIFD-Peg3-C-BSA, where C = cysteine. The same procedure was repeated to generate the scrambled epitope. The BSA conjugated SynEps were immobilized on the plate and probed biotinylated peptide candidates. The peptides are detected by an anti-biotin antibody conjugated to an enzyme that turns over a colorimetric substrate where signal is proportionate to the amount of analyte bound.[21]

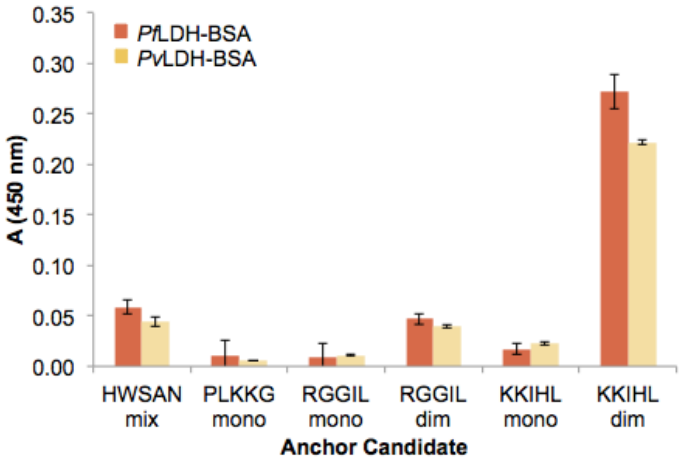

Figure 2-4. Sandwich ELISA of click cyclized CC candidates against the *Pf*LDH-specific SynEp in 0.1% human serum. The hits were tested as a monomer (mono), dimer (dim), or a mixture of both (mix).

The most promising hits from the preliminary ELISA were **cyHWSAN**, **cyPLKGG**, **cyRGGIL**, and **cyKKIHL** (data not shown) which were probed in the epitope binding assay (Figure 2-4). Whilst the best PCC candidate appears to be **cyKKIHL** dimer from this assay, repeats of this experiment demonstrated variations in performance (data not shown). Thus, **cyHWSAN** monomer was selected as the best candidate for *Pf*LDH capture (Figure 2-5A). A sandwich ELISA of **cyHWSAN** demonstrate the selectivity of the PCC for *Pf*LDH over *Pv*LDH and human LDH (hLDH) (Figure 2-5B). The capture

PCC binds to its target with an EC_{50} = 23.4 nM (as determined by ELISA) and K_D = 40.6 nM by fluorescence polarization (Figure 2-5C).[18]

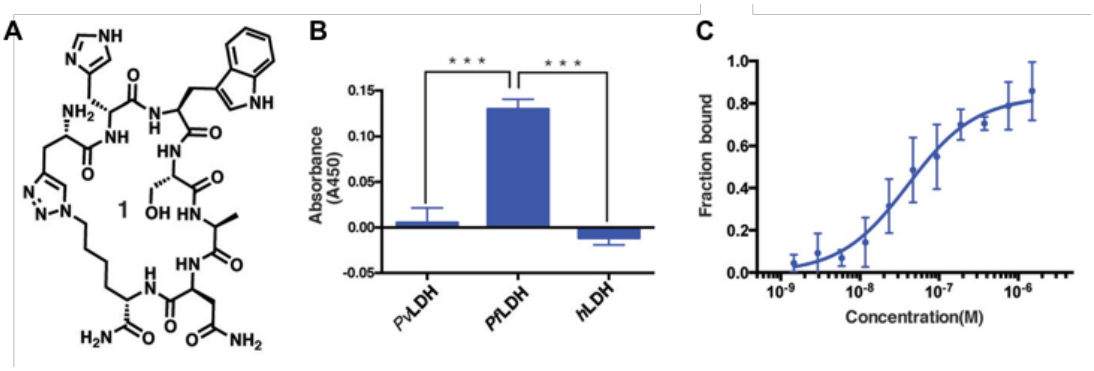

Figure 2-5. (A) The click cyclized **cyHWSAN** is the best candidate as a capture PCC against *Pf*LDH. (B) The PCC is selective for *Pf*LDH. (C) The PCC binds to *Pf*LDH with a K_D = 40.6 nM as measured by fluorescence polarization. Figure reprinted in part with permission.[18]

There is a stark difference in target affinities from PCCs developed from linear and cyclic OBOC peptide libraries. Relative to the nanomolar affinity of **cyHWSAN**, **hevwh** is only a modest binder. Recent PCCs developed with cyclic OBOC peptide libraries within the Heath lab have demonstrated the superiority of conformationally restricted structures in generating affinity agents that bind in the nanomolar regime from a single generation screen.[18,19] Whereas linear peptides possess myriad conformations, peptides restricted through macrocycles are inflexible against many conformational changes. When bound to their target epitopes, cyclic PCCs present functionalities in the optimal positions for recognition without the need to sample or cycle through all possible conformations.

2.3.2 Improving Affinity of the *Pf*LDH Capture PCC Through Olefin Metathesis

In a bid to increase the performance of **cyHWSAN**, we experimented with modifications to the cyclic backbone. All-hydrocarbon stapling, or ring closure through olefin metathesis, has been shown to increase target affinity as well as improving proteolytic resistance and serum half-lives of peptides.[22] The all-hydrocarbon staple induces α-helical structure into the stapled peptide. The staple is constructed by forming a C-C bond with ruthenium-mediated (1st generation Grubbs catalyst) olefin metathesis.[23] We appended a glycine (G) residue onto the **HWSAN** sequence and replaced the click handles with the olefin bearing side chains, (S)-N-Fmoc-2-(4'-pentenyl)alanine and (R)-N-Fmoc-2-(7'-octenyl)alanine, on the C- and N-termini of the peptide, respectively. Treatment of the olefin appended peptide with 1st generation Grubbs catalyst yields an *i, i + 7* hydrocarbon staple, where the *i + 7* specifies 7 residues distance between olefin-bearing side chains.[24] We synthesized **GHWSAN$_{RCM}$** (Figure 2-6) with an *i, i + 7* an staple in addition to an *i, i + 6* variant (not shown). Relative to **cyHWSAN**, **GHWSAN$_{RCM}$** bears a larger, more flexible ring structure that is expected to enforce α-helical structure as detailed in the literature.[22]

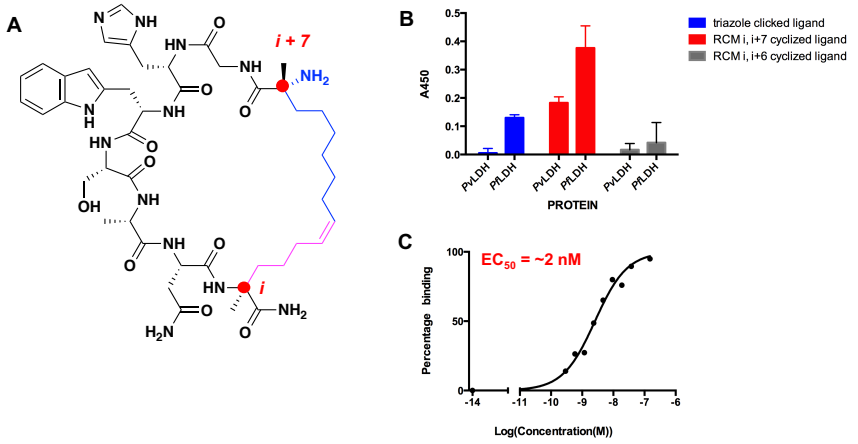

Figure 2-6. (A) The structure of the *i, i + 7* hydrocarbon stapled **GHWSAN$_{RCM}$** PCC. (B) The affinity of the PCC against *Pf*LDH-GST is increased by hydrocarbon stapling (*i, i + 7*), but at a loss of antigen specificity. (C) The EC_{50} of **GHWSAN$_{RCM}$** (*i, i + 7*).

We tested the performances of the stapled peptides to compare their affinities for *Pf*LDH-GST relative to **cyHWSAN**.[21] All hydrocarbon stapling improved the affinity of **GHWSAN$_{RCM}$**, but at a cost of target selectivity (Figure 2-6B,C). The EC_{50} of the *i, i + 7* stapled peptide of binding to *Pf*LDH-GST was improved to 2 nM. However, the hydrocarbon staple also introduces off-target interactions with *Pv*LDH-GST. The *i, i + 6* staple significantly reduces affinity of the PCC for either antigen. Given the increased signal observed for *Pf*LDH-GST in our assays, we opted to use **GHWSAN$_{RCM}$** in further screening for a secondary ligand to further improve the performance of the capture PCC.

2.3.3 Expansion of Anchor PCC Agents into Bivalent Ligands

Prior work on PCC agents within the Heath group has demonstrated that iterative *in situ* click screening to obtain secondary and tertiary ligands[16,17,19,20,25] can greatly improve the affinity and performance of PCCs. We sought to improve upon **hevwh** and **GHWSAN$_{RCM}$** by using our screening methodology to develop bivalent PCCs.

Whereas primary PCCs are developed against SynEps selected from the antigen of interest, screens for secondary ligands utilize the full protein target. The secondary ligand candidates were obtained by screening *Pf*LDH-GST against a click cyclized (triazole bearing) OBOC library. As illustrated in Scheme 2-1, the primary, or anchor, PCC bearing a click handle is first incubated with the full protein to allow binding to the targeted SynEp. The protein:PCC complex is then screened against a OBOC library that bears a complimentary click handle to that on the PCC. Whereas the initial screen for an anchor PCC relies upon the recognition between library elements and the SynEp to promote formation of a click product, the screen for a secondary ligand requires the target to guide the click product. In the target screen, only elements of the library that bind on regions of the target protein in close proximity to where the anchor PCC is already bound will facilitate the formation of the low-yielding click product. In this manner, it is the protein that assembles the bivalent ligand that recognizes two separate sites on the same PCC. The OBOC library is then stripped of any noncovalent binders and probed for the covalent click product. This process can be iterated for additional ligands as needed.[16,17,19,20,25]

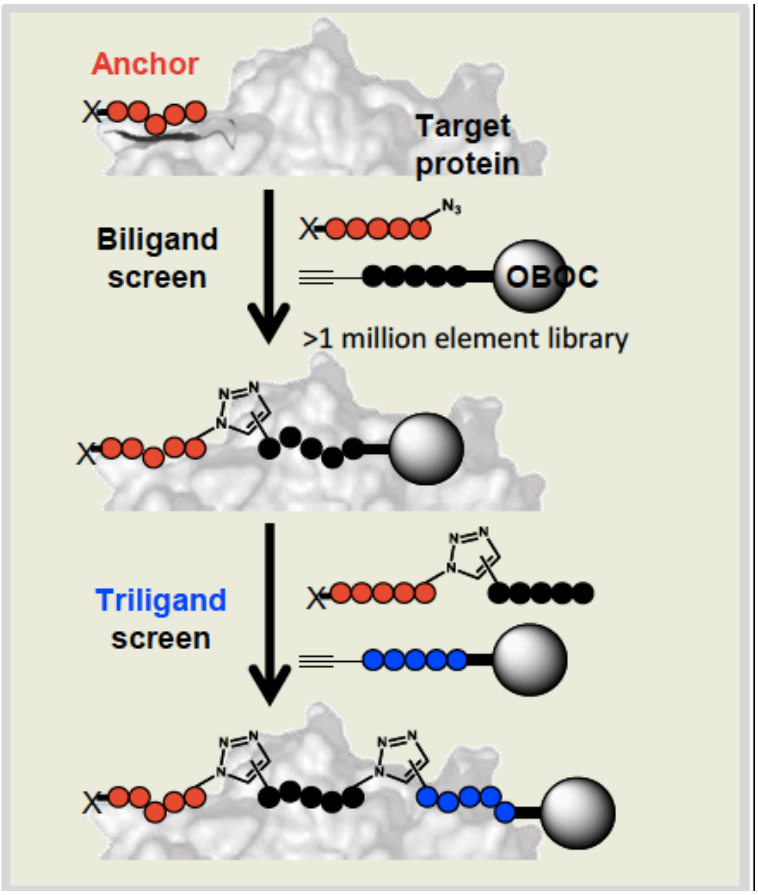

Scheme 2-1. Schematic of target-guided iterative *in situ* click screening methodology for obtaining secondary and tertiary ligands.[16,17,19,20,25]

Two versions of **GHWSAN$_{RCM}$** were prepared for secondary ligand screens guided by the full *Pf*LDH protein (Figure 2-7). The anchor PCC was synthesized with an azide on either the N-terminus or C-terminus. A cyclic OBOC library was prescreened to remove non-specific binding to the detection antibody, human LDH, and the GST fusion tag on *Pf*LDH-GST. The **GHWSAN$_{RCM}$** anchors were incubated separately with *Pf*LDH-GST and screened against batches of the OBOC library. Noncovalent binders were removed and the click products with each anchor were detected and sequenced. The secondary ligand hits are provided in Table 2-2.

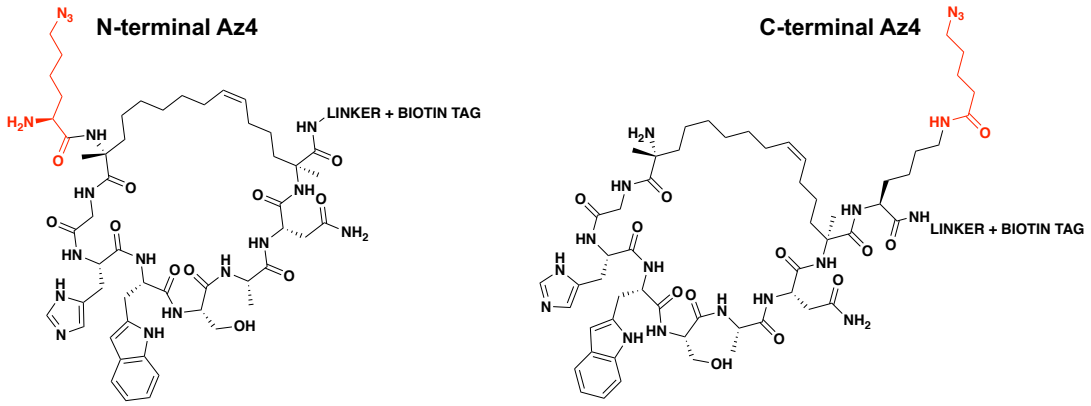

Figure 2-7. The stapled **GHWSAN$_{RCM}$** was used as an anchor PCC in the secondary ligand screens against *Pf*LDH. An azide click handle was appended at the N-terminus (left) or C-terminus (right) of the anchor PCC. Biotin is tethered on to each ligand for detection.

A

X_1	X_2	X_3	X_4	X_5
G	H	S	A	N
G	H	S	A	R
G	H	W	A	R
G	H	H	S	A
D	H	S	A	S
H	H	K	R	R
N	G	N	S	Q
V	G	I	H	Q
R	G	R	R	Y
K	G	N	F	Q
K	R	R	H	R

B

X_1	X_2	X_3	X_4	X_5
H	Y	R	I	Q/T
H	Y	Y	R	Y
H	V	G	Y	T
V	S	Y	H	H
V	P	N	D	E
H	N	D	E	Q
T	R	A	K	T
K	R	L	R	A
R	A	R	R	H
R	A	R	A	H

Table 2-2. Secondary ligand hits for a captyre PCC against *Pf*LDH from screening with **GHWSAN$_{RCM}$** with (A) a C-terminal or (B) N-terminal azide (Az4) click handle sequenced via Edman degradation.

There is a high degree of homology between the two screens. Several hits for the C-terminal secondary ligand screen look nearly alike to **GHWSAN$_{RCM}$**. We hypothesize that it is likely the secondary ligand may have bound to a second copy of *Pf*LDH-GST. There are also repeats of amino acids in the same position in both screens, namely H, A, G, and R residues. In order the test the secondary ligands, the hits were synthesized on

Sieber resin, which allows for retention of protecting groups, and appended to the anchor **GHWSAN$_{RCM}$** PCC (Figure 2-7) by click chemistry. The biligands were examined by sandwich ELISA for *Pf*LDH-GST binding (data not shown).[24] The best biligands were found to be **GHWSAN$_{RCM}$-HYYRY** (N-terminal screen) and **GHWSAN$_{RCM}$-RGRRY** (C-terminal screen) (Figure 2-8).

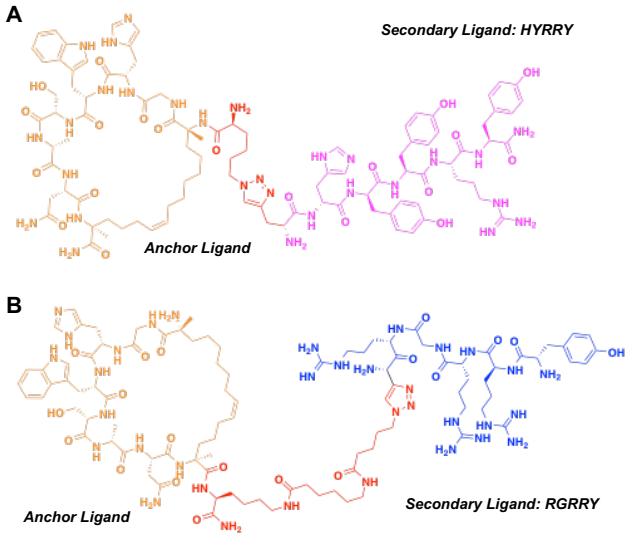

Figure 2-8. Structure of (A) the N-terminal biligand **GHWSAN$_{RCM}$-HYYRY** and (B) the C-terminal biligand **GHWSAN$_{RCM}$-RGRRY**.

The binding affinities of the capture biligand PCCs against *Pf*LDH antigen were determined by sandwich ELISA. Recombinant *Pf*LDH was expressed in house with a FLAG tag and a His6-SUMO tag.[26] The EC_{50} values of the C-terminal PCC **GHWSAN$_{RCM}$-RGRRY** against FLAG-*Pf*LDH and His6-SUMO-*Pf*LDH were found to be 21 nM and 9.5 nM, respectively. Likewise, the analogous EC_{50} values for antigen binding by the N-terminal PCC **GHWSAN$_{RCM}$-HYYRY** were found to be 16 nM and 18 nM (Figure 2-9).[21] Relative to both **cyHWSAN**, the triazole bearing macrocycle, and the hydrocarbon stapled **GHWSAN$_{RCM}$**, neither of the biligands show significant

improvement in affinity. Whilst iterative *in situ* screening for rapid secondary and tertiary ligand discovery has enhanced the affinity of other PCCs developed in the Heath lab, this work shows that this effect may be target dependent. As such, a tertiary ligand screen was not pursued further.

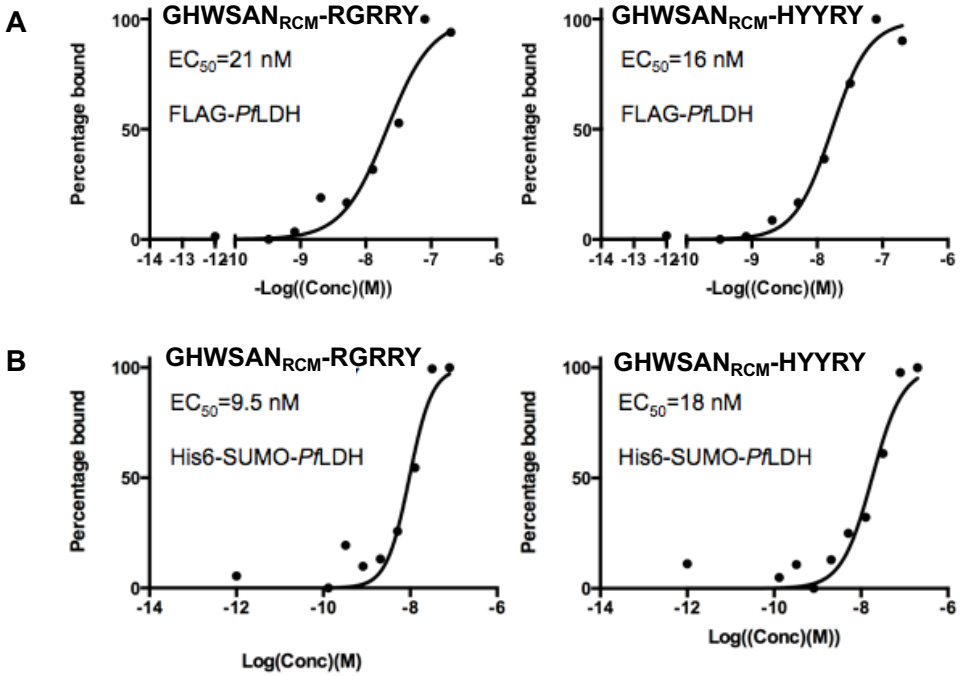

Figure 2-9. The apparent binding affinities, EC_{50} values, of the *Pf*LDH biligands are shown with (A) FLAG-tagged recombinant *Pf*DLH and (B) His6-SUMO-tagged recombinant *Pf*LDH. There is no significant improvement in affinity from expansion of the anchor ligand into bivalent PCCs.

A secondary ligand screen was also performed for improvement of the pan-*Plasmodium* LDH detection PCC, **hevwh**, with a cyclic OBOC library using the same methodology described for the aforementioned biligands. After validation of hits via ELISA (data not shown), the best secondary ligand was a cyclic peptide with the sequence YLGHK. The EC_{50} of the secondary ligand, **cyYLGHK**, was determined to be ~15 nM by sandwich ELISA (data not shown). The anchor and secondary ligand were ligated together

by a triazole to create the bivalent PCC (Figure 2-10A). The EC_{50} of the biligand against *Pf*LDH-GST and *Pv*LDH-GST is 15 nM and 12 nM, respectively (Figure 2-10B). The biligand maintains its performance in up to 5% human serum, which is indicative of little off-target interaction (Figure 2-10C).[26] From these data, we can conclude that the affinity of the biligand is largely dominated by the affinity of the macrocyclic secondary ligand. In this case, the addition of a secondary ligand is beneficial for increasing overall affinity, though the use of **cyYLGHK** alone might demonstrate similar performance.

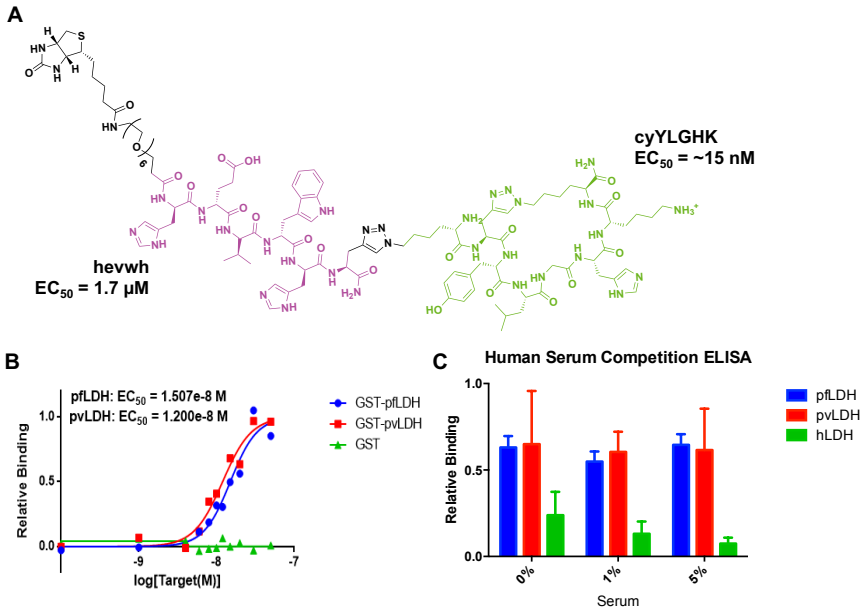

Figure 2-10. (A) The structure of the detection biligand PCC against pan-Plasmodium LDH. (B) The biligand PCC binds to *Pf*LDH-GST and *Pv*LDH-GST in nanomolar affinities with no binding to the GST tag. (C) The performance of the PCC is maintained in up to 5% human serum.

2.4 Conclusion

A pair of synthetic affinity agents were developed as a sandwich set of protein capture agents for the lactate dehydrogenase biomarker of the lethal malaria species, *P. falciparum*. We employed epitope targeted *in situ* click chemistry in conjunction with high throughput screening against OBOC libraries for the rapid discovery of affinity agents. We targeted two distinct epitopes, one that occurred only in *Pf*LDH to engineer antigen specificity into the PCC, and one that was common to the LDH enzyme in multiple *Plasmodium* species.

We developed a monovalent capture PCC against the *Pf*LDH-specific epitope that can selectively bind *Pf*LDH nanomolar affinity despite high similarity between homologous antigen epitopes. The affinity was slightly improved through alteration of the original click cyclized PCC macrocycle into an all-hydrocarbon stapled backbone. However, this increase in affinity came at the cost of target specificity and the altered PCC showed off-target interactions. Using target-guided iterative in situ click screening methodology, we screened new macrocyclic OBOC libraries for suitable secondary ligands. Despite high homology in the hits, we found that for the capture PCC, a bivalent ligand performed similarly to a monovalent affinity agent.

We applied the secondary ligand screening protocols towards the micromolar detection PCC, which was obtained from an initial screen against a linear OBOC peptide library. In this case, the addition of a second ligand obtained from screening against a cyclic OBOC library significantly improved the detection PCC to nanomolar affinity for pan-*Plasmodium* LDH antigens. The improved affinity of the biligand detection PCC was

largely attributed to the macrocyclic secondary ligand. The improved detection PCC was found to perform in up to 5% human serum and showed little off-target interactions.

In this work, the application of epitope-targeting for engineering specificity and the use of entropy restricted macrocyclic peptide libraries were demonstrated. Relative to linear peptide libraries, we found that the use of cyclic libraries dramatically improved the affinities of monovalent PCCs. Using cyclic OBOC peptide libraries in combination with epitope targeting and *in situ* click chemistry methodology provides a platform for the rapid discovery of selective and high-binding affinity agents in a single generation high throughput screen. As demonstrated through the development of a pair of capture and detection PCCs against *Plasmodium* LDH antigens, this platform can be readily applied towards the development of similar affinity agents against other antigens and disease biomarkers.

2.5 Acknowledgments

The *Pf*LDH capture/detection agents were developed by JingXin Liang, Arundhati Nag, Samir Das, Aiko Umeda, and Mary Beth Yu. The *P*LDH detection PCC was developed by Aiko Umeda. Arundhati Nag, Samir Das, Mary Beth Yu, and JingXin Liang developed the *Pf*LDH anchor PCC and biligands.

References

(1) WHO. World Malaria Report 2016. World Health Organization December 2016.

(2) Chiodini, P. L.; Bowers, K.; Jorgensen, P.; Barnwell, J. W.; Grady, K. K.; Luchavez, J.; Moody, A. H.; Cenizal, A.; Bell, D. The Heat Stability of Plasmodium Lactate Dehydrogenase-Based and Histidine-Rich Protein 2-Based Malaria Rapid Diagnostic Tests. *Trans. R. Soc. Trop. Med. Hyg.* **2007**, *101* (4), 331–337.

(3) Birku, Y.; Welday, D.; Ayele, D.; Shepherd, A. Rapid Diagnosis of Severe Malaria Based on the Detection of PfHRP-2 Antigen. *Ethiop Med J* **1999**, *37*.

(4) Endeshaw, T.; Gebre, T.; Ngondi, J.; Graves, P. M.; Shargie, E. B.; Ejigsemahu, Y.; Ayele, B.; Yohannes, G.; Teferi, T.; Messele, A.; et al. Evaluation of Light Microscopy and Rapid Diagnostic Test for the Detection of Malaria under Operational Field Conditions: A Household Survey in Ethiopia. *Malar J* **2008**, *7*.

(5) Moody, A. Rapid Diagnostic Tests for Malaria Parasites. *Clin. Microbiol. Rev.* **2002**, *15* (1), 66–78.

(6) Wongsrichanalai, C. Rapid Diagnostic Techniques for Malaria Control. *Trends Parasitol* **2001**, *17*.

(7) Koczula, K. M.; Gallotta, A. Lateral Flow Assays. *Essays Biochem.* **2016**, *60* (1), 111–120.

(8) Penna-Coutinho, J.; Cortopassi, W. A.; Oliveira, A. A.; França, T. C. C.; Krettli, A. U. Antimalarial Activity of Potential Inhibitors of Plasmodium Falciparum Lactate Dehydrogenase Enzyme Selected by Docking Studies. *PLoS ONE* **2011**, *6* (7), e21237.

(9) Akbulut, E.; Celik, V.; Balik, D. T. Comparative Analysis at the Nucleotide Level of the Genes Encoding the Lactate Dehydrogenase Enzyme of Plasmodium Vivax and Plasmodium Falciparum. *Turk. Parazitol Derg* **2005**, *29*.

(10) Turgut-Balik, D.; Akbulut, E.; Shoemark, D. K.; Celik, V.; Moreton, K. M.; Sessions, R. B.; Holbrook, J. J.; Brady, R. L. Cloning, Sequence and Expression of the Lactate Dehydrogenase Gene from the Human Malaria Parasite, Plasmodium Vivax. *Biotechnol Lett* **2004**, *26*.

(11) Houzé, S.; Boly, M. D.; Le Bras, J.; Deloron, P.; Faucher, J.-F. PfHRP2 and PfLDH Antigen Detection for Monitoring the Efficacy of Artemisinin-Based Combination Therapy (ACT) in the Treatment of Uncomplicated Falciparum Malaria. *Malar. J.* **2009**, *8*, 211–211.

(12) Bashir, I. M.; Otsyula, N.; Awinda, G.; Spring, M.; Schneider, P.; Waitumbi, J. N. Comparison of PfHRP-2/PLDH ELISA, QPCR and Microscopy for the Detection of Plasmodium Events and Prediction of Sick Visits during a Malaria Vaccine Study. *PLOS ONE* **2013**, *8* (3), e56828.

(13) Iqbal, J.; Siddique, A.; Jameel, M.; Hira, P. R. Persistent Histidine-Rich Protein 2, Parasite Lactate Dehydrogenase, and Panmalarial Antigen Reactivity after Clearance of Plasmodium Falciparum Monoinfection. *J. Clin. Microbiol.* **2004**, *42* (9), 4237–4241.

(14) Hurdayal, R.; Achilonu, I.; Choveaux, D.; Coetzer, T. H. T.; Dean Goldring, J. P. Anti-Peptide Antibodies Differentiate between Plasmodial Lactate Dehydrogenases. *Peptides* **2010**, *31* (4), 525–532.

(15) Aydin-Schmidt, B.; Mubi, M.; Morris, U.; Petzold, M.; Ngasala, B. E.; Premji, Z.; Björkman, A.; Mårtensson, A. Usefulness of Plasmodium Falciparum-Specific Rapid Diagnostic Tests for Assessment of Parasite Clearance and Detection of Recurrent Infections after Artemisinin-Based Combination Therapy. *Malar. J.* **2013**, *12* (1), 349.

(16) Agnew, H. D.; Rohde, R. D.; Millward, S. W.; Nag, A.; Yeo, W.-S.; Hein, J. E.; Pitram, S. M.; Tariq, A. A.; Burns, V. M.; Krom, R. J.; et al. Iterative In Situ Click Chemistry Creates Antibody-like Protein-Capture Agents. *Angew. Chem. Int. Ed Engl.* **2009**, *48* (27), 4944–4948.

(17) Millward, S. W.; Henning, R. K.; Kwong, G. A.; Pitram, S.; Agnew, H. D.; Deyle, K. M.; Nag, A.; Hein, J.; Lee, S. S.; Lim, J.; et al. Iterative in Situ Click Chemistry Assembles a Branched Capture Agent and Allosteric Inhibitor for Akt1. *J. Am. Chem. Soc.* **2011**, *133* (45), 18280–18288.

(18) Das, S.; Nag, A.; Liang, J.; Bunck, D. N.; Umeda, A.; Farrow, B.; Coppock, M. B.; Sarkes, D. A.; Finch, A. S.; Agnew, H. D.; et al. A General Synthetic Approach for Designing Epitope Targeted Macrocyclic Peptide Ligands. *Angew. Chem. Int. Ed Engl.* **2015**, *54* (45), 13219–13224.

(19) Farrow, B.; Wong, M.; Malette, J.; Lai, B.; Deyle, K. M.; Das, S.; Nag, A.; Agnew, H. D.; Heath, J. R. Epitope Targeting of Tertiary Protein Structure Enables Target-Guided Synthesis of a Potent In-Cell Inhibitor of Botulinum Neurotoxin. *Angew. Chem. Int. Ed.* **2015**, *54* (24), 7114–7119.

(20) Farrow, B.; Hong, S. A.; Romero, E. C.; Lai, B.; Coppock, M. B.; Deyle, K. M.; Finch, A. S.; Stratis-Cullum, D. N.; Agnew, H. D.; Yang, S.; et al. A Chemically

Synthesized Capture Agent Enables the Selective, Sensitive, and Robust Electrochemical Detection of Anthrax Protective Antigen. *ACS Nano* **2013**, *7* (10), 9452–9460.

(21) Das, S.; Nag, A.; Yu, M. B. *Unpublished Data.*

(22) Verdine, G. L.; Hilinski, G. J. Chapter One - Stapled Peptides for Intracellular Drug Targets. In *Methods in Enzymology*; Wittrup, K. D., Verdine, G. L., Eds.; Academic Press, 2012; Vol. 503, pp 3–33.

(23) Blackwell, H. E.; Grubbs, R. H. Highly Efficient Synthesis of Covalently Cross-Linked Peptide Helices by Ring-Closing Metathesis. *Angew. Chem. Int. Ed.* **1998**, *37* (23), 3281–3284.

(24) Liang, J.; Das, S.; Nag, A.; Yu, M. B. *Unpublished Data.*

(25) Deyle, K. M.; Farrow, B.; Qiao Hee, Y.; Work, J.; Wong, M.; Lai, B.; Umeda, A.; Millward, S. W.; Nag, A.; Das, S.; et al. A Protein-Targeting Strategy Used to Develop a Selective Inhibitor of the E17K Point Mutation in the PH Domain of Akt1. **2015**, *7*, 455.

(26) Umeda, A. *Unpublished Data.*

Chapter 3

A Cocktail of Multi-Epitope Targeted Protein-Catalyzed Capture Agents Against Plasmodium falciparum Histidine-Rich Protein 2

Reproduced in part with permission from:

*S. Das, *A. Nag, **J.X. Liang**, D.N. Bunck, A. Umeda, B. Farrow, M.B. Coppock, D.A. Sarkes, A.S. Finch, H.D. Agnew, S. Pitram, B. Lai, M.B. Yu, A.K. Museth, K.M. Deyle, B. Lepe, F.P. Rodriguez-Rivera, A. McCarthy, B. Alvarez-Villalonga, A. Chen, J. Heath, D.N. Stratis-Cullum, J.R. Heath

Angewandte Chemie International Edition, **2015**, *54(45)*, 13219-13224.

DOI: 10.1002/anie.201505243

3.1 Introduction

As described in Chapters 1 and 2, *P. falciparum* is the most lethal of all malaria species and eradication of this global epidemic is contingent on rapid, accurate, and cost-effective diagnosis as afforded by rapid diagnostic tests (RDTs).[1] *P. falciparum* histidine-rich protein 2 (*Pf*HRP2) is an antigen that is detected by antibody-based malarial RDTs. *Pf*HRP2 is a 30 kDa water soluble protein that is specific to *P. falciparum* infection. It is found in the parasite's food vacuole and cytoplasm. The antigen is also secreted into the erythrocytes of infected human hosts and associated with the cellular membrane.[2] The presence of *Pf*HRP2 in cerebrospinal fluid has also recently been reported.[3] The stability

of the protein makes it an excellent biomarker for the detection of lethal malaria infection.[4] Unfortunately, like other malarial RDTs, antibody-RDTs against *Pf*HRP2 exhibit variable performance which can largely be attributed to the unique nature of the protein.

The *Pf*HRP antigen is encoded by the *pfhrp2* gene, which encodes for 37% alanine (A), 10% aspartic acid (D), and 34% histidine (H) residues. The internal region of PfHRP2 is highly repetitive and contains many patterns of epitopes such as AHHATD, AHHAAD, AHHAHHAAD in its internal region.[5–7] *Pf*HRP2-based RDTs have been shown to perform well at high parasitemia, but exhibit variations in sensitivity at low parasite densities (<200 parasites/μL) which has been correlated with the well documented genetic variation in *Pf*HRP2.[7–9] As many as 80 unique sequences of *Pf*HRP2 per country have been reported and over 400 isolates exist worldwide.[8] Antigen polymorphism has not been shown to greatly affect diagnosis by antibody-based RDTs in clinical malaria infection where parasite load is great. On the other hand, the variable performance of these lateral flow assays at low parasite densities has been linked to the deletion or variations in the number of repeated motifs (Table 3-1) as well as cross-reactivity with the homologous *Pf*HRP3.[5,7] It is possible that monoclonal antibodies in such assays display variations in signal if targeted against these inconsistent repetitive motifs. All *Pf*HRP2 sequences are expected to have conserved Type 1 (AHHAHHVAD) and Type 12 (AHHAAAHHEAATH) repeats. Whilst the number of repeats may vary, Type 2 (AHHAHHAAD) and Type 6 (AHHATD) epitopes within the internal region of *Pf*HRP2 are found in 100% of isolates studied.[7] The use of two antibodies that recognize different epitopes to compensate for reduced numbers of one antigenic motif has been proposed as a strategy for addressing the effect of *Pf*HRP2 polymorphism.[7]

Code	Repeat sequences	Antigens observed	
		PfHRP2	PfHRP3
1	AHHAHHVAD	+	+
2	AHHAHHAAD	+	+
3	AHHAHHAAY	+	−
4	AHH	+	+
5	AHHAHHASD	+	−
6	AHHATD	+	−
7	AHHAAD	+	+
8	AHHAAY	+	−
9	AAY	+	−
10	AHHAAAHHATD	+	−
11	AHN	+	−
12	AHHAAAHHEAATH	+	−
13	AHHASD	+	−
14	AHHAHHATD	+	−
15	AHHAHHAAN	−	+
16	AHHAAN	−	+
17	AHHDG	−	+
18	AHHDD	−	+

Table 3-1. Repeated motifs in the internal region of *Pf*HRP2. Figure reproduced from the literature.[7]

In this chapter, we describe the development of a combination, or cocktail, of synthetic affinity agents known as protein-catalyzed capture agents (PCCs) as alternatives to antibodies for application in a *Pf*HRP2-based RDT.[10] We employ a multi-epitope targeting strategy where we developed five PCCs, one for capture and four for detection, for a system of built-in signal amplification as a means to address antigen polymorphism. With a cocktail of PCCs, any decrease or absence of an epitope bound by one affinity agent can be compensated for through detection of other another epitope. Using epitope targeting in conjunction with *in situ* click screening methodology developed with cyclic one-bead-one-compound (OBOC) peptide libraries,[10] we describe the rapid discovery of PCCs that bind in with nanomolar to picomolar affinities, which is within the range of monoclonal antibodies.[11]

3.2 Materials and Methods

All reagent acquisitions, syntheses, and screening protocols were followed as described in Chapter 2 and the literature.[10] The screening methodology was identical with the exception of the product screens where synthetic epitopes were incubated at 10 μM overnight at 4°C. The screens were developed from 30 to 55 minutes. Recombinant *Pf*HRP2 with a GST tag (*Pf*HRP2-GST, UniProt Sequence: P90582, 98.9% identical to ITG strain) was obtained from CTK Biotech.

3.3 Results and Discussion

3.3.1 A Multi-Epitope Targeting Strategy

The design of a cocktail of affinity agents begins with epitope selection for the construction of synthetic epitopes (SynEps) for screening. In order to develop a set of reagents for *Pf*HRP2 detection, the antigen needs to be specifically pulled down over other proteins in a biological matrix and then detected with PCCs in a manner that can provide reasonable signal. This requires targeting an epitope unique to *Pf*HRP2 for antigen-specific capture and multiple orthogonal epitopes for detection.

One of the many existent primary amino acid sequences of *Pf*HRP2 (UniProt Sequence: P90582, 98.9% identical to ITG strain) is illustrated in Figure 3-1. As shown in Table 3-1, the Type 12 epitope, AHHAAAHHEAATH, is specific to *Pf*HRP2 and is reported to be universally conserved.[7] We constructed a SynEp containing the Type 6 and Type 12 motifs, AHHATDAHHAAAHHEAATHC, which are unique to *Pf*HRP2 for the development of a capture PCC. Four epitopes were targeted for detection: Type 2, AHHAHHAAD; Type 6, AHHATD; Type 2 variant, AHHAADAHHA; and a sequence

near the N-terminus that is expected to be conserved, LHETQAHVD (Figure 3-1). Unlike previous screens where antigens with defined secondary structure were targeted and longer epitopes might be expected to have some degree of static conformation,[10,12–14] unbound *Pf*HRP2 has no defined structure.[15,16] This means that no static or secondary structure can be obtained even with the selection of longer SynEps and these epitopes lack conformational or entropic restrictions.

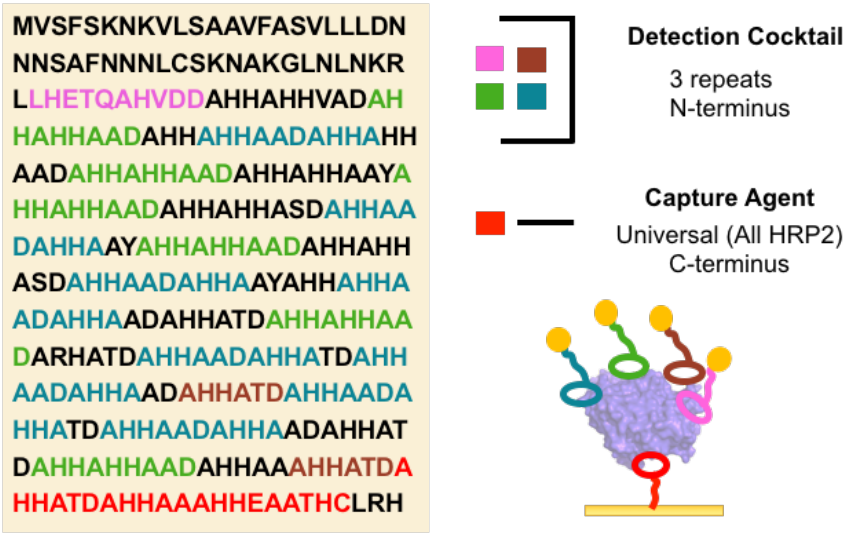

Figure 3-1. A schematic of a cocktail of multi-epitope targeted PCCs against PfHRP2 (cartoon in lower right). Three repeat motifs (AHHATD, AHHAHHAAD, and AHHAADAHHA) as well as a singly occurring epitope (LHETQAHVDD) were targeted for detection. An epitope specific to *Pf*HRP2 (AHHATDAHHAAAHHEAATHC) was targeted for capture.

The SynEps for the five targeted epitopes were synthesized for screening where the epitopes had an alkyne-bearing (Pra) side chain on their C-termini.[10] All cyclic OBOC libraries used for the development of anti-*Pf*HRP2 PCCs were prescreened to remove off-target binders to detection antibodies and human sera. An additional prescreening step was added for detection PCC screens with the Type 12 epitope to minimize cross-reactivity.

3.3.2 Development of a Capture Agent Against *Pf*HRP2

The capture PCC was developed against an *i, i + 7* hydrocarbon stapled library afforded by olefin metathesis (Figure 3-2).[10] Following the standard screening protocols, eight hit sequences were obtained and tested in a sandwich ELISA (data not shown) for binding to the recombinant full PfHRP2-GST protein. The best PCC candidate turned out to be **GSTEWL**, denoted here as **GSTEWL$_{RCM}$** to indicate the stapled backbone. The binding affinity of **GSTEWL$_{RCM}$** was determined by sandwich ELISA (EC_{50}) to be 20 nM, which agreed very well with fluorescence polarization measurements using fluorescein isothiocyanate as a reporter where the K_D was found to be 54.2 nM (Figure 3-3A).

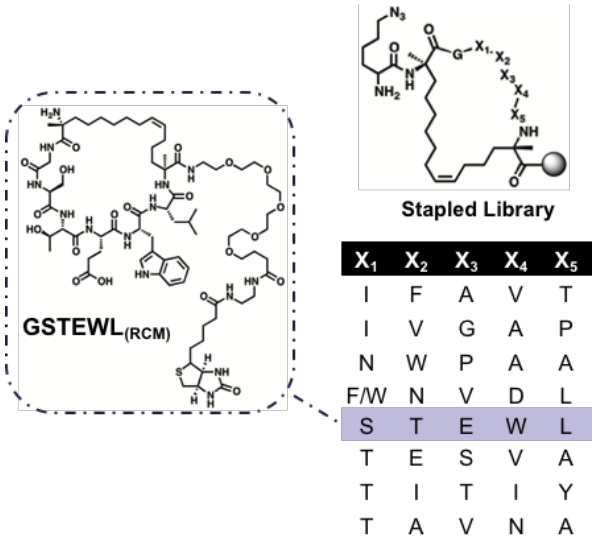

X_1	X_2	X_3	X_4	X_5
I	F	A	V	T
I	V	G	A	P
N	W	P	A	A
F/W	N	V	D	L
S	T	E	W	L
T	E	S	V	A
T	I	T	I	Y
T	A	V	N	A

Figure 3-2. Structure of the best PCC candidate (**GSTEWL$_{RCM}$**) for the capture of *Pf*HRP2 obtained by screening with a OBOC hydrocarbon stapled library.[10] The eight hits from the screen are shown.

As a capture PCC, **GSTEWL$_{RCM}$** proved successful in capture *Pf*HRP2-GST over *Pf*LDH-GST and pure GST, which demonstrated the intended specificity of the affinity agent (Figure 3-3B). Additionally, the capture PCC retained most of its performance in

1% human serum, showing only a 16% decrease, which is indicative of a small amount of off-target interactions (Figure 3-3C).[10]

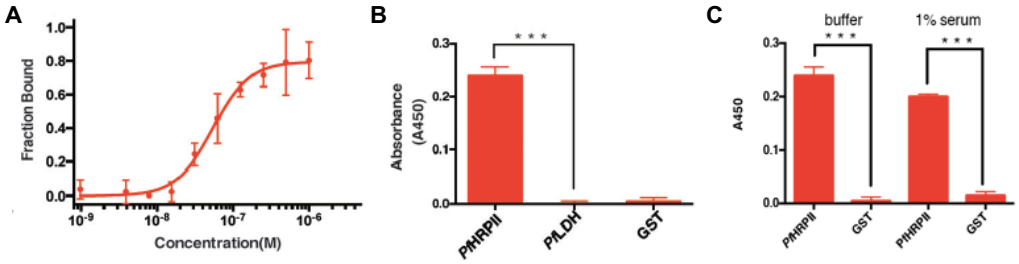

Figure 3-3. (A) The anchor PCC, **GHWSAN$_{RCM}$**, binds to full length recombinant *Pf*HRP2-GST with a K_D = 54.2 nM by fluorescence polarization. (B) **GHWSAN$_{RCM}$** binds selectively to *Pf*HRP2 over *PfLDH* and the GST tag. (C) The binding of **GHWSAN$_{RCM}$** with 25 nM of *Pf*HRP2-GST and the GST tag in 0 or 1% human serum. The signal of the PCC is attenuated by ~16%, indicating little off-target interactions. Figure reproduced with permission.[10]

3.3.3 Development of the Capture and Detection PCCs Against *Pf*HRP2

Four epitopes of various lengths were synthesized as SynEps for screening against pentameric click cyclized OBOC libraries, which afforded a smaller and more rigid backbone than the hydrocarbon stapled library used for the development of the capture PCC. The click cyclized OBOC libraries now also employed the addition of para-fluoro-phenylalanine, adding a 19th amino acid to the combinations possible in the pentameric peptide libraries.[10]

The selection of the para-fluoro-phenylalanine (^{4F}F) amino acid side chain is observed in the hit sequences of the detection PCC candidates screened against the SynEp of the Type 2 epitope variant, AHHAADAHHA, in *Pf*HRP2 (Table 3-2). There is a large degree of homology observed in the hits that include stretches of three tyrosine (Y) residues

in a row and the selection of charge residues such as lysine (K) and arginine (R) in the X_4 and X_5 positions.

X_1	X_2	X_3	X_4	X_5
^{4F}F	Y	Y	G	L
Y	Y	V	N	R
Y	Y	K	L	Y
Y	Y	Y	N	K
Y	Y	G	K	L
Y	Y	Y	K	N
R	^{4F}F	Q	Y	Y
Y	Y	Q	L	L
L	G	Y	Y	Y
Y	Y	Y	N	V
Y	Y	Y	K	S
L	K	Y	Y	Y

Table 3-2. Hits against the Type 12 (AHHAADAHHA) SynEp as sequenced by Edman degradation. The best hit before optimization was **cyYYYNV**.

The hits were synthesized after sequencing and assessed in a sandwich ELISA against the full recombinant *Pf*HRP2-GST protein (Figure 3-4). From these data, the best PCCs contain the YY motif at the N-terminal end of the pentameric sequence, which include **cyYYYKV** and **cyYYYNV**.[17] The macrocyclic ligand, **cyYYYKV**, was selected as the best candidate for a detection PCC against the Type 2 variant.

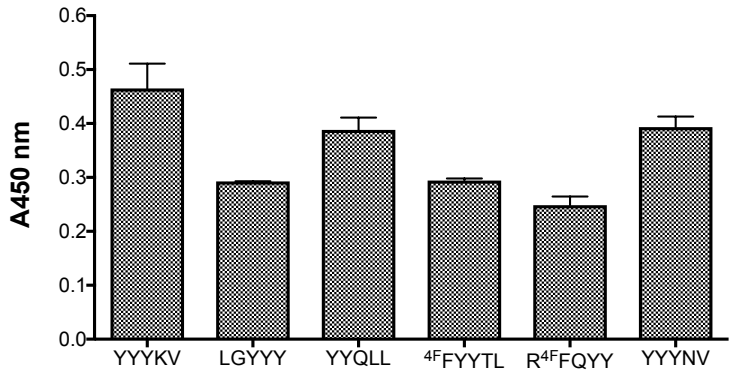

Figure 3-4. A sandwich ELISA comparing AHHAADAHHA-screened hits against the full length recombinant *Pf*HRP2-GST protein.

Recent literature has shown that the substitution of Y residues with ^{4F}F can significantly improve the inherent affinity of a peptide-based affinity agent.[18] We experimented with ^{4F}F substitution in place of Y for **cyYYYKV** as well as K with R and assessed the altered PCCs in a sandwich ELISA (Figure 3-5). Replacement of K with R improved the signal of the detection PCC. Further replacement of Y in the X_2 position with ^{4F}F yielded a superior PCC, **cyY^{4F}FYRV** (Figure 3-6).

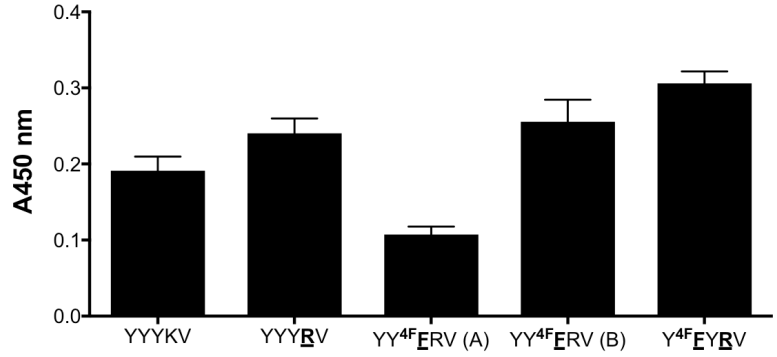

Figure 3-5. Sandwich ELISA assessment of variants of **cyYYYKV** binding to full length *Pf*HRP2-GST after amino acid substitutions.[17]

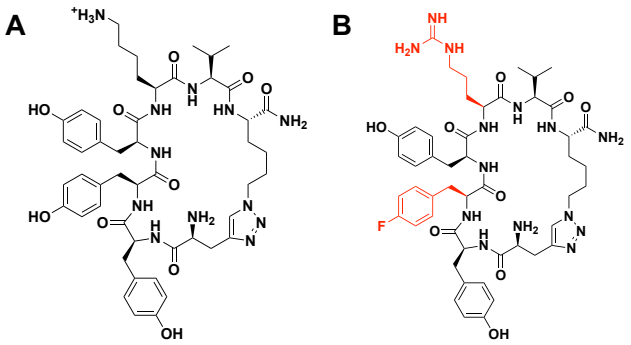

Figure 3-6. (A) The **cyYYYKV** PCC as obtained from sequencing of hits. (B) Structure of the improved second-generation PCC, **cyY^{4F}FYRV**, after two amino acid substitutions.

The binding affinity (EC_{50}) of **cyY^{4F}FYRV** for *Pf*LDH-GST was measured in a sandwich ELISA and found to be 540 pM (Figure 3-7A). The performance of the PCC and the PCC with *Pf*HRP2-GST was also assessed in a sandwich ELISA in human serum (Figure 3-7B). In the absence of protein, the PCC demonstrates some non-specific interactions with the detection antibody against the GST tag, which may be attributed to either the antibody of the PCC. In the presence of 1% human serum, **cyY^{4F}FYRV** maintains over 80% of its performance. At 5% of serum, the performance of **cyY^{4F}FYRV** drops to almost 50%, indicating competitive off-target interactions when the concentration of proteins increases.[17]

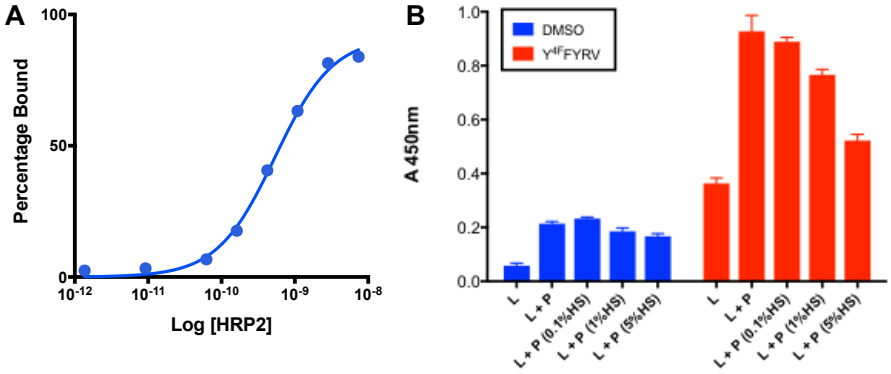

Figure 3-7. (A) The EC_{50} of **cyY^{4F}FYRV** was determined to be 540 pM by sandwich ELISA.[10] (B) The specific capture of *Pf*LDH-GST by **cyY^{4F}FYRV** in 0 to 5% human

serum is demonstrated. At higher human serum concentrations, the ligand performance is diminished by ~ 50% by off-target interactions. DMSO is used as a control for protein.

The same screening methodology and ELISAs were used to obtain a detection PCC against the SynEp of the Type 2 epitope, AHHAHHAAD.[10] The best macrocyclic hit obtained from the click cyclized OBOC library was **cyYKYYR**, which was synthesized as both a monomer and a dimer[19] (Figure 3-8). Due to the high molar loading on the resins used for peptide synthesis on solid support, peptide dimers can spontaneously form as a result of intramolecular cyclization. Thus, both versions of the PCC were assayed.

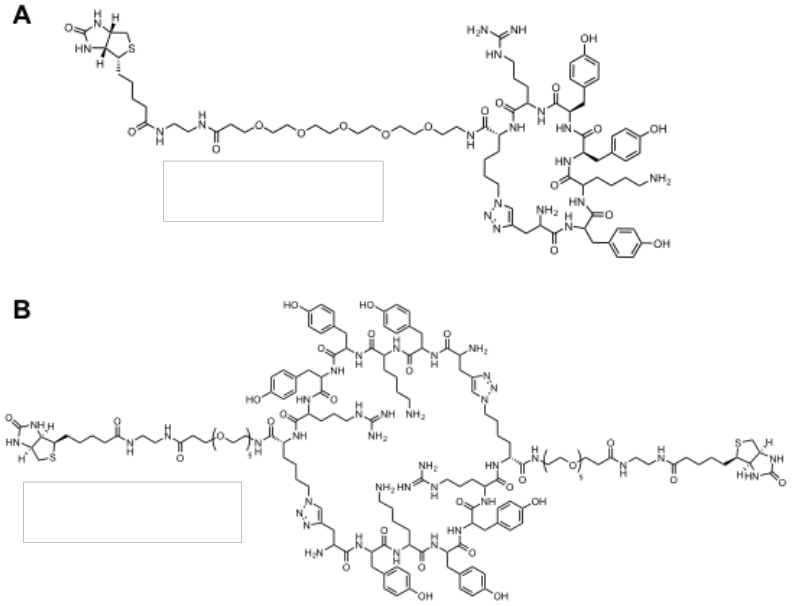

Figure 3-8. (A) Chemical structure of the **cyYKYYR** monomer, developed against the Type 12 epitope, AHHAHHAAD. (B) Chemical structure of the **cyYKYYR** dimer[19] that formed through intramolecular cyclization. Both PCCs are shown with biotin tags separated by polyethylene glycol linkers.

The binding affinities of the monomer and dimer versions of **cyYKYYR** were determined using standard sandwich ELISA (Figure 3-9). From a single generation screen without modification of any amino acids, the affinity of **cyYKYYR** against *Pf*LDH-GST

was found to be 218 nM.[10] Dimerization of **cyYKYYR** by intramolecular cyclization improved the affinity by over five-fold, to 40.7 nM.[19] However, single point measurements demonstrate that whilst the affinity is drastically improved, the signal of the **cyYKYYR** dimer is only improved over the monomer by two-fold (Figure 3-9B). The **cyYKYYR** dimer also exhibits more off-target interactions, as evidenced by single point assays in human serum. With increasing concentrations of human serum, the signal of **cyYKYYR** dimer is attenuated in greater magnitude than that of **cyYKYYR** monomer. In this case, whilst **cyYKYYR** dimer shows greater affinity and better signal, **cyYKYYR** monomer might be a more ideal ligand for minimal cross-reactivity in performance.

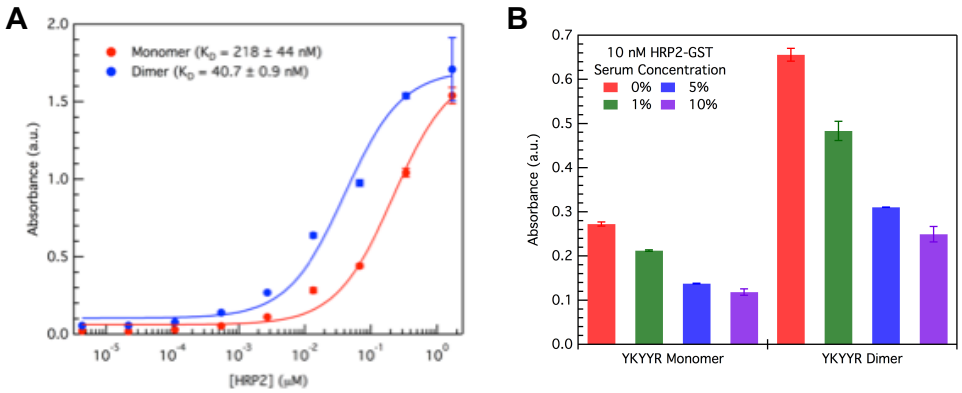

Figure 3-9. (A) The binding affinities of **cyYKYYR** monomer and dimer to the full *Pf*LDH-GST protein determined by sandwich ELISA are 218 nM and 40.7 nM, respectively. (B) The **cyYKYYR** dimer shows more rapid decline in signal, i.e., nonspecific interactions, than the monomer in human serum.[19]

The last PCC successfully developed was against the N-terminal epitope, LHETQAHVDD. Like the other screens, the hits obtained from *in situ* click screening with a macrocyclic OBOC peptide library bear a degree of homolog (Table 3-3). The candidate PCCs contain a preponderance of R residues, though less Y than the PCCs against the Type 2 variations. From these hits, the best PCC against LHETGAHVDD was

determined via single point sandwich ELISA to be **cyRYKHY**. The EC_{50} of **cyRYKHY** by sandwich ELISA was found to be 4.1 nM without any alteration to the chemical structure (Figure 3-10A).[10] We sought to improve the affinity of be **cyRYKHY** through amino acid substitutions as performed on **cyY^{4F}FYRV**. The Y in the X_5 position of be **cyRYKHY** was substituted to ^{4F}F and para-cyano-phenylalanine, ^{CN}F. However, single point assays showed that the ^{4F}F substitution had negligible effect on the performance of this PCC. Replacement of the Y at X_5 with ^{CN}F actually abolished over 50% of PCC performance and increased non-specific interactions. However, this study did show that the Y residue at X_5 played an essential role in recognition and that the cyano group may have contributed electron donation through resonance that significantly impacted the electron density of the phenyl ring.

X_1	X_2	X_3	X_4	X_5
R	Y	K/L	H	Y
R	K/L	Y	Y	V
A	K	L	L	L
R	R	Q	S	R
F	Q	R	R	F
K	F	K	L	Y
P	K/L	R	T/G	F
S	Y	K	Y	Y
A	Y	Y	K/L	K/L

Table 3-3. Candidate PCC hits against the N-terminal, LHETQAHVDD. The best hit was **cyRYKHY**.

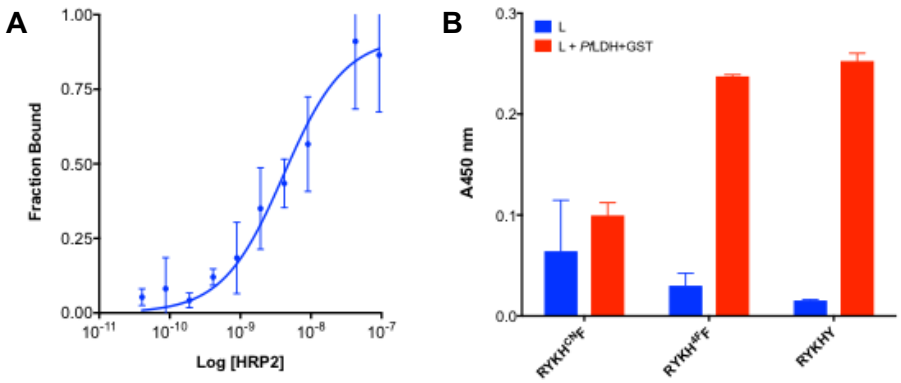

Figure 3-10. (A) The EC_{50} of **cyRYKHY** obtained was 4.1 nM. (B) The performance of **cyRYKHY** was dampened by replacement of the Y residue at X_5.

3.3.4 A Limitation to Epitope Targeting

Whilst high affinity PCCs were successfully developed for the C-terminal, N-terminal, and Type 2 variant epitopes, no affinity agent was obtained against the Type 6 motif, AHHATD. Compared to the other SynEps, AHHATD is extremely short and bears only six amino acids. From a preliminary sandwich ELISA assay (data not shown), the best hit was **cyPWEVH** (Figure 3-11). However, it was not feasible to obtain a binding curve for this PCC. A comparison of **cyPWEVH** with other PCCs demonstrated its low signal and inferior relative performance (Figure 3-12).

A

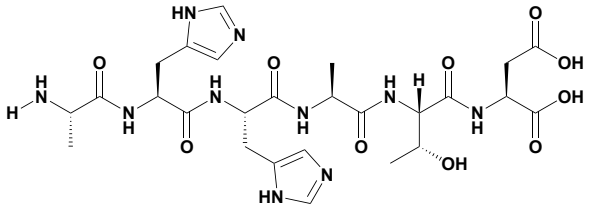

B

S	D	V	W	A
T	A	A	W	N
G	A	L	W	A
N	D	Y	W	A
P	W	E	V	H
T	G	Q	W	A
A	D	A	T	W

Figure 3-11. (A) Chemical structure of the Type 6 epitope, AHHATD. (B) List of hits against the Type 6 SynEp where the best candidate, **cyPWEVH**, is highlighted.

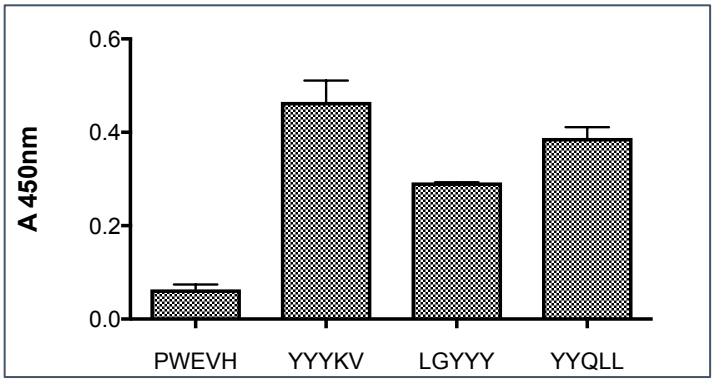

Figure 3-12. Sandwich ELISA comparing the performance of **cyPWEVH** against other PCCs developed against *Pf*HRP2.

These data demonstrate that there are limitations to the epitope targeting strategy for the rapid discovery of affinity agents. All the other SynEps constructed against malarial epitopes within this thesis have been a minimum of ten amino acids in length. The failed development of a suitable PCC against AHHATD suggests that six amino acids is too short in length and may not provide enough contacts for the recognition events that result in tight binding. If we consider the pentameric structure presented by the OBOC library, the macrocyclic backbone likely does not present functional groups in a linear manner for maximal contact with short epitopes. A further hypothesis, which has not yet been tested, is that the residues present in the SynEp may be important. For example, the inclusions of more hydrophobic residues or charged side chains may result in more π-stacking or electrostatic bonding interactions, respectively.

3.3.5 Assessment of a Multi-Epitope Targeted Cocktail of PCCs

In the final study, several of the PCCs were combined to determine their efficiency at binding to *Pf*HRP2-GST. A sandwich ELISA was performed where the performance of

the single PCCs, **GSTEWL$_{RCM}$**, **cyY^{4F}FYRV**, and **cyYKYYR** was compared to dual mixtures.[20] From the data provided in Figure 3-13, the performance of **cyYKYYR** on its own stands out. Whilst **cyYKYYR** displays the most off-target interactions as evidenced by the high signal in the DMSO control in the absent of protein, it most successfully binds to *Pf*HRP2-GST. Despite the higher binding affinity of **cyY^{4F}FYRV**, this PCC also underperforms in *Pf*HRP2-GST capture relative to **cyYKYYR**. Of the dual ligand combinations, the pairing of **cyY^{4F}FYRV** and **cyYKYYR** is observed as the best performing set followed by **cyYKYYR** with **GSTEWL$_{RCM}$**. Overall, the strength of the best performing cocktail duos seems to be largely dominated by the superior ability of **cyYKYYR** to bind *Pf*HRP2-GST. We can conclude that the PCCs can also stand on their own in pulling down *Pf*HRP2-GST as the combinations do not significantly outperform their constituents.

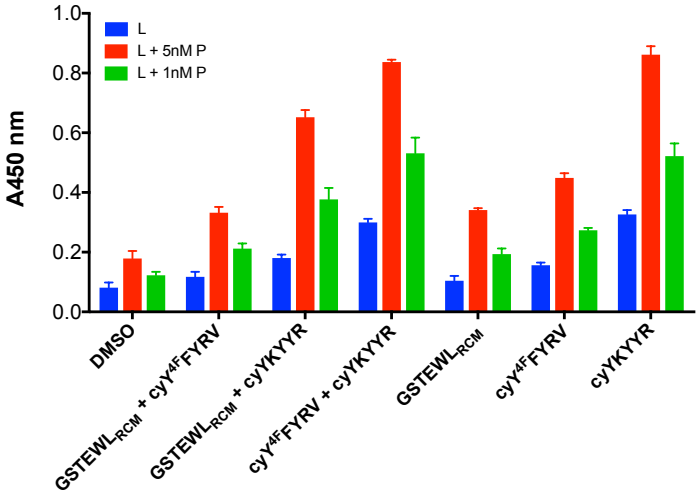

Figure 3-13. Sandwich ELISA comparing combinations of the PCCs with the performance of the standalone affinity agents at two low-*Pf*HRP2-GST concentrations.

An important consideration to be made is that the cocktail developed here was tested on just a single *Pf*HRP2 antigen so the performance of this particular PCC

combination cannot be generalized across all variants of this protein. As shown in Figure 3-1, this particular *Pf*HRP2 has a lot of AHHAHHAAD, or Type 2, repeat motifs which may contribute to the high signal of **cyYKYYR**. The preponderance of Type 2 variants may also contribute to the high affinities of **cyYKYYR** and **cyY^{4F}FYRV**, where binding interactions between PCC and *Pf*HRP2 may be additive. In the case of the single occurring epitopes, such as the N-terminal and C-terminal motifs, the binding affinity may reflect the true strength of recognition rather than avidity effects.

3.4 Conclusion

A cocktail of protein-catalyzed capture agents was developed to simultaneously target multiple regions in a single malarial protein biomarker*, P. falciparum* HRP2. This strategy was developed to address variations in sensitivity of antibody-based RDTs that detect the *Pf*HRP2 biomarker. Antibodies typically target a single epitope and may exhibit variations in signal with the absence or variation of the target region. Through simultaneously targeting multiple epitopes, we provide a means for built-in signal amplification and compensation for absent peptide motifs. The PCCs developed have affinities in the high picomolar to low nanomolar range, similar to that of monoclonal antibodies. We demonstrate that the PCCs can function as a cocktail of reagents whilst retaining excellent performance in *Pf*HRP2 capture as standalone agents. This work stands as a generalizable strategy for the successful development of affinity agents against a polymorphic and unstructured protein target.

3.5 Acknowledgments

The work described in this chapter was performed by JingXin Liang in collaboration with Arundhati Nag, Samir Das, David Bunck, and John Heath. Arundhati Nag and Samir Das developed the PCC against the C-terminus of *Pf*HRP2. JingXin Liang conceived of the multiple-epitope targeting strategy and developed PCCs against the N-terminus and internal repeat motif, AHHAADAHHA. David Bunck developed the PCC against AHHAHHAAD. John Heath participated in the screening process for PCCs. We received aid in the form of proteins and meaningful academic discussions in collaboration with the Gates foundation and PATH, Seattle.

References

(1) Moody, A. Rapid Diagnostic Tests for Malaria Parasites. *Clin. Microbiol. Rev.* **2002**, *15* (1), 66–78.

(2) Howard, R. J.; Uni, S.; Aikawa, M.; Aley, S. B.; Leech, J. H.; Lew, A. M.; Wellems, T. E.; Rener, J.; Taylor, D. W. Secretion of a Malaria Histidine Rich Protein (Pf HRP II) from Plasmodium Falciparum- Infected Erythrocytes. *J Cell Biol* **1986**, *103*.

(3) Pal, P.; Daniels, B. P.; Oskman, A.; Diamond, M. S.; Klein, R. S.; Goldberg, D. E. Plasmodium Falciparum Histidine-Rich Protein II Compromises Brain Endothelial Barriers and May Promote Cerebral Malaria Pathogenesis. *mBio* **2016**, *7* (3).

(4) Dondorp, A. M.; Desakorn, V.; Pongtavornpinyo, W.; Sahassananda, D.; Silamut, K.; Chotivanich, K.; Newton, P. N.; Pitisuttithum, P.; Smithyman, A. M.; White, N. J.; et al. Estimation of the Total Parasite Biomass in Acute Falciparum Malaria from Plasma PfHRP2. *PLoS Med* **2005**, *2*.

(5) Rock, E. P.; Marsh, K.; Saul, A. J.; Wellems, T. E.; Taylor, D. W.; Maloy, W. L.; Howard, R. J. Comparative Analysis of the Plasmodium Falciparum Histidine Rich Proteins HRP-I, HRP-II, and HRP-III in Malaria Parasites of Diverse Origin. *Parasitology* **1987**, *95*.

(6) Panton, L. J.; McPhie, P.; Maloy, W. L.; Wellems, T. E.; Taylor, D. W.; Howard, R. J. Purification and Partial Characterization of an Unusual Protein of Plasmodium Falciparum: Histidine Rich Protein II. *Mol Biochem Parasitol* **1989**, *35*.

(7) Baker, J.; McCarthy, J.; Gatton, M.; Kyle, D. E.; Belizario, V.; Luchavez, J.; Bell, D.; Cheng, Q. Genetic Diversity of Plasmodium Falciparum Histidine Rich Protein 2 (PfHRP2) and Its Effect on the Performance of PfHRP2-Based Rapid Diagnostic Tests. *J Infect Dis* **2005**, *192*.

(8) Baker, J.; Ho, M.-F.; Pelecanos, A.; Gatton, M.; Chen, N.; Abdullah, S.; Albertini, A.; Ariey, F.; Barnwell, J.; Bell, D.; et al. Global Sequence Variation in the Histidine-Rich Proteins 2 and 3 of Plasmodium Falciparum: Implications for the Performance of Malaria Rapid Diagnostic Tests. *Malar. J.* **2010**, *9* (1), 129.

(9) Kumar, N.; Singh, J. P.; Pande, V.; Mishra, N.; Srivastava, B.; Kapoor, R.; Valecha, N.; Anvikar, A. R. Genetic Variation in Histidine Rich Proteins among Indian Plasmodium Falciparum Population: Possible Cause of Variable Sensitivity of Malaria Rapid Diagnostic Tests. *Malar. J.* **2012**, *11*, 298–298.

(10) Das, S.; Nag, A.; Liang, J.; Bunck, D. N.; Umeda, A.; Farrow, B.; Coppock, M. B.; Sarkes, D. A.; Finch, A. S.; Agnew, H. D.; et al. A General Synthetic Approach for Designing Epitope Targeted Macrocyclic Peptide Ligands. *Angew. Chem. Int. Ed Engl.* **2015**, *54* (45), 13219–13224.

(11) Landry, J. P.; Ke, Y.; Yu, G.-L.; Zhu, X. D. Measuring Affinity Constants of 1,450 Monoclonal Antibodies to Peptide Targets with a Microarray-Based Label-Free Assay Platform. *J. Immunol. Methods* **2015**, *417*, 86–96.

(12) Farrow, B.; Wong, M.; Malette, J.; Lai, B.; Deyle, K. M.; Das, S.; Nag, A.; Agnew, H. D.; Heath, J. R. Epitope Targeting of Tertiary Protein Structure Enables Target-Guided Synthesis of a Potent In-Cell Inhibitor of Botulinum Neurotoxin. *Angew. Chem. Int. Ed.* **2015**, *54* (24), 7114–7119.

(13) Deyle, K. M. Development of Protein-Catalyzed Capture (PCC) Agents with Application Ot the Specific Targeting of the E17K Point Mutation of Akt1, California Institute of Technology, 2014.

(14) Millward, S. W.; Henning, R. K.; Kwong, G. A.; Pitram, S.; Agnew, H. D.; Deyle, K. M.; Nag, A.; Hein, J.; Lee, S. S.; Lim, J.; et al. Iterative in Situ Click Chemistry Assembles a Branched Capture Agent and Allosteric Inhibitor for Akt1. *J. Am. Chem. Soc.* **2011**, *133* (45), 18280–18288.

(15) Schneider, E. L.; Marletta, M. A. Heme Binding to the Histidine-Rich Protein II from Plasmodium Falciparum. *Biochemistry (Mosc.)* **2005**, *44* (3), 979–986.

(16) Lynn, A.; Chandra, S.; Malhotra, P.; Chauhan, V. S. Heme Binding and Polymerization by Plasmodium Falciparum Histidine Rich Protein II: Influence of PH on Activity and Conformation. *FEBS Lett.* **1999**, *459* (2), 267–271.

(17) Liang, J. Unpublished Data.

(18) Middendorp, S. J.; Wilbs, J.; Quarroz, C.; Calzavarini, S.; Angelillo-Scherrer, A.; Heinis, C. Peptide Macrocycle Inhibitor of Coagulation Factor XII with Subnanomolar Affinity and High Target Selectivity. *J. Med. Chem.* **2017**, *60* (3), 1151–1158.

(19) Bunck, D. N. Unpublished Data.

(20) Liang, J.; Bunck, D. N.; Mishra, A.; Heath, J. R. Inhibition of Heme Sequestration of Histidine-Rich Protein 2 Using Multiple Epitope-Targeted Peptides. *Submitted. August 2017*.

Chapter 4

A Linker Screen for Bivalent Ligands in an Unstructured Protein Landscape Using *In Situ* Click Chemistry

4.1 Introduction

Epitope targeted *in situ* click chemistry has allowed for the rapid discovery of high affinity ligands, or protein-catalyzed capture agents (PCCs), in a single generation high throughout screen. Developed within the Heath lab, high-binding and selective agents of molecular recognition are discovered by screening against one-bead-one-compound (OBOC) macrocyclic peptide libraries. As detailed in Chapters 2 and 3, the use of macrocyclic over linear peptide libraries[1] can easily generate picomolar and nanomolar binders against both structured and unstructured protein targets without the need for secondary or tertiary ligands. However, prior work on linear peptidomimetic PCCs has demonstrated the utility of expanding monovalent ligands into bi- or triligand compounds to drastically improve affinity.[2–7]

As described in Chapter 2, the expansion of primary, or anchor, PCCs into multi-ligand molecules is accomplished in a step-wise fashion. The anchor PCC, fitted with a click handle, is incubated against the full protein and allowed to recognize, i.e., bind, to the epitope against which it was first developed. The anchor:protein complex is then subjected to a prescreened OBOC library that bears the complementary click handle to that on the anchor. Elements of the OBOC library that bind tightly and in close proximity to the

primary ligand facilitate the formation of a click product which is then detected, sequenced, and tested.[2] This process can be iterated to produce additional ligands.

In general, the expansion of an anchor PCC into a multivalent ligand has relied on a static and defined protein structure. The tertiary structure of the protein provides a solid basis upon which to guide the self-assemblage of secondary and tertiary ligand arms, i.e., target-guided click. Within our lab, we have demonstrated the use of the tertiary structure of botulinum neurotoxin to assemble a biligand.[6] In this work, two unique epitopes were targeted for the development of two distinct PCCs. Instead of screening for a secondary ligand, the two anchor PCCs were linked by screening with a linker library of varying length, i.e., the protein target selected its own ideal ligator between PCCs bound to adjacent sites. *In situ* click screening methodology was also employed in selection of the ideal linker.[6]

Thus far, the development of biligands and triligands within the Heath lab has relied on a defined, tertiary structure. In this chapter, we explore whether this screening methodology can be applied to an intrinsically disordered protein, *P. falciparum* histidine-rich protein 2 (*Pf*HRP2), which exhibits no secondary structure when it is not sequestering heme molecules in its native state.[8,9] We use the PCCs developed within Chapter 3[1] against four distinct epitopes in *Pf*HRP2 as anchors for an *in situ* click chemistry linker screen using OBOC libraries. We find that the *Pf*HRP2 antigen structure selects for a specific length of semi-rigid ligation and apply these linkers towards the development of biligand PCC structures.

4.2 Materials and Methods

General Information. All materials for assays, solid phase peptide synthesis, and screening were obtained by vendors described in Chapter 2. The additional unnatural amino acid used within this study, aminoisobutyric acid (Aib), was obtained from Sigma-Aldrich. In the case of proline and leucine, the D-stereochemistry amino acids were used for library synthesis. The protocols for immunoassay, chemical synthesis, compound characterization, and purification are identical to general procedures provided in previous chapters.

OBOC Linker Library. The anchor PCCs **cyYKYYR** and **cyY^{4F}FYRV** were each synthesized on 100 mg scale on TentaGel resin (Rapp Polymere, 0.29 mmol/g) separated from the bead by a methionine residue. Successful synthesis and click cyclization of the anchor PCCs were confirmed by Edman degradation. Split-and-mix synthesis was employed to generate a linker region by successive couplings of D-proline, glycine, D-leucine, and aminoisobutyric acid. At each of the five coupling step, ¼ of the resin was not treated with coupling solutions to generate linkers that varied from 0 to 5 amino acids in length. An alkyne click handle was appended to the N-terminus of the variable linker region.

Linker Screens. The standard binding buffer as described for screening in Chapter 2 was used for the linker screens. The OBOC linker libraries were precleared against the detection antibody (Antibiotin-AP) and all four anchor PCCs. Full recombinant *Pf*HRP2 protein without a fusion tag (PATH, ITF strain) was used as the target to guide the linker

product screen. Following full washing and stripping of the OBOC library after the prescreen, the library was blocked in 1% BSA in binding buffer. For each separate screen, the beads were incubated with 5 μM of the desired anchor and 100 nM of recombinant *Pf*HRP2 protein for 6 hours at ambient temperature. The beads were washed 3X in standard buffer, 1 hour with guanidine hydrochloride (pH 2), and 10X with standard buffer. The library was blocked overnight in 1% BSA in binding buffer at 4°C. Afterwards, the library was incubated with 1:10000 antibiotin-AP in standard buffer for 1 hour at ambient temperature. The beads were then washed 3X with standard buffer, 3 x 15 minutes with high salt TBS, 1 hour with high salt TBS, 3X in BCIP buffer, and developed with BCIP/ NBT for a maximum of 30 minutes. The hits (purple beads) were isolated, washed, and sequenced via Edman degradation to identify hits.

Synthesis, Purification, and Characterization of Fmoc-L-Pra-OtBu. The alkyne bearing unnatural amino acid, Fmoc-L-propargylglycine-OH, was protected on the C-terminus with an OtBu by treatment with t-But-2,2,2-trichloroacetimidate in dichloromethane. The reaction was heated up to 55°C and refluxed for five hours (Scheme 1). The resultant molecule, herein termed Fmoc-L-Pra-OtBu, was extracted with saturated $NaHCO_3$, followed by an extraction with brine. The compound was dried with the addition of anhydrous $MgCl_2$. The crude molecule was concentrated under vacuum.

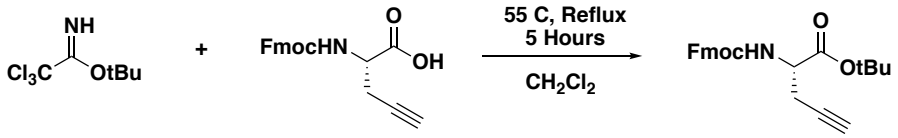

Scheme 1. Addition of the OtBu protecting group onto Fmoc-L-Propargylglycine-OH.

Fmoc-L-Pra-OtBu was purified by silica gel chromagraphy, using a mobile phase of 10:1 hexanes:ethyl acetate, and monitored with thin layer chromatography. Spots with the product were identified by UV absorption at 254 nm. The product fractions were concentrated under vacuum and characterized by NMR spectroscopy by addition of a methyl peak in ^{1}H spectrum.

4.3 Results and Discussion

4.3.1 Target-Guided Linker Screens

To identify the ideal linker between *Pf*HRP2-targed PCCs as described in Chapter 3, high throughput linker screens were performed with the full non-tagged *PfHRP2* antigen.[10] As illustrated in Figure 4-1, the library had one static region, which was an anti-*Pf*HRP2 PCC, and a variable linker region. Two anchor PCCs were synthesized on bead: **cyYKYYR** and **cyY^{4F}FYRV**, which were developed against Type 2 epitope variants.[1,11] These libraries bore alkyne (Pra) click handles at their N-termini. These libraries were prescreened against off-target interactions. Three of the anti-PfHRP2 PCCs were synthesized and utilized off-bead: **cyRYKHY** (N-terminal targeted PCC), **GWNVDL$_{RCM}$** (another hit against the C-terminus of *Pf*HRP2 from Chapter 3), and **cyYKYYR** (Type 2 targeted PCC). These anchor PCCs were appended with azide (Az4) click handles on their C-termini which were complementary to those on the linker libraries. The anchor PCCs in solution were pre-incubated with the full *Pf*HRP2 protein. The anchor:protein complex was then screened against the OBOC library bearing another PCC and the variable linker region (Figure 4-2). Four amino acids were selected (D-proline, glycine, D-leucine, and

aminoisobutyric acid) to create linkers that were semi-rigid or barriers against complete free rotation around the amide bonds.

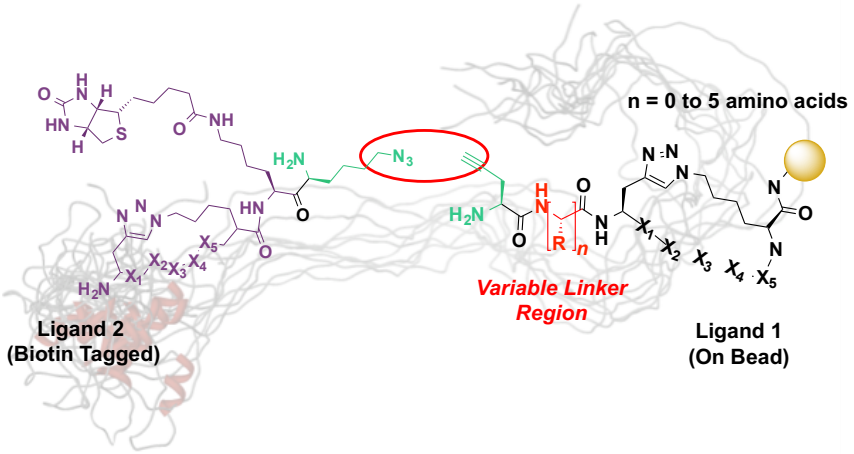

Figure 4-1. Schematic for linker screen between two ligands binding to distal regions on *Pf*HRP2. One ligand is synthesized on bead with the variable linker library, appended with an alkyne (Pra) click handle. The second ligand, bearing the azide (Az4) click handle, is prepared in solution and incubated with the OBOC library.

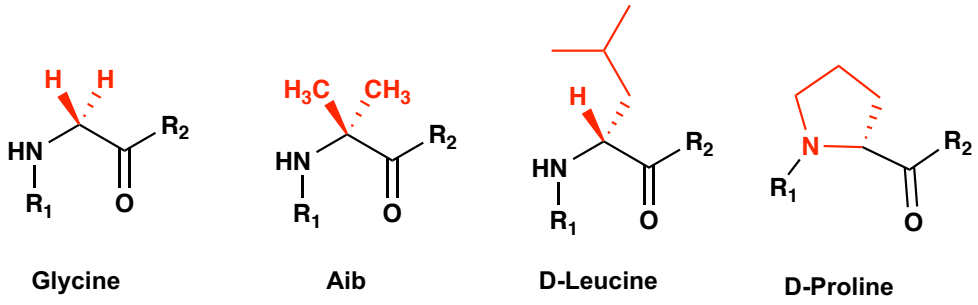

Figure 4-2. Amino acids used in the on-bead variable linker region. Aminoisobutyric (Aib) acid is an unnaturally occurring side chain.

The results of the linker screen are shown in Figure 4-3. Since only four different amino acids are used in the screen, no conclusive argument can be made for sequence or residue homology. However, it is important to note that despite varying linker lengths and an intrinsically disordered protein structure, the full *Pf*HRP2 antigen has selected for

linkers that are four amino acids in length. The four amino acid length encompasses over 55% of the total hits.

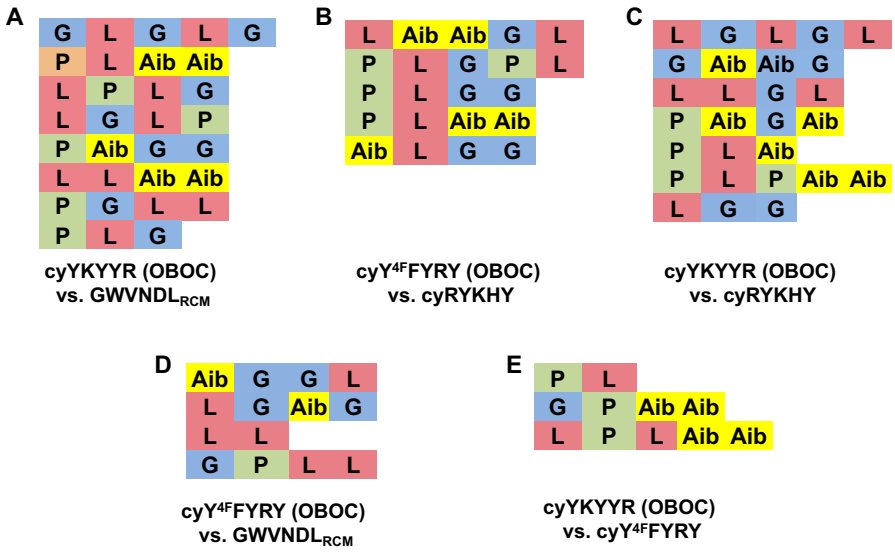

Figure 4-3. Sequenced hits obtained from the linker screens.

4.3.2 Comparison of *Pf*HRP2 Biligands to Anchor PCCs

The biligands were synthesized with the PCC pairs as indicated in Figure 4-3 and the variable linkers. A representative chemical structure of the biligand **cyY^{4F}FYRV – p-l-Aib – cyYKYYR** is shown in Figure 4-4. All the biligands were constructed in this manner by synthesis of the constant PCC from the library on solid support, followed by the linker amino acids, and the coupling of Fmoc-L-Pra-OtBu. The traizole was assembled by clicking an azide bearing amino acid with the alkyne (Pra) group. The synthesis of the secondary ligand was finished before the entire biligand was cleaved off solid support, purified, and quantified for immunoassay.

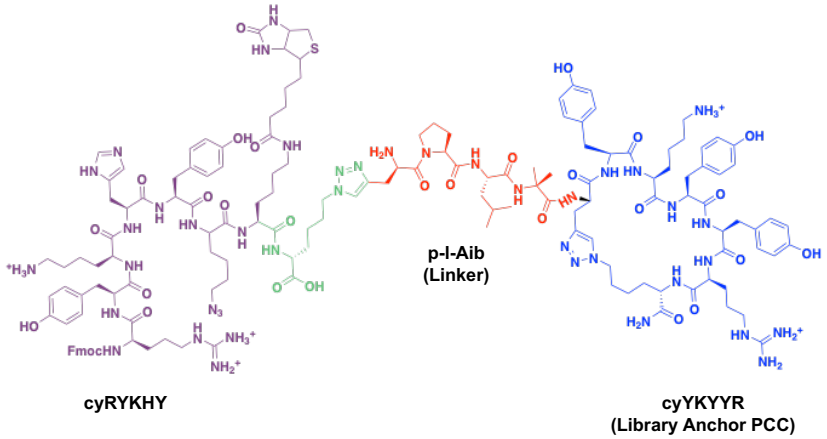

Figure 4-4. Representative chemical structure of all biligands in this study. Biligand are synthesized on solid support from the C- to N-terminus. The biligands are composed of two anchor PCCs against *Pf*HRP2, a triazole, and a linker region.

A set of biligands containing PCCs developed against the Type 2 variants in *Pf*HRP2 and the N-terminal epitope, LHETQAHVDD, were synthesized following the schematic in Figure 4-4. Their linker regions comprised four to five amino acids in length. The biligands were **cyY^{4F}FYRV - p l Aib Aib – cyRYKHY**, **cyYKYYR - l g l g l – cyRYKHY**, and **cyYKYYR - p Aib p Aib – cyRYKHY**. These ligands were compared to their anchor constituents in a sandwich ELISA (Figure 4-5). As observed in the results, only one biligand, **cyY^{4F}FYRV - p l Aib Aib – cyRYKHY**, showed significant signal in binding *Pf*HRP2-GST in the assay. The two other biligands perform poorly. Despite the high signal, however, **cyY^{4F}FYRV - p l Aib Aib – cyRYKHY** displays a large degree of non-specific binding as observed in the lane containing no protein. We hypothesize that the extreme non-specific binding may be due to the hydrophobic nature of the linker region in addition to any off-target interactions from the constituent PCCs. All three of these biligands were discarded as viable candidates and further molecules were synthesized for testing.

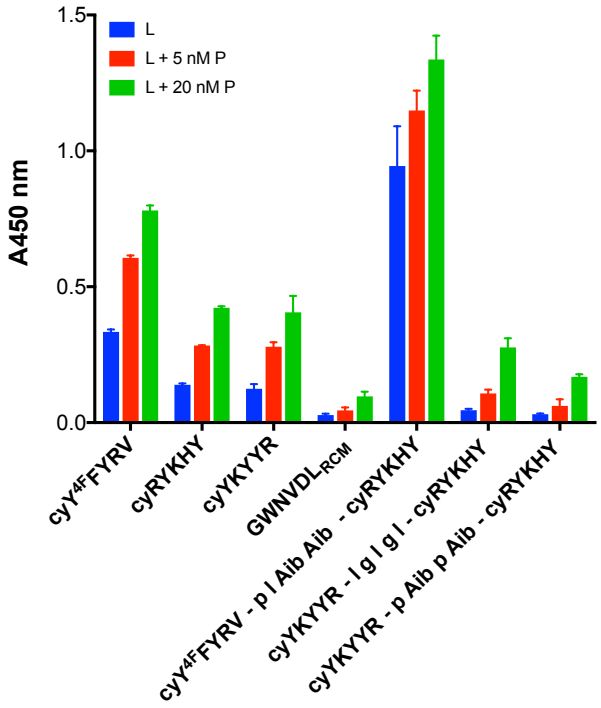

Figure 4-5. Sandwich ELISA comparing several biligands obtained from the linker screen to their constituents.

4.3.3 Comparison of Dual PCC Cocktails to Biligands

Several other biligands obtained from the linker screen were synthesized, but demonstrated far too much nonspecific binding in the absence of protein to reasonably justify their application as capture agents against *Pf*HRP2.[10] Attempts to attain binding curves to assess the EC_{50} values of the biligands were not successful. Due to the high degree of non-specific binding presented by these biligands, it was difficult to obtain sufficient signal after background subtraction to have saturated isotherms that allowed for fitting of EC_{50} values (data not shown).

Instead, we investigated the assemblage of biligands through ligation with a polyethylene glycol unit to determine whether it was possible to increase performance without introducing more off-target interactions. A biligand was developed by ligating

two **cyYKYYR** molecules,[12] the anchor PCC, which proved to provide the greatest signal in the capture of *Pf*HRP2-GST as demonstrated in Chapter 3 (Figure 4-6).

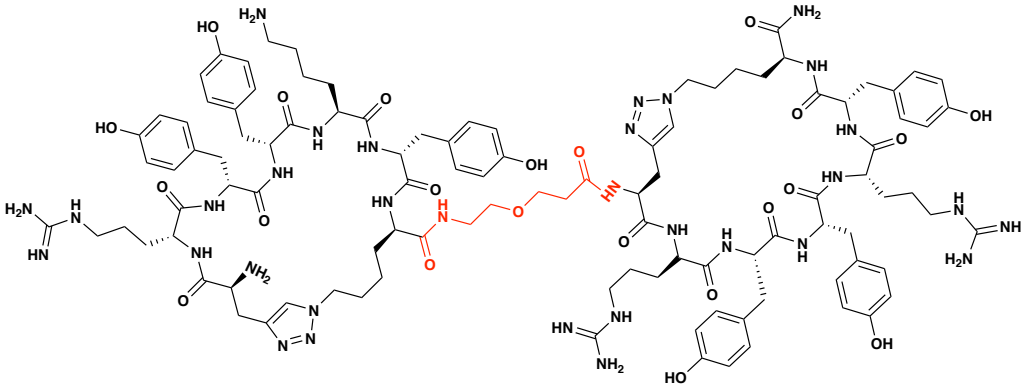

Figure 4-6. Two equivalents of **cyYKYYR** are ligated by a polyethylene glycol unit.[12]

The ligated dimer, **cyYKYYR-Peg1-cyYKYYR**, was tested in an ELISA assay against dual PCC cocktails and a linker screened biligand, **cyY^{4F}FYRV – p l g p l – cyRYKHY** (Figure 4-7). Relative to the linker obtained from the linker screen, **cyYKYYR-Peg1-cyYKYYR** is a superior performer. The non-specific interactions between the two biligands are similar when examining the protein-free condition of the assay. However, **cyYKYYR-Peg1-cyYKYYR** exhibits significantly greater signal for *Pf*HRP2-GST binding. Relative to any other biligand, combination, or single PCC in this assay, **cyYKYYR-Peg1-cyYKYYR** also retains good performance in human serum.

From these data, it was concluded that biligands created by Peg1 ligation might afford better performance than using the amino acids from the linker screen. Based on the success of **cyYKYYR-Peg1-cyYKYYR**, a second biligand was constructed containing the two anchor PCCs developed against the Type 2 epitope variants, **cyYKYYR-Peg1-cyY^{4F}FYRV** (Figure 4-8).[12] As described in Chapter 5, **cyYKYYR-Peg1-cyY^{4F}FYRV**

displays nanomolar binding affinity to *Pf*HRP2-GST and demonstrates a functional application in attenuating the role of this antigen in heme sequestration.

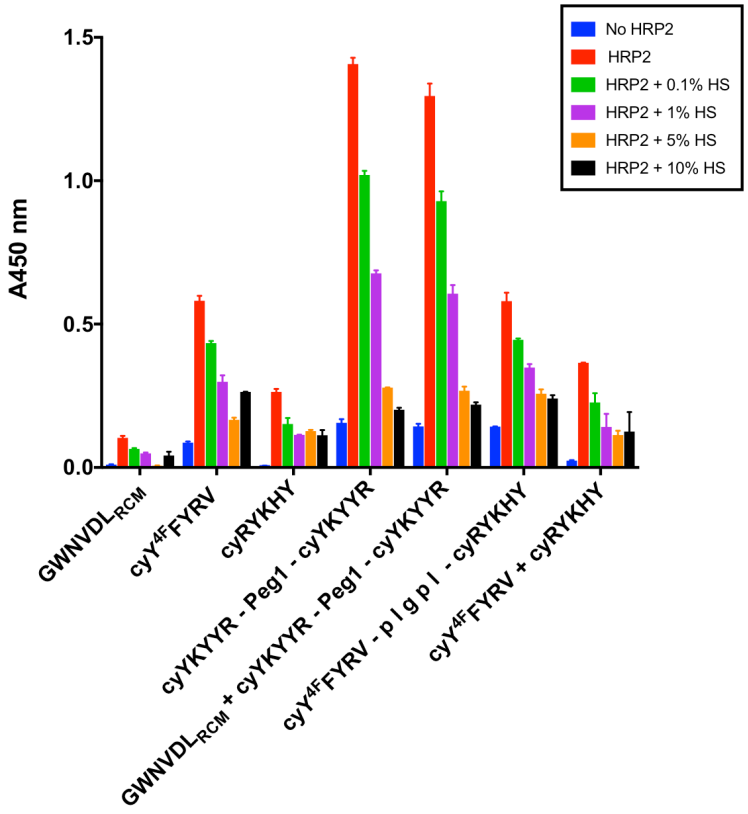

Figure 4-7. Sandwich ELISA comparing the performance of single PCCs, combinations, and biligands in human serum.

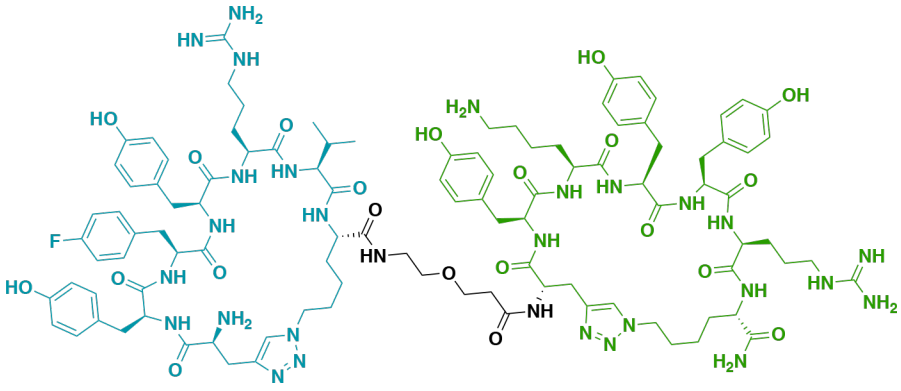

Figure 4-8. Biligand (**cyYKYYR-Peg1-cyY^{4F}FYRV)** obtained from Peg1 ligation.

4.4 Conclusion

Using the full *Pf*HRP2 antigen as a guide for *in situ* assemblage of bivalent ligands. Screens were performed using OBOC libraries with a variable region composed of unnatural amino acids for linkers. Whilst this strategy of target guided selection of linkers from a combinatorial library has proved successful with a structured protein,[6] the development of biligands from this screening methodology produced molecules with a high-degree of off-target interactions despite the high homology in lengths selected by the screens. This work has demonstrated that *in situ* linker screens guided by an intrinsically disordered, unstructured protein have not yielded high-performing PCCs, though this it not necessarily generalizable to all disordered proteins. From this study, the development of biligands from ligation using a single unit polyethylene glycol linker proved to be a facile means of generating bivalent molecules that yield superior performance over linkers obtained from a high throughput screen.

4.5 Acknowledgements

The linker screen was designed by JingXin Liang with guidance from Blake Farrow.[6] The linker screens were executed by JingXin Liang with Amy McCarthy. Molecular synthesis, characterization, purification, and assays were performed by JingXin Liang, Amy McCarthy, and Anvita Mishra.

References

(1) Das, S.; Nag, A.; Liang, J.; Bunck, D. N.; Umeda, A.; Farrow, B.; Coppock, M. B.; Sarkes, D. A.; Finch, A. S.; Agnew, H. D.; et al. A General Synthetic Approach for Designing Epitope Targeted Macrocyclic Peptide Ligands. *Angew. Chem. Int. Ed Engl.* **2015**, *54* (45), 13219–13224.

(2) Agnew, H. D.; Rohde, R. D.; Millward, S. W.; Nag, A.; Yeo, W.-S.; Hein, J. E.; Pitram, S. M.; Tariq, A. A.; Burns, V. M.; Krom, R. J.; et al. Iterative In Situ Click Chemistry Creates Antibody-like Protein-Capture Agents. *Angew. Chem. Int. Ed Engl.* **2009**, *48* (27), 4944–4948.

(3) Millward, S. W.; Agnew, H. D.; Lai, B.; Lee, S. S.; Lim, J.; Nag, A.; Pitram, S.; Rohde, R.; Heath, J. R. In Situ Click Chemistry: From Small Molecule Discovery to Synthetic Antibodies. *Integr. Biol. Quant. Biosci. Nano Macro* **2013**, *5* (1), 87–95.

(4) Nag, A.; Das, S.; Yu, M. B.; Deyle, K. M.; Millward, S. W.; Heath, J. R. A Chemical Epitope-Targeting Strategy for Protein Capture Agents: The Serine 474 Epitope of the Kinase Akt2. *Angew. Chem. Int. Ed.* **2013**, *52* (52), 13975–13979.

(5) Deyle, K. M. Development of Protein-Catalyzed Capture (PCC) Agents with Application Ot the Specific Targeting of the E17K Point Mutation of Akt1, California Institute of Technology, 2014.

(6) Farrow, B.; Wong, M.; Malette, J.; Lai, B.; Deyle, K. M.; Das, S.; Nag, A.; Agnew, H. D.; Heath, J. R. Epitope Targeting of Tertiary Protein Structure Enables Target-Guided Synthesis of a Potent In-Cell Inhibitor of Botulinum Neurotoxin. *Angew. Chem. Int. Ed.* **2015**, *54* (24), 7114–7119.

(7) Farrow, B.; Hong, S. A.; Romero, E. C.; Lai, B.; Coppock, M. B.; Deyle, K. M.; Finch, A. S.; Stratis-Cullum, D. N.; Agnew, H. D.; Yang, S.; et al. A Chemically Synthesized Capture Agent Enables the Selective, Sensitive, and Robust Electrochemical Detection of Anthrax Protective Antigen. *ACS Nano* **2013**, *7* (10), 9452–9460.

(8) Lynn, A.; Chandra, S.; Malhotra, P.; Chauhan, V. S. Heme Binding and Polymerization by Plasmodium Falciparum Histidine Rich Protein II: Influence of PH on Activity and Conformation. *FEBS Lett.* **1999**, *459* (2), 267–271.

(9) Schneider, E. L.; Marletta, M. A. Heme Binding to the Histidine-Rich Protein II from Plasmodium Falciparum. *Biochemistry (Mosc.)* **2005**, *44* (3), 979–986.

(10) Liang, J.; Mishra, A.; McCarthy, A. Unpublished Data.

(11) Baker, J.; McCarthy, J.; Gatton, M.; Kyle, D. E.; Belizario, V.; Luchavez, J.; Bell, D.; Cheng, Q. Genetic Diversity of Plasmodium Falciparum Histidine Rich Protein 2 (PfHRP2) and Its Effect on the Performance of PfHRP2-Based Rapid Diagnostic Tests. *J Infect Dis* **2005**, *192*.

(12) Heath, J. R.; Agnew, H.; Farrow, B.; Bunck, D. N.; Liang, J.; Lai, B. T.; Pitram, S. M.; Nag, A.; Das, S. IL-17F Specific Capture Agents, Compositions, and Methods of Using and Making. 20170052199.

Chapter 5

Inhibition of heme sequestration of Histidine-Rich Protein 2 using multiple epitope-targeted peptides

Reprinted with permission from Biochemistry, submitted for publication:

J.X. Liang, D. N. Bunck, A. Mishra, M. Idso, J. R. Heath

5.1 Introduction

Plasmodium falciparum is the most lethal malarial species attributed to the infectious Plasmodium species.[1,2] During the intra-erythrotic stage of the parasite's life cycle, P. falciparum ingests over 75% of the host hemoglobin for nutrients,[2] releasing cytotoxic free heme.[3–5] The toxic byproduct is remediated by the parasite through conversion into hemozoin, an inert biomineral comprising a network of heme dimers linked by hydrogen bonds. The heme dimer is structurally identical to β-hematin, where each heme unit is connected through coordination of its propionate group on the porphyrin to the iron center of its cognate heme.[6]

Numerous antimalarial drugs target hemozoin formation. The antimalarial drug chloroquine prevents nucleation of new heme layers in hemozoin by binding to the surfaces of β-hematin crystals. In turn, this leads to retention of toxic free heme concentrations within the protozoan, thus inducing parasite death.[7,8] Artemesinin is another antimalarial drug used to treat *P. falciparum* infection. While the exact mechanism of artemisinin is

unknown, it is suggested to inhibit hemozoin formation through terminal capping of heme dimers, thus preventing aggregation of the dimeric units necessary for biocrystallization.[9]

While inert to the parasite, heme byproducts are harmful to human hosts, even after parasite clearance. Chronic bone loss has been correlated with the persistence of accumulated hemozoin in bone marrow after *P. falciparum* infection.[10] The retained hemozoin also modulates immune responses and bone homeostasis, so inhibition of heme biocrystallization might reduce disease related complications.[10] Despite numerous therapeutic compounds that hinder hemozoin formation, resistance against established single and combination drug therapies persists as a barrier against malaria eradication.[1] For example, one means of chloroquine resistance by *P. falcipar*um arises from a genetic mutation that prevents uptake of the drug. Similarly, other genetic mutations or selection of resistant isolates by drug pressure confer resistance to the *P. falciparum* species.[11] Many antimalarial drugs work through targeting heme via a host of biomolecules such as lipids and proteins that have been implicated in biocrystallization.[12] An alternative avenue of reduction hemozoin formation might be to target key biomolecules that are associated with this process.

A key *P. falciparum* specific protein implicated in heme binding is histidine-rich protein 2 (HRP2). The protein is secreted into the cytosol of erythrocytes and recruited in the parasitic food vacuole with hemoglobin.[13] HRP2 is composed almost exclusively of histidine (37%), alanine, and aspartic acid residues (Figure 5-1), with multiple, discrete Ala-His-His-Ala-Ala-Asp (AHHAAD) and AHHAHHAAD fragments repeated throughout its internal region. These subunits function as heme binding motifs, aiding in the formation of β-hematin, the precursor to hemozoin. Unbound HRP2 is a random coil,

adopting secondary structure only when bound to heme.[14,15] One HRP2 copy can bind up to 15-17 equivalents of heme, ligating the central iron atom with two imidazoles on histidine side-chains.[13,16] Dendritic structures bearing peptides AHHAHHAADA and the variant AHHAHHAANA have been shown to both bind heme and facilitate hemozoin formation.[17] Interestingly, while HRP2 sequesters heme and aids in biocrystallization, *Plasmodium* clones lacking genes for HRP2 and the homologous HRP3, can still produce hemozoin. Murine parasites lacking in HRP2 can also form hemozoin.[18] Outside of heme sequestration, HRP2 has been implicated in cerebral malarial pathogenesis by weakening the brain endothelial barrier.[19] Given the multiple roles assigned to HRP2, it is worthwhile to explore methods of inhibiting its activity and function.

MVSFSKNKVLSAAVFASVLLLDNNNSAFNNNLCSKNAKGLNLNKRLLHETQAH
VDDAHHAHHVADAHHAHHAADAHHAADAHHAHHAADAHHAHHAAYAHHAHH
AADAHHAHHASAHHAHHAADAHHDAHHAADAHHAAYAHHAHHAADAHHAHH
ASDAHHAADAHHAAYAHHAHHAADAHHAADAHHATDAHHAHHAADARHATD
AHHAADAHHATDAHHAADAHHAADAHHATDAHHAADAHHATDAHHAADAHH
AADAHHATDAHHAHHAADAHHAAAHHATDAHHATDAHHAAAHHEAATHCLRH

Figure 5-1. *P. falciparum* HRP2 contains numerous internal repeats of AHH, AHHAAD, and AHHAHHAAD motifs that participate in heme sequestration, as well as more chemically diverse regions at the C- and N-termini. The epitopes targeted in this study are colored by type. (UniProt: P90582, 98,9% similarity to ITG strain).

HRP2 holds diagnostic utility as a biomarker for acute and chronic *P. falciparum* infection. We recently reported on the development of protein-catalyzed capture agents (PCCs) that bind to HRP2.[20] We developed several PCCs as a cocktail for simultaneously recognizing multiple sites within HRP2, including several heme-binding epitopes (Figure 5-2).[20] Here, we explore the utility of those PCCs for inhibiting the formation of a heme:protein complex with HRP2-GST and an untagged, ITG strain of HRP2, herein

termed HRP2 (ITG). We find that the inhibitory potency of these PCCs can be enhanced through multimerization of the PCC agents. The reported approach provides a novel, proof-of-concept strategy that demonstrates protein targeting with engineered peptides can be used as functional inhibitors of protein and biomolecule interactions as demonstrated in the heme-binding properties of *P. falciparum* HRP2.

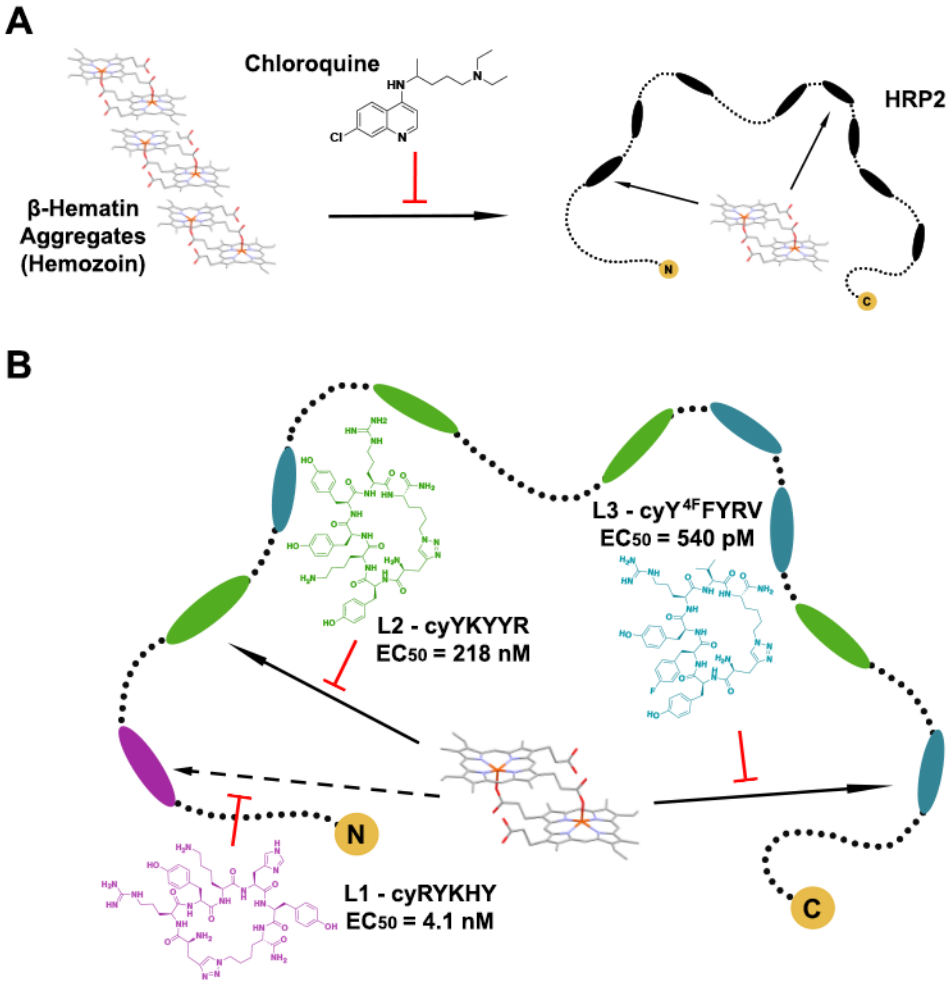

Figure 5-2. (A) Heme complexes with histidine rich regions in *Plasmodium falciparum* HRP2, and formation of those complexes can be hindered using the antimalarial drug chloroquine (**CQ**). (B) Macrocyclic peptides (**L1**, **L2**, **L3**) developed against the color-matched epitopes in HRP2 prevent formation of the heme:HRP2 complex by directly targeting the protein instead of heme. The EC_{50} binding strengths of the peptide ligands are indicated in the figure.

5.2 Materials and Methods

Materials. Recombinant *Plasmodium falciparum* HRP2 with a glutathione s-transferase tag (HRP2-GST) was obtained from CTK Biotech (A3000, 60 kDa, UniProt Sequence: P90582). All dilutions were made from reconstitution of the protein pellet with deionized water as per manufacturer instructions. The HRP2-GST stock was quantified by Bradford assay to yield a 37 and 47 μM stock, dependent on protein lot, from which all dilutions were made. Glutathione s-transferase (GST) from equine liver, hemin chloride, chloroquine diphosphate, and HEPES were all obtained from Sigma-Aldrich. Native *Plasmodium falciparum* HRP2 (ITG strain, 29 kDa, 24 μM) was kindly provided by collaborators from PATH. The primary sequence of HRP2 (ITG) is 98.9% similar to UniProt Sequence: P90582. All microplate heme binding assays were performed in 96-well clear bottom plates with non-binding surfaces obtained from Corning. Electronic absorption spectra for microtiter plate assays were obtained on a Flexstation 3 Multi-Mode Microplate Reader (Molecular Devices) at ambient temperature. Electronic absorption spectra for ligand and heme interaction studies were obtained on a Cary 300 UV-Vis spectrophotometer in 1 cm quartz cuvette at ambient temperature.

Ligand Synthesis and Purification. All ligands were synthesized on Rink Amide MBHA resin (Aapptec, 0.68 mmol/g loading) from their C to N termini using standard solid phase peptide synthesis techniques and commercially available L-amino acids (Aapptec, Anaspec, or Chempep). The resin was pre-swelled in N-methylpyrrolidone (NMP, BDH Chemicals) for a minimum of 2 hours prior to synthesis. The Fmoc group was removed by treatment for 2, 5, 25 minutes in 20% piperidine (Alfa Aesar) in NMP. An azide click handle was

attached by coupling of 4 equivalents of Fmoc-Lys(N_3)-OH with 4 equivalents of HATU (Chempep) used as a coupling agent and 12 equivalents of N,N-Diisopropylethylamine (DIEA, Sigma-Aldrich). Elongation of the peptide chain was accomplished on the Titan 357 Peptide Synthesizer (Aaaptec). An alkyne click handle was installed through coupling of Fmoc-L-Propargylglycine onto the N-termini of the peptides in the same reagent excess as azide attachmebt. The terminal Fmoc group was removed and the peptide ligands were cyclized by treatment overnight with 2 equivalents of copper iodide (Sigma-Aldrich) and 5 equivalents of L-Ascorbic Acid (Sigma-Aldrich) in 20% piperidine in NMP. After cyclization, the resin was rinsed liberally with NMP. For synthesis of ligands with two cycles, the cyclization step was repeated for 5 hours after the first overnight reaction. Following the click reaction, the resin was washed liberally with NMP. The remaining copper was removed by washing with a 2% w/v solution of sodium diethyldithiocarbamate trihydrate (Chem-Impex International) and 2% v/v solution of DIEA in NMP until the wash turned from dark brown to clear. The resin was then rinsed liberally with NMP, followed by methanol, and dichloromethane (DCM). The resin was dried under vacuum. Peptides were cleaved off solid support by treatment with 95% trifluoroacetic acid (TFA, Chem-Impex International), 2.5% triethylsilane (TES, Sigma-Aldrich), and 2.5% deionized water for 2 hours with agitation. The cleaved peptides were precipitated with diethyl ether and centrifuged for 45 minutes. The supernatant was discarded and the peptides were dissolved in 50/50 acetonitrile/water. The peptides were purified via preparatory scale reversed phase HPLC on a Dionex Ultimate3000 instrument on a Kinetex 5 μm XB-C18 100 column. Fractions containing the compound were lyophilized, recombined, and purified again via reversed phase semi-preparatory scale chromatography. Repurification was accomplished

on either a Beckman Coulter HPLC instrument with a Luna 10 μm C18(2) 100A column or a Dionex Ultimate3000 UHPLC (ThermoScientific) on a Hypersil GOLD C18 250 x 10 mm column (ThermoScientific). Chromatographic fractions containing the desired peptide products were characterized via MALDI-TOF MS (Bruker) using α-Cyano-4-hydroxycinnamic acid matrix (10 mg in 50/50 acetronitrile/water with <0.1% TFA). All peptides were quantified on a ThermoFisher Nanodrop 2000c UV-Vis spectrometer at A280 nm using extinction coefficients of 2560 cm^{-1} M^{-1} (Arg-Tyr-Lys-His-Tyr and Tyr-(4F)Phe-Tyr-Arg-Val), 3840 cm^{-1} M^{-1} (Tyr-Lys-Tyr-Tyr-Arg), and 6400 cm^{-1} M^{-1} (Tyr-Lys-Tyr-Tyr-Arg ligated to Tyr-(4-Fluoro)Phe-Tyr-Arg-Val).

Heme Binding Assays. A 1 mM solution of heme was prepared fresh for each experiment by dissolving ~ 13.1 mg of hemin chloride (Sigma-Aldrich) into 20 mL of 0.1 M NaOH where solution volumes were dispensed by serological pipettes for uniformity. The 0 to 21 μM heme stocks were prepared in 100 mM pH 7.0 HEPES (Sigma-Aldrich) buffer by individual dilutions from the 1 mM solution. From the 0 to 21 μM heme stocks, 450 μL of each solution was transferred into individual microcentrifuge tubes. For the protein containing solutions, 490 nM of HRP2-GST was added from the 37 μM or 47 μM stock. For the inhibition experiments, 10 μM of ligand or chloroquine was dispensed into each microcentrifuge tube requiring ligand. The solutions were protected from light and allowed to equilibrate at room temperature for 20 minutes. The solutions were then transferred onto a microwell plate and their electronic absorption spectra were read at ambient temperature on a platereader from 325 – 700 nm at 3 nm resolution. Absorbance at 415 nm was analyzed for the formation and inhibition of a heme:protein complex. All variable assays

were performed in the presence a control to yield four conditions: (i) heme (varied), (ii) heme (varied) + protein (constant), (iii) heme (varied) + ligand (constant), and (iv) heme (varied) + protein (constant) + ligand (constant). Contributions to the Soret band at 415 nm were determined in the control by spectral subtraction of {heme + protein} – {heme} at each point to obtain the difference spectra. For the ligand inhibition assays, the difference spectra are calculated by subtracting {heme + ligand} from {heme + protein + ligand}, which removes optical contributions from heme and ligand interactions. Thus, the final difference spectra are representative of contributions made only by formation of the heme:protein complex. From these data, ΔA415 are abstracted to generate heme binding curves. For ligand containing assays, ΔA415 values for the control are averaged over 26 data points. All ΔA415 values for the ligands were measured in at least triplicate with few exceptions.

Enzyme-Linked Immunosorbent Assays. All ELISA measurements of ligand binding to HRP2-GST were obtained on clear 96 well NeutrAvidin high-binding capacity plates (ThermoScientific). Assays were performed in TBS buffer (pH 7.5) with 0.05% Tween20 and 0.1% BSA. All plate washing as well as ligand, proteins, and antibody solutions were prepared in this buffer. The plates were washed 1X before incubation with a biotinylated ligand solution for 2 hours at ambient temperature. The plates were than washed 3X before blocking with 5% milk in buffer either at ambient temperature for 2 hours or overnight (~16 hours) at 4°C. After blocking, the plates were washed 3X with buffer, followed by incubation with HRP2-GST at ambient temperature for 2 hours or overnight (~16 hours) at 4°C. The plates were then washed 3X and incubated with 1:2000 dilution of anti-GST

horse radish peroxidase (Abcam) for 1 hour at ambient temperature. The plates were washed 3X with buffer and 1X with pure TBS before development with TMB ELISA substrate (ThermoFisher) for 5 minutes. The development was quenched with 1M H_2S0_4 before absorbance measurements were taken on a Flexstation 3 Platereader. To account for nonspecific binding of HRP2-GST, all binding assays were performed with a control, non-interacting ligand of polyethylene glycol (PEG_5) on the same microtiter plate as the variable ligand. This background ligand was immobilized in a manner identical to the variable ligand. Non-specific binding to both the microtiter plate and PEG5 were background subtracted from the absorbance of the variable ligands.

Circular Dichroisim Spectroscopy. Circular dichroism spectroscopy was performed on an Aviv Biomedical Model 410 spectrophotometer. Solutions of native HRP2 (ITG) protein were prepared in concentrations of 2, 3, and 4 μM. The spectra of HRP2 (ITG) were measured from 198 to 280 nm at 1 nm resolution in quartz cells (Hellma Analytics) of 1 mm pathlength. **L2-P1-L3** was titrated into the cuvettes containing HRP2 (ITG), aspirated gently with a pipette tip, and their spectra measured again. The titrations were continued until the peak at 199 nm was saturated for each protein concentration.

Size Exclusion Chromatography. Size exclusion chromatography was performed on a Biorad X FPLC using a Superdex 200 10/300 column. Solutions for HRP2-GST and GST were separately prepared at 500 nM and eluted via an isocratic PBS gradient.

5.3 Results and Discussion

5.3.1 Development of Macrocylic Peptide Ligands

Developing ligands for the detection of HRP2 is challenging because the protein exhibits significant sequence diversity across malaria endemic regions.[21–23] We used the epitope-targeted in situ click chemistry screening method[20] to develop three macrocyclic peptide ligands against conserved motifs within the protein (Figure 5-2B). For this method, polypeptides representing the targeted epitopes were synthesized, affixed with a click handle, and screened against combinatorial macrocyclic peptide libraries that presented the complementary click handle. This screen selects for library elements that bind to the synthetic HRP2 epitopes in just the right orientation to promote the (non-catalyzed) copper-free click reaction. Candidate PCCs are then screened for selective binding to the full length protein.

Using this method, three anti-HRP2 macrocyclic PCCs were developed against epitopes of the HRP2 protein of Figure 5-1. The *in vitro* binding characteristics of these PCCs were previously reported.[20] A macrocycle bearing the sequence Arg-Tyr-Lys-His-Tyr (cyRYKHY or **L1**; EC_{50} = 4.1 nM) was developed against the singly occurring Leu-His-Glu-Thr-Gln-Ala-His-Val-Asp-Asp (LHETQAHVDD) epitope located near the N-terminus. The other two targeted epitopes, AHHAADAHHA and AHHAHHAAD, are heme binding motifs in the internal region of HRP2 that are present in most HRP2 genotypes, but with different repeat frequencies.[21,23] These PCCs have sequences Tyr-Lys-Tyr-Tyr-Arg (cyYKYYR, **L2**; EC_{50} = 218 nM) and Tyr-(4F)Phe-Tyr-Arg-Val (cyY4FFYRV, **L3**; EC_{50} = 540 pM), respectively (Figure 5-2B). For PCC macrocycles developed against different targets, we have recently reported that qualitative EC_{50} values,

measured using the methods used here, agree, within a factor of 2, with quantitative binding constant (K_D) values measured using fluorescence polarization.[24]

The apparent binding affinity of **L3** is particularly high. For both **L2** and **L3**, the targeted epitopes represent repeating motifs, which could contribute to the measured avidity, likely scaling with the numbers of repeats.[23] The **L1** ligand is apparently a strong inherent binder of its target epitope. In comparison to the peptide macrocycles developed herein, the affinity of heme to HRP2 has been reported as 940 nM.[25] We thus reasoned that our ligands might competitively inhibit the formation of the heme:HRP2 complex.

5.3.2 Heme Binding Assays

We characterized free and bound heme using UV-Vis absorption spectroscopy in microwell plates. Digestion of hemoglobin to liberate free heme occurs in the digestive vacuole of the parasite *P. falciparum* between pH 4.8-5. At pH 5.5, the coordination state of heme is identical to that at pH 7.0. In the presence of HRP2 it polymerizes through saturated binding of the protein. Saturation at pH 7.0 occurs without polymerization or precipitation with retention of the initial heme coordination geometry.[15] We conducted the microtiter assays at pH 7.0 in 100 mM HEPES buffer, as adapted from reported protocols, using HRP2-GST.[15] The UV-Vis spectrum of free heme exhibits a broad peak at 386 nm that shifts to a sharp Soret band at 415 nm indicative of the heme:HRP2-GST complex (Figure 5-3A, B). The characteristic weakly absorbing α/β bands at 568 nm/535 nm are also observed in bound heme. The environment and interactions of heme can be monitored through these spectroscopic features.

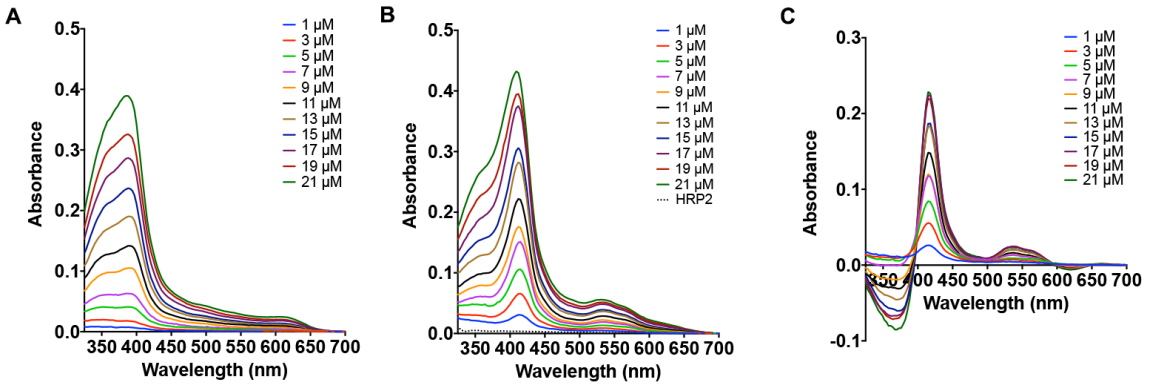

Figure 5-3. Electronic absorption spectra of (A) 0 to 21 μM free heme and (B) with 490 nM HRP2-GST taken in 100 mM HEPES (pH 7.0) after incubation at ambient temperature for 20 minutes. Free heme exhibits a broad peak centered at 385 nm. The heme:HRP2-GST complex produces a sharp Soret band at 415 nm with low intensity bands at 568 nm/535 nm, while HRP2-GST by itself (blacked dotted trace) is optically transparent through this region. (C) The signature of HRP2-GST binding to heme can be quantified by taking the difference spectra as shown, isolating the optical feature at 415 nm.

The impact of **CQ**, **L1**, **L2**, and **L3** binding on heme:HRP2 formation were determined by replicating heme titrations in the presence of ligand. We measured the UV-Vis absorption spectra of 0 to 21 μM heme solutions, with and without HRP2-GST. The heme and HRP2-GST solutions were equilibrated at room temperature for 20 minutes before transfer to a microtiter plate for optical absorption measurements. The formation of the heme:HRP2-GST complex was monitored by the growth of the Soret band at 415 nm. Taking the difference spectra between free and bound heme isolated the Soret band, thus permitting a quantitative assessment of the change in absorbance (ΔA415, Figure 5-3C).

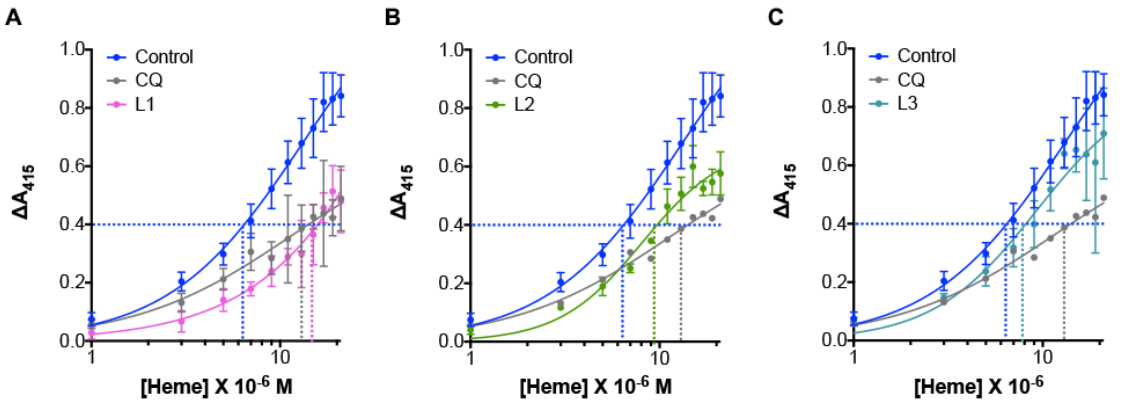

Figure 5-4. The influence of 10 μM epitope-targeted PCCs on inhibiting the formation of the heme:HRP2-GST complex is demonstrated. Chloroquine (**CQ**), which binds to heme and inhibits the formation of heme:HRP2-GST, provides a reference ligand. (A) **L1**, which binds to a singly occurring N-terminal epitope is about as effective as CQ. (B) **L2** and (C) **L3**, which bind against histidine-rich repeat motifs throughout HRP2, show weak inhibition relative to **CQ**. All assays were performed from 0 to 21 μM heme, 10 μM total ligand, and 490 nM of HRP2-GST in 100 mM HEPES (pH 7.0) at ambient temperature.

A saturation curve for the heme:HRP2-GST complex is generated by plotting ΔA415 against [Heme] (Figure 5-4). In the control, the growth in the ΔA415 correlates with the abundance of the heme:HRP2-GST complex. Inhibition of heme:HRP2-GST binding results in attenuation of this optical feature. An additional titration of GST with heme was performed to confirm that the fusion tag does not display significant optical features at low heme concentrations (Figure 5-S1). However, GST has been reported to bind heme so further assays were performed with a non-tagged HRP2. In addition, we also performed the heme:HRP2-GST inhibition experiments using the cyclic peptide Asn-Tyr-Arg-Trp-Leu (NYRWL), which was previously developed against botulinum toxin serotype A light chain (Figures S2).[20] We selected this ligand for the presence of the Tyr and Arg residues, which are also present in **L2** and **L3**. The NYRWL peptide displays no

inhibitory function despite bearing identical two residues in the same order as **L2** and **L3**. This result speaks to the specificity of the ligands developed via epitope-targeting against proteins of interest.

The effect of the anti-HRP2 peptides (**L1**, **L2**, and **L3**) was determined (Figure 5-4) using UV-Vis absorption spectroscopy. For these measurements, the formation of the heme:HRP2-GST complex was recorded by titrating [Heme] into a 490 nM HRP2-GST solution in the presence of 10 μM ligand or a **CQ** control. Chloroquine (**CQ**) is a known inhibitor of hemozoin formation (Figure 5-S3). It binds strongly to heme in a 2:1 ratio with a K_D = 37 nm and does not interact with HRP2.[25] **CQ** thus competes with the protein for heme sequestration.[25]

Ligand	**[Heme] A415=0.40**	**10 μM Heme ΔA415**	**% Inhibition Relative to Control**
0 μM	6 μM	0.56	0
10 μM **CQ**	13 μM	0.24	57
10 μM **L1**	15 μM	0.25	55
10 μM **L2**	9 μM	0.40	28
10 μM **L3**	8 μM	0.47	16
5 μM **L2-P1-L3**	20 μM	0.16	65
10 μM **L2-P1-L3**	32 μM	0.11	80
5 μM **L1** + 5 μM **L3**	13 μM	0.29	48
5 μM **L2** + 5 μM **L3**	12 μM	0.33	41

Table 1. Inhibition of Anti-HRP2 PCC Agents.
Inhibitory potency was assessed at 50% saturation of the heme:HRP2-GST complex (Abs = 0.40) and at equimolar heme / ligand concentrations (10 μM) from the plots in Figures 4-4 and 4-5.

The effect of **CQ** on heme:HRP2-GST formation can be observed by attenuation of the ΔA415 across heme concentrations. Like the control, saturation curves for the

heme:HRP2-GST complex in the presence of ligand were constructed by monitoring ΔA415 across heme concentrations. The plots in Figures 4 and 5 are reminiscent of inhibition curves, but with the caveat that multiple copies of heme, as well as most of the PCCs, bind to a single copy of HRP2-GST, so saturation in these solution phase assays is difficult to establish. Furthermore, the primary targets of **CQ** and the PCCs are not the same. This makes determination of absolute IC_{50} values for inhibiting heme:HRP2 complex formation difficult. However, relative comparisons between the PCCs and **CQ** can be made by fitting each of the data sets in Figures 4 and 5 to a Hill function (Table 1). We then selected the value of Abs = 0.40, or ~50% saturation, of the ΔA415 heme:HRP2-GST Soret band as a reference point (this value is reached at [Heme] = 6 μM). Addition of 10 μM **CQ** inhibits heme:HRP2-GST formation so that 13 μM heme is required to achieve an Abs = 0.40 value for the Soret band. The relative inhibition afforded by the anti-HRP2 peptides can be assessed in a similar way. All the anti-HRP2 PCC agents require similar or lesser amount of heme to achieve Abs = 0.40 except for **L2-P1-L3**, which requires 32 μM heme.

Given the strong binding strength of **L2** and **L3** to their respective heme-binding (i.e., AHHAAD-containing) epitopes, we expected those ligands to exhibit potent inhibitory effects on heme:HRP2-GST complex formation. In HRP2-GST, the AHHAHHAAD epitope is repeated 8 times whereas the analogous AHHAADAHHA motif is repeated 12 times (Figure 5-1). The repetitions of these two epitopes are not additive as they are variants of one another, but we had anticipated **L2** and **L3** to be the strongest inhibitors given the frequency of these motifs. Surprisingly, **L1** is the strongest of the single peptide cycle inhibitors. **L1** performed similarly to **CQ**, despite targeting a singly

occurring epitope not implicated in heme binding (Figure 5-4A and Figure 5-S4). However, **L1** is the only peptide macrocycle which contains a histidine residue which may participate in coordination with the iron center in heme, similar to the histidine residues in HRP2. **L2** and **L3** are significantly weaker than **CQ** (Fig 3-4B, C and Figures 3-S5, 6), despite the preponderance of repeated epitopes against which they were developed.

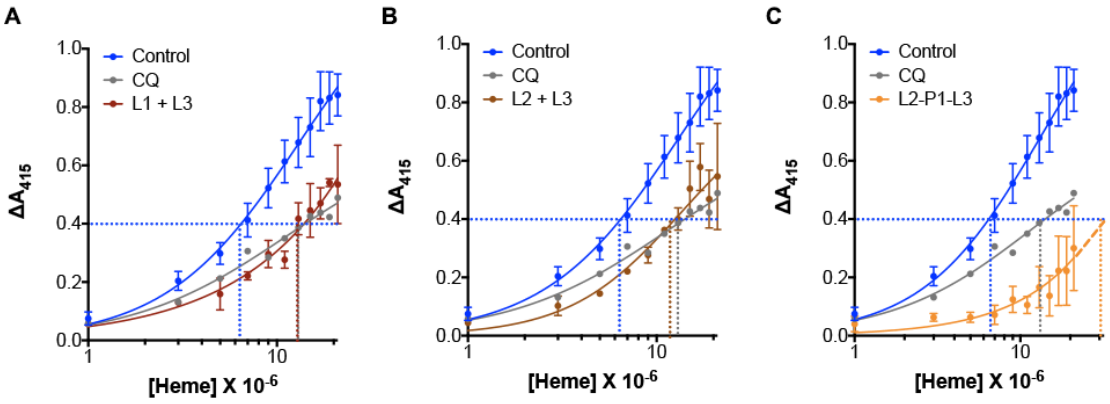

Figure 5-5. Combinations of (A) 5 μM **L1** + 5 μM **L3** and (B) 5 μM **L2** + 5 μM **L3** inhibit with a strength similar to **CQ**. (C) The most potent inhibition is afforded by addition of 10 μM of the bivalent ligand, **L2-P1-L3**. All assays were performed from 0 to 21 μM heme, 10 μM total ligand, and 490 nM of HRP2-GST in 100 mM HEPES (pH 7.0) at ambient temperature.

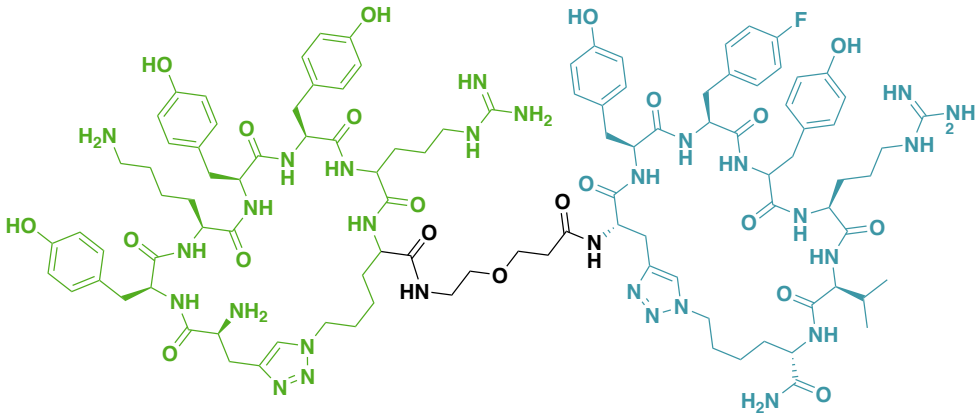

Figure 5-6. Chemical structure of the bivalent ligand **L2-P1-L3**. The two ligands, **L2** (green) and **L3** (teal), are ligated by a polyethylene glycol to afford a semi-flexible molecule.

We also investigated whether a cocktail of ligands could enhance inhibition. A mixture of **L1** + **L3** and **L2** + **L3** (each ligand supplied at 5 μM concentration) had about the same potency as 10 μM of **CQ** (Figure 5-5A, B). The **L2** + **L3** cocktail is more effective than its individual constituents. The improved potencies can be viewed as additive potencies through increased concentration of competitive peptides. We explored whether we could introduce cooperativity in inhibition by tethering **L2** and **L3** with a 9-atom polyethylene glycol (PEG) linker, yielding the bivalent ligand **L2-P1-L3** (Figure 5-6). We reasoned that a PEG linker would allow the new ligand to span two spatially separated regions in the unstructured protein target without significant loss of overall conformational rigidity. The heme binding assay was repeated with 10 μM of **L2-P1-L3** (Figure 5-5C and Figure 5-S7) and the inhibition effect was more pronounced than any single ligand, cocktail, or **CQ** in the same dose, with a value of about 32 μM [Heme] at 50% saturation (extrapolated). As 10 μM of **L2-P1-L3** would be equivalent to 10 μM of **L2** and **L3** individually, we also performed the heme:HRP2-GST assay with 5 μM of **L2-P1-L3** (Figure 5-7). At 50% saturation, treatment of heme:HRP2-GST with 5 μM of **L2-P1-L3** would require 20 μM of heme to overcome inhibition. A similar quantitative assessment of inhibition can be made by comparing ΔA415 at 10 μM of heme across all the assays. At this concentration, the 10 μM of ligand added is in equimolar competition with heme binding. **CQ** performs similarly to **L1** and inhibit 57% to 55% of heme:HRP2-GST relative to the control, respectively. By this assessment, **L2-P1-L3** shows an almost two-fold improved inhibition over **CQ** by inhibiting 80% of the heme:HRP2 complex. At half concentration, 5 μM of **L2-P1-L3** inhibits 65% of the heme:HRP2-GST complex and outperforms any single molecule or combination tested. An additional assay of

heme:HRP2 inhibition was performed with a cocktail combination of 10 μM **L2** + 10 μM **L3**, which is the equivalent of adding 10 μM of **L2-P1-L3** (Figure 5-7).

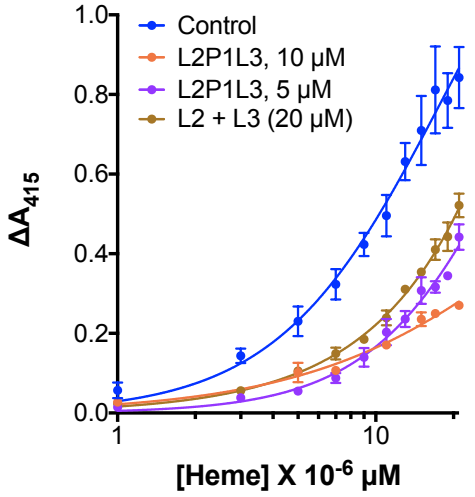

Figure 5-7. Comparison of heme:HRP2 complex inhibition by cocktail combinations of **L2** and **L3** versus **L2-P1-L3**. A combination of 10 μM of **L2** and 10 μM of **L3** exhibits similar potency to 5 μM of **L2-P1-L3**, indicating 2 equivalents of each individual ligand are required to approach the performance of the biligand.

5.3.3 Heme Binding by Native HRP2

The GST tag on HRP2-GST is expected to have some ability to sequester heme. We thus investigated the differences between heme binding by native, non-tagged HRP2 (ITG) and HRP2-GST fusion tag. The assays were repeated with HRP2 (ITG) at 1, 5, 7, and 21 μM of heme. At lower heme concentrations, the amount of complex formed is comparable. At higher heme concentrations, HRP2 (ITG) saturates before HRP2-GST (Figure 5-8).

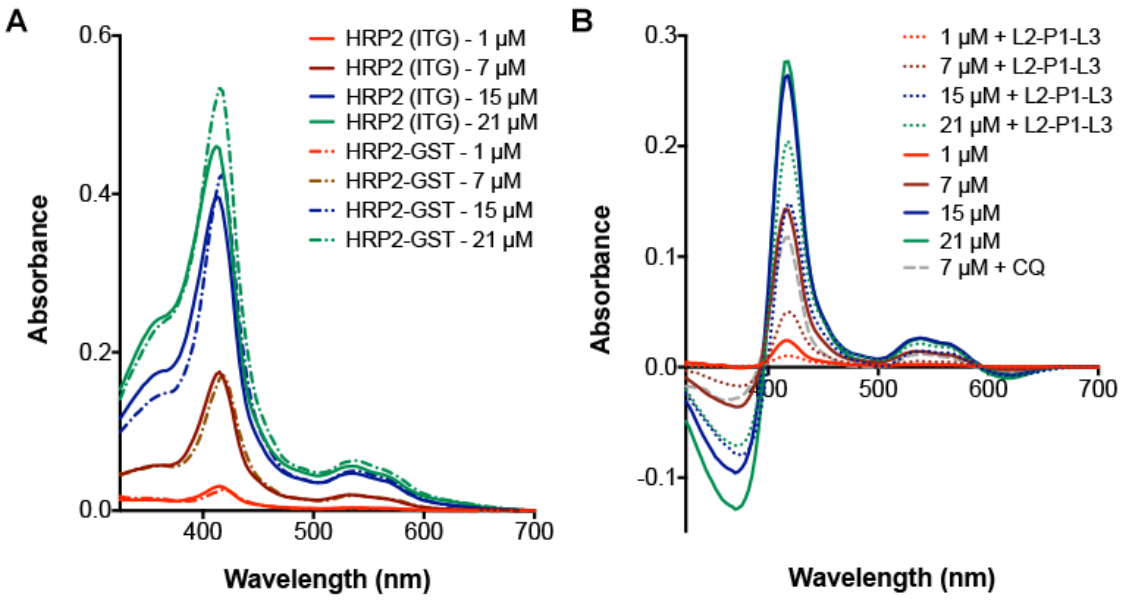

Figure 5-8. A comparison of heme binding capacities between 490 nM HRP2-GST and 360 nM HRP2 (ITG) indicates similar sequestration at lower concentrations. The assay was performed with 1, 7, 15, and 21 µM of heme. (A) HRP2-GST and HRP2 (ITG) exhibit the same heme binding capacity at 1 and 7 µM. HRP2-GST exhibits greater heme and protein complex formation at higher heme concentrations. (B) Heme:HRP2 (ITG) was subjected to 5 µM of L2-P1-L3. Inhibition is the most pronounced up to 15 µM of heme. At 7 µM of heme, treatment of the heme:HRP2 (ITG) complex with 10 µM of **CQ** (grey dashed line) demonstrates relatively weaker inhibitory potency.

The heme:HRP2 (ITG) complex was subjected to 5 µM of **L2-P1-L3** following the same protocol as the other microtiter plate assays (Figure 5-9). We compare the performance of **L2-P1-L3** to **CQ** at 7 µM heme, which represents the steepest part of the heme binding curve. At 7 µM of heme, 10 µM of **CQ** affords just 14% inhibition of heme:HRP2 (ITG). The addition of 5 µM of **L2-P1-L3** induces 64% inhibition of heme:HRP2 (ITG) at 7 µM of heme. The differences between inhibition of a heme:protein complex with and without the GST fusion tag are shown in Figure 5-9. This data shows

that the potency of heme:protein complex inhibition by **L2-P1-L3** is retained with HRP2 (ITG).

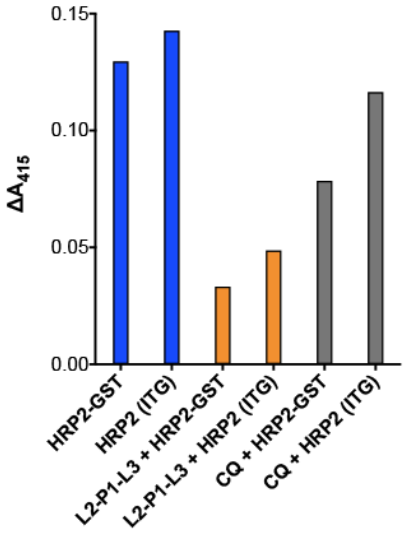

Figure 5-9. Comparison of ΔA415 at 7 μM of heme, shows similar quantities of complex formation between HRP2-GST and HRP2 (ITG). The addition of 5 μM **L2-P1-L3** compared to 10 μM of **CQ** demonstrates the relative superior inhibitory potency of the bivalent inhibitor.

5.3.4 The Potency of a Bivalent Ligand

The data of Figure 5-5 indicates that the **L2-P1-L3** bivalent ligand is a significantly better inhibitor of heme:HRP2 binding than **CQ**. The potency of 10 μM **L2-P1-L3** is largely retained with 5 μM of the biligand until concentrations of heme exceed 15 μM (Figure 5-7). **L2-P1-L3** inhibits heme:HRP2 across all heme concentrations explored. We explored whether this increased potency arose from cooperative binding. We have shown that optimally linking two epitope targeted PCCs onto the surface of a structured protein can significantly enhance binding affinity.[24,26] However, the random coil structure of HRP2, plus the repetitive heme binding epitope motifs within HRP2 does not lend itself

towards such a straightforward picture. We obtained EC_{50} curves using enzyme-linked immunosorbent assays (ELISAs) to compare the **L2**, **L3**,[20]a and **L2-P1-L3** protein interactions (Figure 5-S8, Table 3-S1). The **L2-P1-L3** titration curve is interpretable as the sum of two curves, one reflecting an EC_{50} value (6.3 ± 1.7 nM) close to that of **L1** (4.1 ± 1.0 nM) and the second reflecting an EC_{50} value (850 ± 270 pM) similar to **L3** (540 ± 130 pM). This is not reflective of a traditional cooperative binder where the K_D can approach the product of the affinities of the component binders. Thus, it is likely that the increased potency of **L2-P1-L3** arises from concentration effects, i.e., when one ligand is bound to HRP2, the local concentration of the second ligand is high. However, it does not appear that both ligands bind simultaneously.

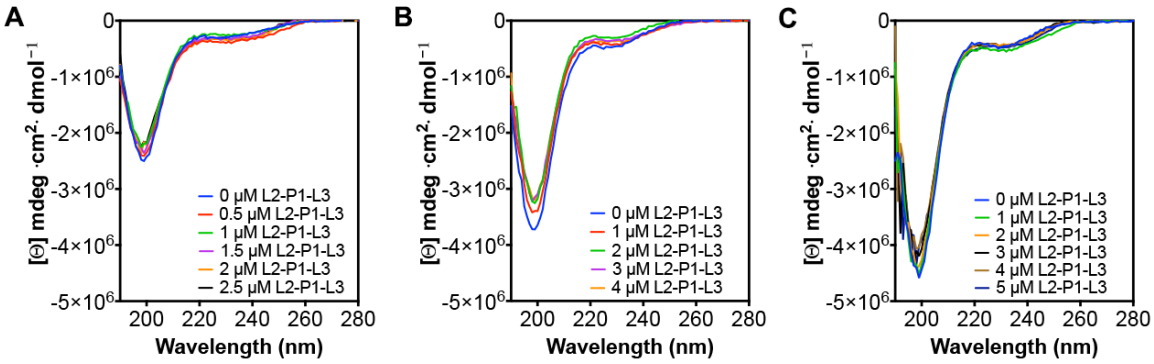

Figure 5-10. Circular dichroism spectra were obtained of the titration of HRP2 (ITG) at (a) 2 μM, (b) 3 μM, and (c) 4 μM with **L2-P1-L3** in 20 mM sodium phosphate buffer, pH 7.0.[16] The spectra of HRP2 across concentrations is that of a random coil with a single, broad peak at 199 nm. Titration of **L2-P1-L3** slightly diminishes the intensity of this peak until saturation.

We also queried whether **L2-P1-L3** might influence the intrinsically disordered nature of HRP2. Solution phase HRP2 exhibits a characteristic random coil structure via circular dichroism (CD) spectroscopy.[14] Heme binding events by HRP2 might facilitate disulfide bridge formation between protein monomers, perhaps enforcing a secondary

helical structure onto the protein that increases heme concentration.[16] We studied the interaction of **L2-P1-L3** and HRP2 (ITG) using CD spectroscopy (Figure 5-10). The CD spectra of 2 μM, 3 μM and 4 μM of native HRP2 indicate a random coil with a sharp peak at 199 nm and a broad, low absorption strength peak centered around 235 nm. Titration of **L2-P1-L3** into the native HRP2 solutions slightly, but consistently, diminishes the peak at 199 nm. However, it does not induce any secondary structural change that is detectable by CD. Thus, although heme may induce and stabilize secondary structure in HRP2, **L2-P1-L3** may just stabilize the random coil structure. We propose that **L2-P1-L3** might create an enthalpic energy barrier to the heme-binding conformation of HRP2. This is consistent with the observations reported in this paper, but challenging to quantitatively prove.

Prior work with antimalarial molecules has shown that complexes between compounds and heme exhibit peak maxima distinct from the Soret band of heme:HRP2 at 415 nm.[27,28] Such is the case in **CQ**, where a distinct peak at 424 nm can be observed in the difference spectra of heme with and without the inhibitor (Figure 5-S19). A trough is observed at 382 nm for heme:**CQ**, similar to that in the difference spectra of the heme:HRP2 complex. We titrated the peptide ligands against heme in the absence of protein and found that similar optical features in their difference spectra could be observed, though with low extinction coefficients (Figures S11 - 15). At low concentrations of heme (1 to 10 μM), the heme:ligand interaction is weak and manifests as a low absorbance strength, broadened band. However, this peak grows more distinct at greater quantities of heme. Interestingly, the most distinct band for a heme:ligand complex is observed with **L1** (Figures S11), indicating that specific heme:ligand interaction is likely the strongest. Due to the presence of histidine in **L1**, this result is anticipated. The imidazole of the histidine

likely participates in ligation with the iron center of heme, much like the imidazoles in HRP2. Indicative of a similar interaction of **L1** with heme to heme:HRP2 is the rise of the heme:**L1** peak at 414 nm, whereas all the other ligands absorb at or beyond 420 nm. The interaction of **L2**, **L3**, and **L2-P1-L3** with heme may arise from the preponderance of tyrosine residues in these ligands, since these aromatic residues may contribute to non-polar π-stacking interactions with the electron clouds in the porphyrin structure of heme. We compared the relative strength of heme, ligand, and **CQ** interactions at ΔA424 nm (Figure 5-S15 – S17). From these data, we can estimate EC_{50} values in the few μM range, with **L3** the strongest binder, and **L2** the weakest. Compared to the high apparent affinity of the peptide ligands for HRP2, which are low nanomolar to high picomolar, the heme:ligand interactions are relatively weaker.

The heme and ligand data, in addition to affinity assays of the ligands, point to two modes of inhibitory action with the anti-HRP2 PCC agents. First, the PCC agents can prevent binding of heme to HRP2 through directly targeting of AHHAAD-containing motifs. The higher potency of **L2-P1-L3** supports the notion that interaction with the target epitopes provides a mode of inhibition. The additional weaker interactions of the peptide ligands with heme may also influence inhibitory potency.

5.4 Conclusions

The malaria parasite digests hemoglobin in infected erythrocytes as a source of nutrients, liberating toxic heme in the process. The most lethal *P. falciparum* species has evolved a means of protection by converting this molecule to the inert biomineral hemozoin through a mechanism in which HRP2 has been implicated. Heme:HRP2 binding and heme

sequestration is promoted by repetitious heme-binding motifs within the protein, such as AHHAAD. We explored a class of epitope-targeted peptide macrocycles, called PCCs, as inhibitors of heme-HRP2 binding. The PCCs had been selected for binding to two closely related, genetically conserved heme-binding motifs, as well as a mostly genetically conserved, singly occurring epitope near the HRP2 N-terminus of the protein. We explored several combinations of these PCCs for blocking heme:HRP2. The combinations included individual ligands, cocktails of two PCCs, and a covalently linked PCC biligand. Our findings indicate that it is possible to inhibit heme:HRP2 association by competitively binding to heme sequestration epitopes on HRP2.

We find that heme:HRP2 complex formation is inhibited through both ligand:protein and, to a lesser extent, ligand:heme interactions. The peptide macrocycle **L1** targeted against the N-terminus of HRP2 was the most potent single PCC for blocking heme:HRP2, with an inhibitory performance similar to the antimalarial drug chloroquine. Although the N-terminal epitope is not an expected heme-binding region of HRP2, **L1** contains a histidine residue. Recent work on heme-detoxification protein (HDP), which contains multiple dispersed histidine residues, has suggested the importance of this amino acid in coordinating with the iron center of heme to seed hemozoin production.[29,30] The interaction of ligands with heme may provide a secondary mechanism for inhibition of HRP2:heme complexation.

The most potent inhibitor, **L2-P1-L3**, was composed of PCCs developed for binding to the same HRP2 epitopes that are associated with heme sequestration. The biligand outperformed **CQ** for blocking heme:HRP2 formation by more than two-fold (Figure 5-3, Table 3-1). The evidence herein points to an additive binding effect of this

biligand on HRP2. We propose also that stabilization of the random coil structure of HRP2 by **L2-P1-L3** binding may also prevent HRP2 from adopting the conformation necessary to sequester heme.

The technology for engineering ligands that bind to predetermined, unstructured regions of target proteins is a generalizable strategy unique to our approach, and permitted this exploration of the molecular nature of heme-sequestration by HRP2. Whilst the translation of such molecules into viable intracellular therapeutics would require engineering them for cell penetrance and bioavailability, we demonstrate a general proof-of-concept for the use of epitope-targeted peptide macrocycles as inhibitors of function through disruption of protein and biomolecule interactions.

5.5 Acknowledgements

The experimental program and manuscript preparation were executed by JingXin Liang and James R. Heath. JingXin Liang, David Bunck, and Anvita Mishra developed the PCC ligands. JingXin Liang executed all experiments associated with heme:HRP2/HRP2-GST. Matthew Idso assisted in ligand synthesis. David Bunck and JingXin Liang contributed to innovation of the biligands as described in "Il-17f-specific capture agents, compositions, and methods of using and making" (US Patent Pending, 15/211,759), filed July 15, 2016.

References

(1) WHO. World Malaria Report 2016. World Health Organization December 2016.

(2) Francis, S. E.; Sullivan, D. J.; Goldberg, and D. E. Hemoglobin metabolism in the malaria parasite Plasmodium falciparum. *Annu. Rev. Microbiol.* **1997**, *51* (1), 97–123.

(3) Papalexis, V.; Siomos, M.-A.; Campanale, N.; Guo, X.; Kocak, G.; Foley, M.; Tilley, L. Histidine-Rich Protein 2 of the Malaria Parasite, Plasmodium Falciparum, Is Involved in Detoxification of the by-Products of Haemoglobin Degradation. *Mol. Biochem. Parasitol.* **2001**, *115* (1), 77–86.

(4) Loria, P.; Miller, S.; Foley, M.; Tilley, L. Inhibition of the Peroxidative Degradation of Haem as the Basis of Action of Chloroquine and Other Quinoline Antimalarials. *Biochem. J.* **1999**, *339* (Pt 2), 363–370.

(5) Goldberg, D. E.; Slater, A. F.; Cerami, A.; Henderson, G. B. Hemoglobin Degradation in the Malaria Parasite Plasmodium Falciparum: An Ordered Process in a Unique Organelle. *Proc. Natl. Acad. Sci. U. S. A.* **1990**, *87* (8), 2931–2935.

(6) Pagola, S.; Stephens, P. W.; Bohle, D. S.; Kosar, A. D.; Madsen, S. K. The Structure of Malaria Pigment [Beta]-Haematin. *Nature* **2000**, *404* (6775), 307–310.

(7) Olafson, K. N.; Ketchum, M. A.; Rimer, J. D.; Vekilov, P. G. Mechanisms of Hematin Crystallization and Inhibition by the Antimalarial Drug Chloroquine. *Proc. Natl. Acad. Sci.* **2015**, *112* (16), 4946–4951.

(8) Combrinck, J. M.; Mabotha, T. E.; Ncokazi, K. K.; Ambele, M. A.; Taylor, D.; Smith, P. J.; Hoppe, H. C.; Egan, T. J. Insights into the Role of Heme in the Mechanism of Action of Antimalarials. *ACS Chem. Biol.* **2013**, *8* (1), 133–137.

(9) Robert, A.; Coppel, Y.; Meunier, B. Alkylation of Heme by the Antimalarial Drug Artemisinin. *Chem. Commun.* **2002**, No. 5, 414–415.

(10) Xu Kelly, J.; Winter, R.; Riscoe, M.; Peyton, D. H. A Spectroscopic Investigation of the Binding Interactions between 4,5-Dihydroxyxanthone and Heme. *J. Inorg. Biochem.* **2001**, *86* (2–3), 617–625.

(11) Lee, M. S. J.; Maruyama, K.; Fujita, Y.; Konishi, A.; Lelliott, P. M.; Itagaki, S.; Horii, T.; Lin, J.; Khan, S. M.; Kuroda, E.; et al. Plasmodium Products Persist in the Bone Marrow and Promote Chronic Bone Loss. *Sci. Immunol.* **2017**, *2* (12).

(12) Le Bras, J.; Durand, R. The Mechanisms of Resistance to Antimalarial Drugs in Plasmodium Falciparum. *Fundam. Clin. Pharmacol.* **2003**, *17* (2), 147–153.

(13) Pandey, A. V.; Babbarwal, V. K.; Okoyeh, J. N.; Joshi, R. M.; Puri, S. K.; Singh, R. L.; Chauhan, V. S. Hemozoin Formation in Malaria: A Two-Step Process Involving Histidine-Rich Proteins and Lipids. *Biochem. Biophys. Res. Commun.* **2003**, *308* (4), 736–743.

(14) Sullivan, D. J.; Gluzman, I. Y.; Goldberg, D. E. Plasmodium Hemozoin Formation Mediated by Histidine-Rich Proteins. *Science* **1996**, *271*.

(15) Lynn, A.; Chandra, S.; Malhotra, P.; Chauhan, V. S. Heme Binding and Polymerization by Plasmodium Falciparum Histidine Rich Protein II: Influence of PH on Activity and Conformation. *FEBS Lett.* **1999**, *459* (2), 267–271.

(16) Choi, C. Y. H.; Cerda, J. F.; Chu, H.-A.; Babcock, G. T.; Marletta, M. A. Spectroscopic Characterization of the Heme-Binding Sites in Plasmodium Falciparum Histidine-Rich Protein 2. *Biochemistry (Mosc.)* **1999**, *38* (51), 16916–16924.

(17) Schneider, E. L.; Marletta, M. A. Heme Binding to the Histidine-Rich Protein II from Plasmodium Falciparum. *Biochemistry (Mosc.)* **2005**, *44* (3), 979–986.

(18) Kumari, P.; Sahal, D.; Chauhan, V. S. Dendrimeric Template of Plasmodium Falciparum Histidine Rich Protein II Repeat Motifs Bearing Asp→Asn Mutation Exhibits Heme Binding and β-Hematin Formation. *PLoS ONE* **2014**, *9* (11), e112087.

(19) Sullivan, D. J. Theories on Malarial Pigment Formation and Quinoline Action. *Malar. Prog. Probl. Plans Genomic Era* **2002**, *32* (13), 1645–1653.

(20) Pal, P.; Daniels, B. P.; Oskman, A.; Diamond, M. S.; Klein, R. S.; Goldberg, D. E. Plasmodium Falciparum Histidine-Rich Protein II Compromises Brain Endothelial Barriers and May Promote Cerebral Malaria Pathogenesis. *mBio* **2016**, *7* (3).

(21) Das, S.; Nag, A.; Liang, J.; Bunck, D. N.; Umeda, A.; Farrow, B.; Coppock, M. B.; Sarkes, D. A.; Finch, A. S.; Agnew, H. D.; et al. A General Synthetic Approach for Designing Epitope Targeted Macrocyclic Peptide Ligands. *Angew. Chem. Int. Ed Engl.* **2015**, *54* (45), 13219–13224.

(22) Baker, J.; McCarthy, J.; Gatton, M.; Kyle, D. E.; Belizario, V.; Luchavez, J.; Bell, D.; Cheng, Q. Genetic Diversity of Plasmodium Falciparum Histidine Rich Protein 2 (PfHRP2) and Its Effect on the Performance of PfHRP2-Based Rapid Diagnostic Tests. *J Infect Dis* **2005**, *192*.

(23) Kumar, N.; Singh, J. P.; Pande, V.; Mishra, N.; Srivastava, B.; Kapoor, R.; Valecha, N.; Anvikar, A. R. Genetic Variation in Histidine Rich Proteins among Indian Plasmodium Falciparum Population: Possible Cause of Variable Sensitivity of Malaria Rapid Diagnostic Tests. *Malar. J.* **2012**, *11*, 298–298.

(24) Baker, J.; Ho, M.-F.; Pelecanos, A.; Gatton, M.; Chen, N.; Abdullah, S.; Albertini, A.; Ariey, F.; Barnwell, J.; Bell, D.; et al. Global Sequence Variation in the Histidine-Rich Proteins 2 and 3 of Plasmodium Falciparum: Implications for the Performance of Malaria Rapid Diagnostic Tests. *Malar. J.* **2010**, *9* (1), 129.

(25) Lai, B. T.; Wilson, J. A.; Malette Loredo, J.; Pitram, S. M.; LaBerge, N. A.; Heath, J. R.; Agnew, H. Epitope Targeted Macrocyclic Peptide Ligand with Picomolar Cooperative Binding to Interleukin-17F. *Chem. – Eur. J.* n/a-n/a.

(26) Pandey, A. V.; Bisht, H.; Babbarwal, V. K.; Srivastava, J.; Pandey, K. C.; Chauhan, V. S. Mechanism of Malarial Haem Detoxification Inhibition by Chloroquine. *Biochem. J.* **2001**, *355* (Pt 2), 333–338.

(27) Farrow, B.; Wong, M.; Malette, J.; Lai, B.; Deyle, K. M.; Das, S.; Nag, A.; Agnew, H. D.; Heath, J. R. Epitope Targeting of Tertiary Protein Structure Enables Target-Guided Synthesis of a Potent In-Cell Inhibitor of Botulinum Neurotoxin. *Angew. Chem. Int. Ed.* **2015**, *54* (24), 7114–7119.

(28) Kannan, R.; Sahal, D.; Chauhan, V. . Heme-Artemisinin Adducts Are Crucial Mediators of the Ability of Artemisinin to Inhibit Heme Polymerization. *Chem. Biol.* **2002**, *9* (3), 321–332.

(29) Choi, C. Y. .; Schneider, E. L.; Kim, J. M.; Gluzman, I. Y.; Goldberg, D. E.; Ellman, J. A.; Marletta, M. A. Interference with Heme Binding to Histidine-Rich Protein-2 as an Antimalarial Strategy. *Chem. Biol.* **2002**, *9* (8), 881–889.

(30) Nakatani, K.; Ishikawa, H.; Aono, S.; Mizutani, Y. Identification of Essential Histidine Residues Involved in Heme Binding and Hemozoin Formation in Heme Detoxification Protein from Plasmodium Falciparum. *Sci. Rep.* **2014**, *4*, 6137.

(31) Nakatani, K.; Ishikawa, H.; Aono, S.; Mizutani, Y. Heme-Binding Properties of Heme Detoxification Protein from Plasmodium Falciparum. *Biochem. Biophys. Res. Commun.* **2013**, *439* (4), 477–480.

5.6 Appendix: Supplementary Information

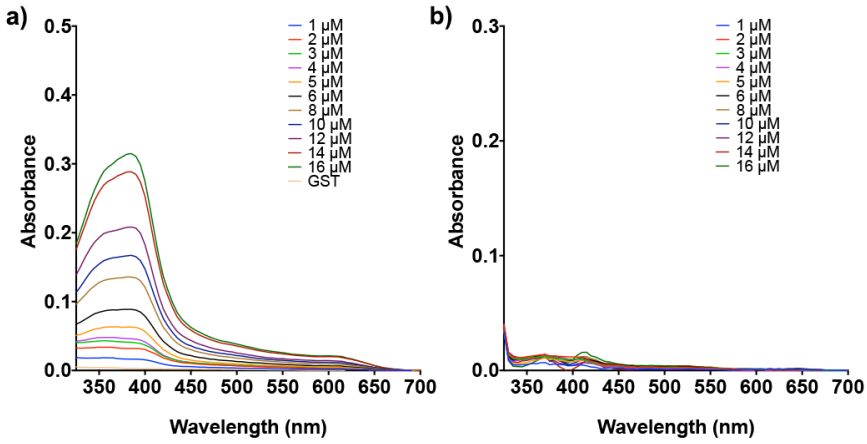

Figure 5-S1. UV-Vis absorption spectra of heme binding assay with GST control. UV-Vis absorption spectra for 440 nM GST titrated with 0 to 16 µM heme. (a) The spectra for heme + GST has a peak at 385 nm indicative of free heme. (b) The difference spectra of {Heme + GST} – {Heme} shows no optical features to suggest significant GST binding to heme.

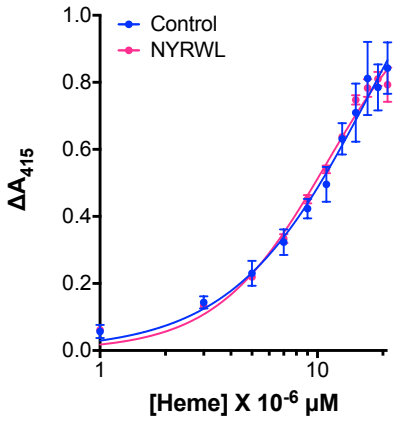

Figure 5-S2. Heme-Binding Assay with NYRWL. The heme and HRP2-GST binding curve was constructed with 490 nM protein. The heme and protein complex was treated with 10 µM of NYRWL. Measurement of ΔA415 nm indicates no inhibitor potency of NYRWL against the formation of the heme:HRP2-GST complex.

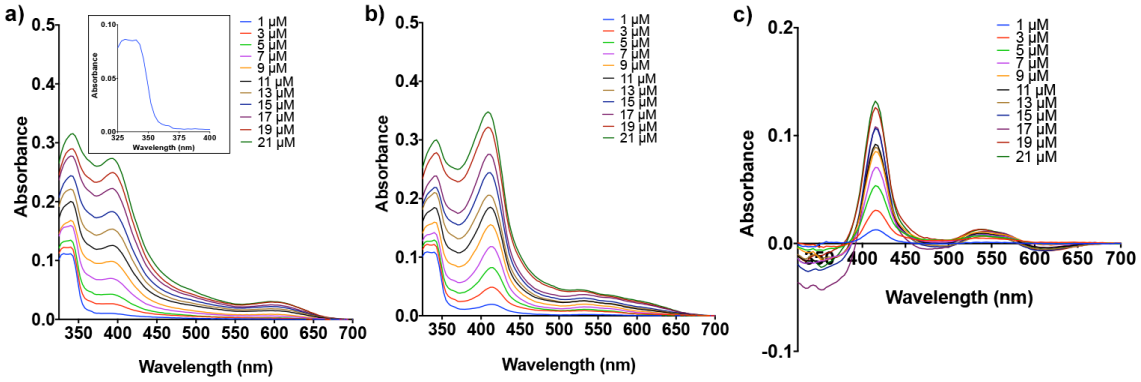

Figure 5-S3. Heme binding assay with CQ. UV-Vis absorption spectra for (a) 0 to 21 µM free heme with 10 µM **CQ** (inset), (b) 0 to 21 µM free heme with 10 µM **CQ** and 490 nM HRP2-GST, and (c) {Heme + HRP2-GST + **CQ**} – {Heme + **CQ**} difference spectra for quantitation of the diminished heme:HRP2-GST peak at 415 nm. The contribution of **CQ** to the blue region of the optical spectra is observed and does not contribute to the features of interest at 385/415 nm.

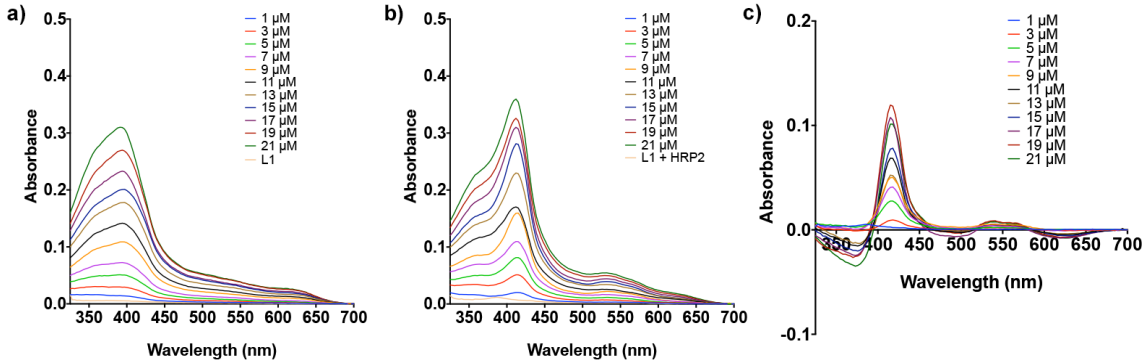

Figure 5-S4. Heme binding assay with L1 (cyRYKHY). UV-Vis absorption spectra for (a) 0 to 21 µM free heme with 10 µM **L1**, (b) 0 to 21 µM free heme with 10 µM **L1** and 490 nM HRP2-GST, and (c) {Heme + HRP2-GST + **L1**} – {Heme + **L1**} difference spectra. The intensity of the 415 nm feature is diminished relative to the control assay without ligand. Some interaction of **L1** with heme may be inferred from (a) where the heme + **L1** spectra are broadened relative to the heme control.

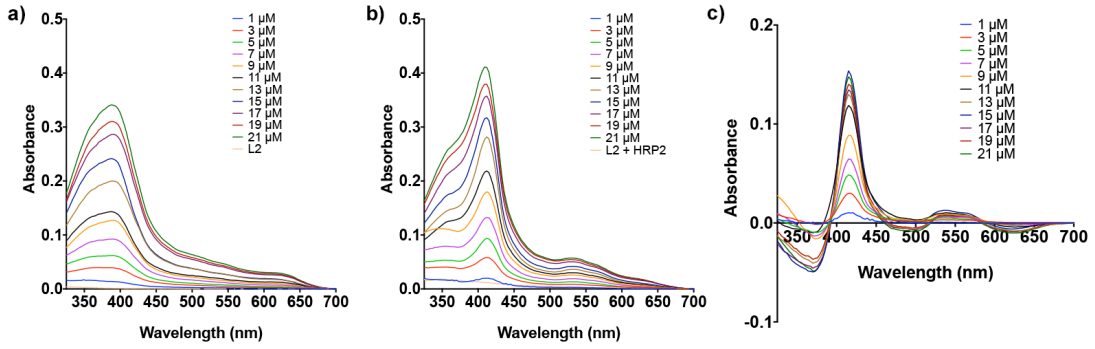

Figure 5-S5. **Heme binding assay with L2 (cyYKYYR).** UV-Vis absorption spectra for (a) 0 to 21 µM free heme with 10 µM **L2**, (b) 0 to 21 µM free heme with 10 µM **L2** and 490 nM HRP2-GST, and (c) the difference spectra of {Heme + HRP2-GST + **L2**} – {Heme + **L2**}. The spectra of heme with **L2** shows slight broadening and redshifting of the peak from 385 nm.

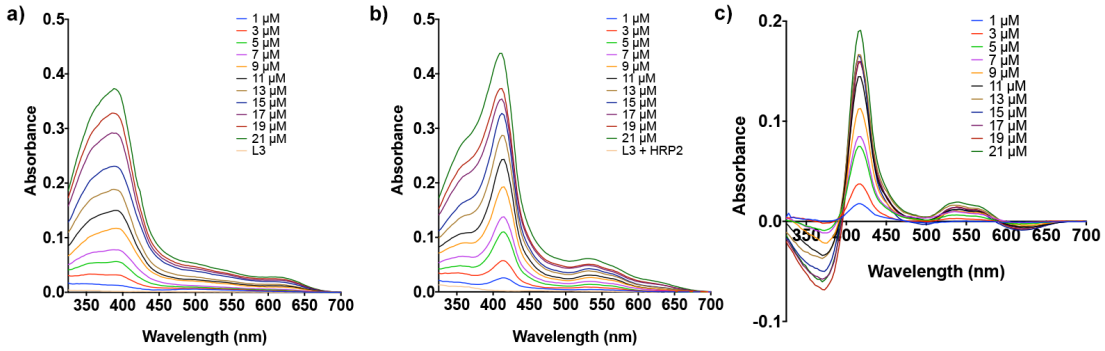

Figure 5-S6. **Heme binding assay with L3 (cyY^{4F}FYRV).** UV-Vis absorption spectra for (a) 0 to 21 µM free heme with 10 µM **L3**, (b) 0 to 21 µM free heme with 10 µM **L3** and 490 nM HRP2-GST, and (c) {Heme + HRP2-GST + **L3**}– {Heme + **L3**} difference spectra. As with the other ligands, addition of **L3** to free heme results in spectral broadening. Relative to the other ligands, **L3** is a weaker inhibitor of the heme:HRP2-GST complex.

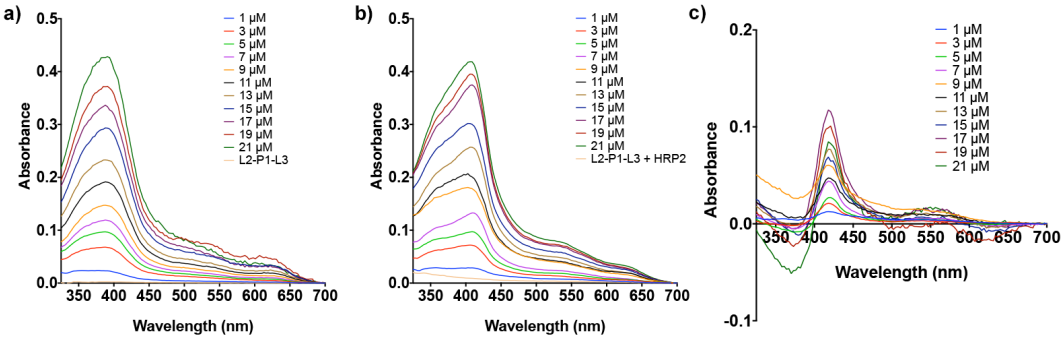

Figure 5-S7. **Heme binding assay with L2-P1-L3.** UV-Vis absorption spectra for (a) 0 to 21 μM free heme with 10 μM **L2-P1-L3** added, (b) 0 to 21 μM free heme with 10 μM **L2-P1-L3** and 490 nM HRP2-GST, and (c) {Heme + HRP2-GST + **L2-P1-L3**} – {Heme + **L2-P1-L3**} difference. The addition of HRP2-GST in the presence of **L2-P1-L3** does not produce the prominent optical feature at 415 nm that is indicative of the heme:HRP2-GST complex.

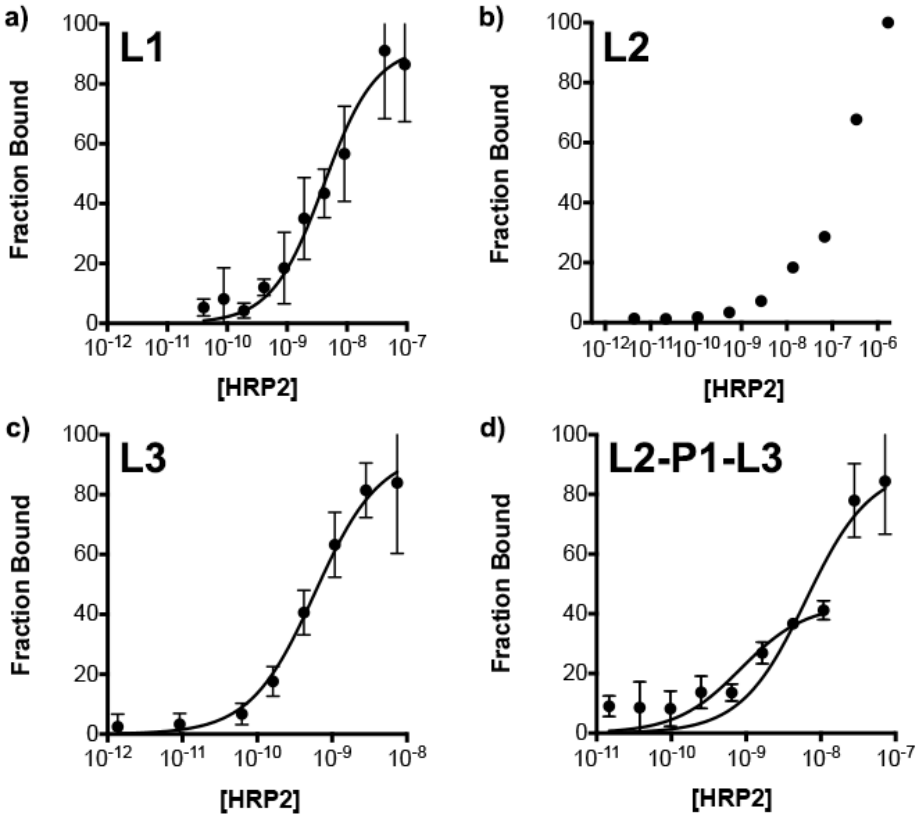

Figure 5-S8. EC50 binding curves for L1, L2, L3, and L2-P1-L3. The EC_{50} values for peptides **L1**, **L2**, **L3**, and **L2-P1-L3** were obtained via ELISA-type immunoassays using a biotinylated 5 unit polyethylene glycol (PEG_5) as a background ligand. For these assays,

biotinylated PCC was immobilized on a high binding capacity NeutrAvidin plate (ThermoFischer) from a 200 nM solution. Recombinant HRP2 with a GST tag was titrated at the indicated concentrations, and surface-captured HRP2 was detected using a (1:2000 dilution) anti-GST-HRP antibody (Abcam). Background and non-specific binding of HRP2-GST was removed by subtraction of an identical protein titration with biotinylated PEG_5. (a) **L1** has an $EC_{50} = 4.1 \pm 1.0$ nM, fitted using Prism (one site specific binding with Hill constant = 1). (b) **L2**, while not quite saturated, has an $EC_{50} = 218 \pm 44$ nM (fitted in Igor to the Hill equation without constraints). (c) **L3** fits to an $EC_{50} = 540 \pm 130$ pM (Prism, one site specific binding with Hill constant =1.1). (d) The **L2-P1-L3** biligand exhibits the sum of two binding isotherms. Below [HRP2] = 70 μM, the EC_{50} = 850±270 pM (Hill constant =1). A fit over the full [HRP2] titration yields an $EC_{50} = 6.3 \pm 1.7$ nM (Hill constant =1).

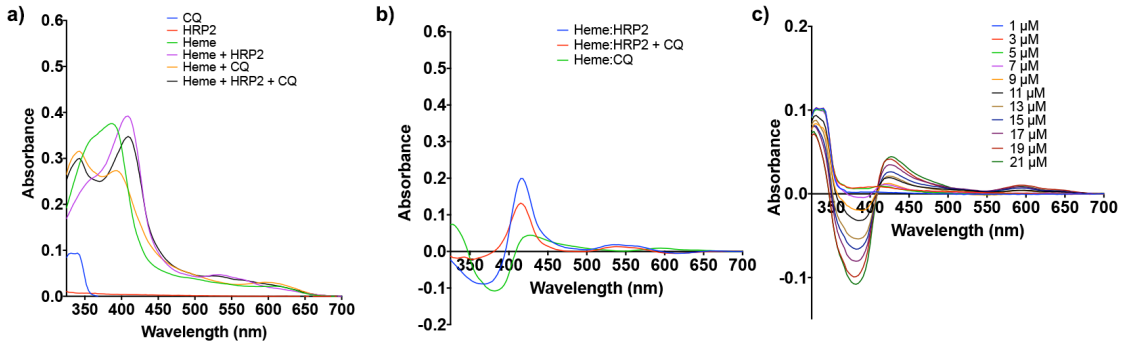

Figure 5-S9. UV-Vis Spectra of CQ interactions with heme. (a) UV-Vis absorption spectra of 10 μM **CQ** with 21 μM heme and 490 nM HRP2-GST. (b) The formation of complexes with heme can be observed in the difference spectra. The optical feature at 415 nm is diminished in the presence of **CQ**. Heme and **CQ** form a complex that yields a broad peak at 424 nm and a trough at 382 nm by measuring {Heme + **CQ**} – {Heme}. (c) The heme:**CQ** complex grows with increasing concentrations of heme.

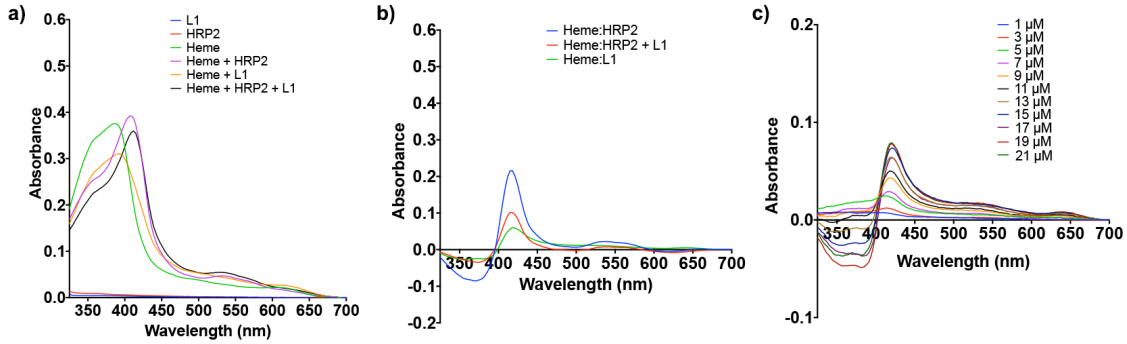

Figure 5-S10. UV-Vis absorption spectra of L1 with heme. (a) UV-Vis absorption spectra of 10 µM **L1** with 21 µM heme and 490 nM HRP2-GST. (b) Addition of **L1** significantly dampens the 415 nm peak for heme:HRP2-GST. (c) The difference spectra between {Heme + **L1**} – {Heme}.

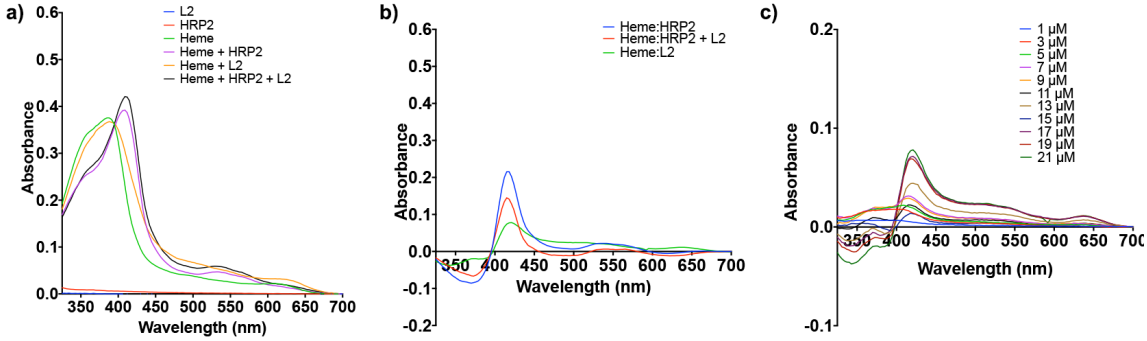

Figure 5-S11. UV-Vis absorption spectra of L2 Interaction with heme. (a) UV-Vis absorption spectra of 10 µM **L2** with 21 µM heme and 490 nM HRP2-GST. (b) The heme:HRP2-GST signal is attenuated in the presence of **L2**. (c) The difference spectra between {Heme + **L2**} – {Heme}. The broad, low absorbing peak that arises at higher heme concentrations is not attributed to formation of a complex with the ligand.

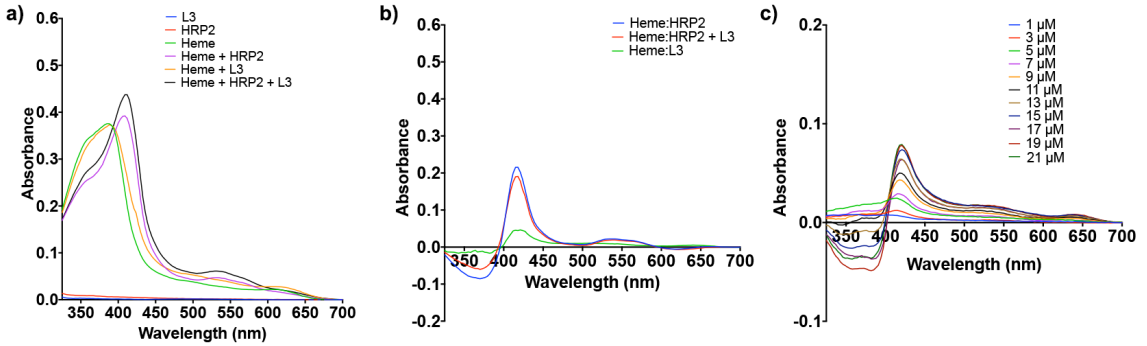

Figure 5-S12. UV-Vis absorption spectra of L3 Interaction with heme. (a) UV-Vis absorption spectra of 10 µM **L3** with 21 µM heme and 490 nM HRP2-GST. (b) **L3**

diminishes heme:HRP2-GST, but not appreciably at 21 μM heme. (c) The difference spectra between {Heme + **L3**} – {Heme}.

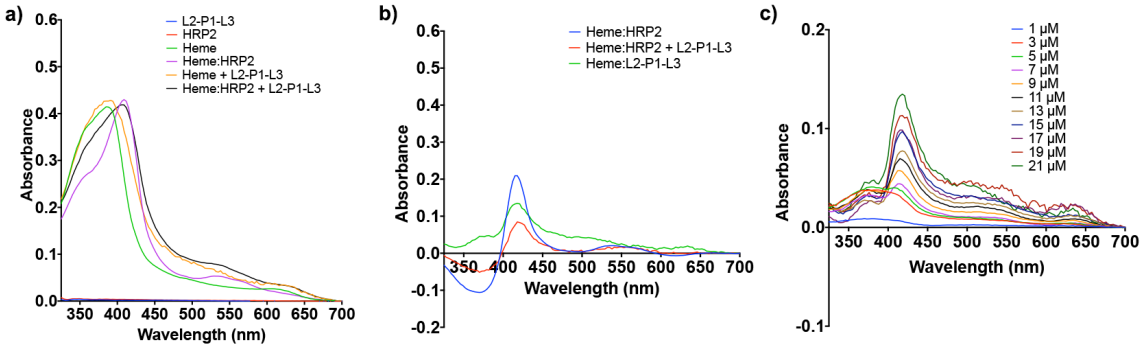

Figure 5-S13. UV-Vis absorption spectra of L2-P1-L3 Interaction with Heme. (a) UV-Vis absorption spectra of 10 μM **L2-P1-L3** with 21 μM heme and 490 nM HRP2-GST. (b) The addition of 10 μM **L2-P1-L3** shows the most pronounced inhibitory effect on formation of heme:HRP2-GST. (c) The difference spectra between {Heme + **L2-P1-L3**} – {Heme} does not indicate a significant interaction or complex formation between heme and the ligand.

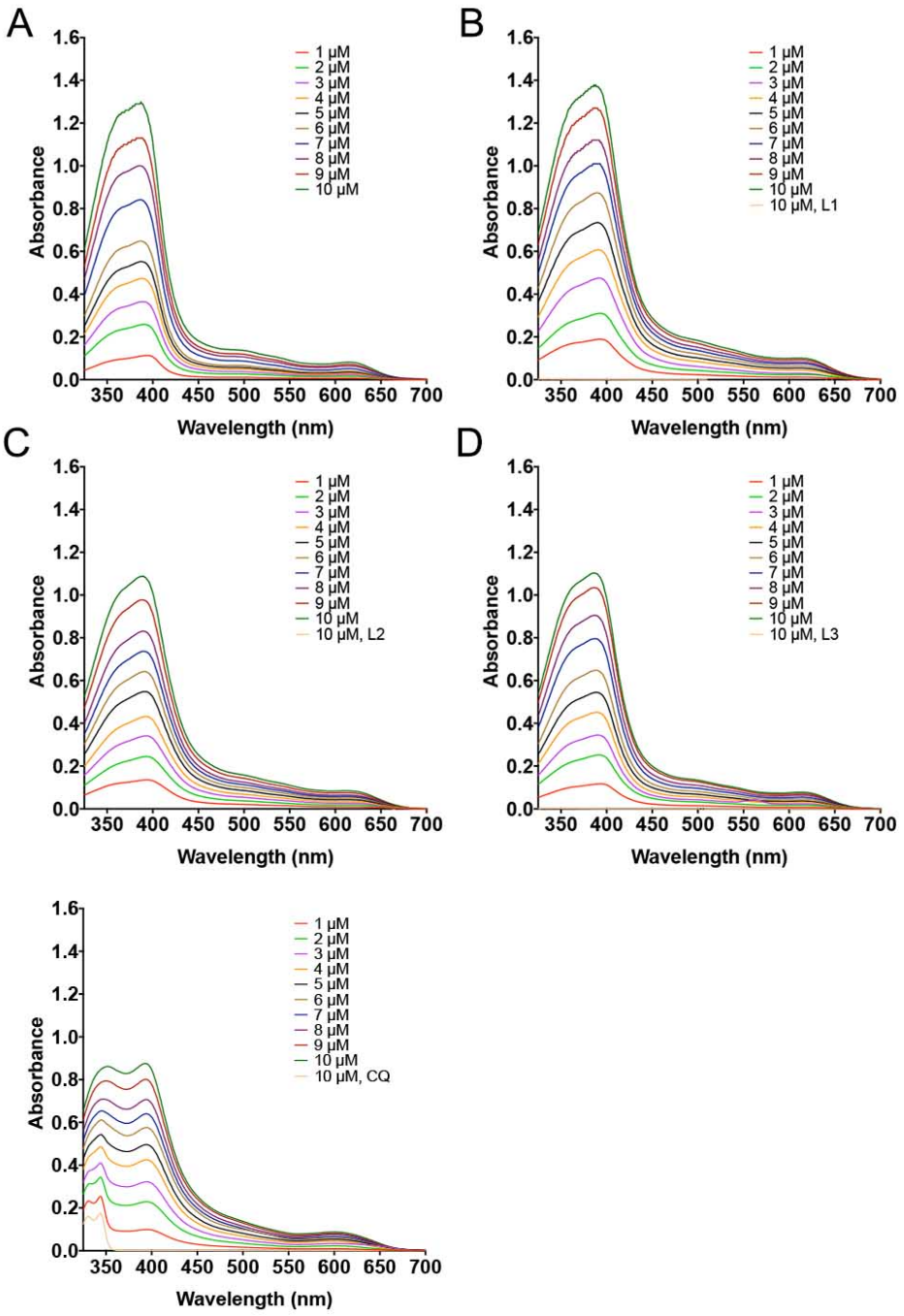

Figure 5-S14. Absorption spectra of heme and ligands. Absorption spectra obtained on a Cary 300 of (A) 1 to 10 µM heme, (B) 1 to 10 µM heme + 10 µM **L1**, (C) 1 to 10 µM heme + 10 µM **L2**, (D) 1 to 10 µM heme + 10 µM **L3**, and (E) 1 to 10 µM heme + 10 µM **CQ**.

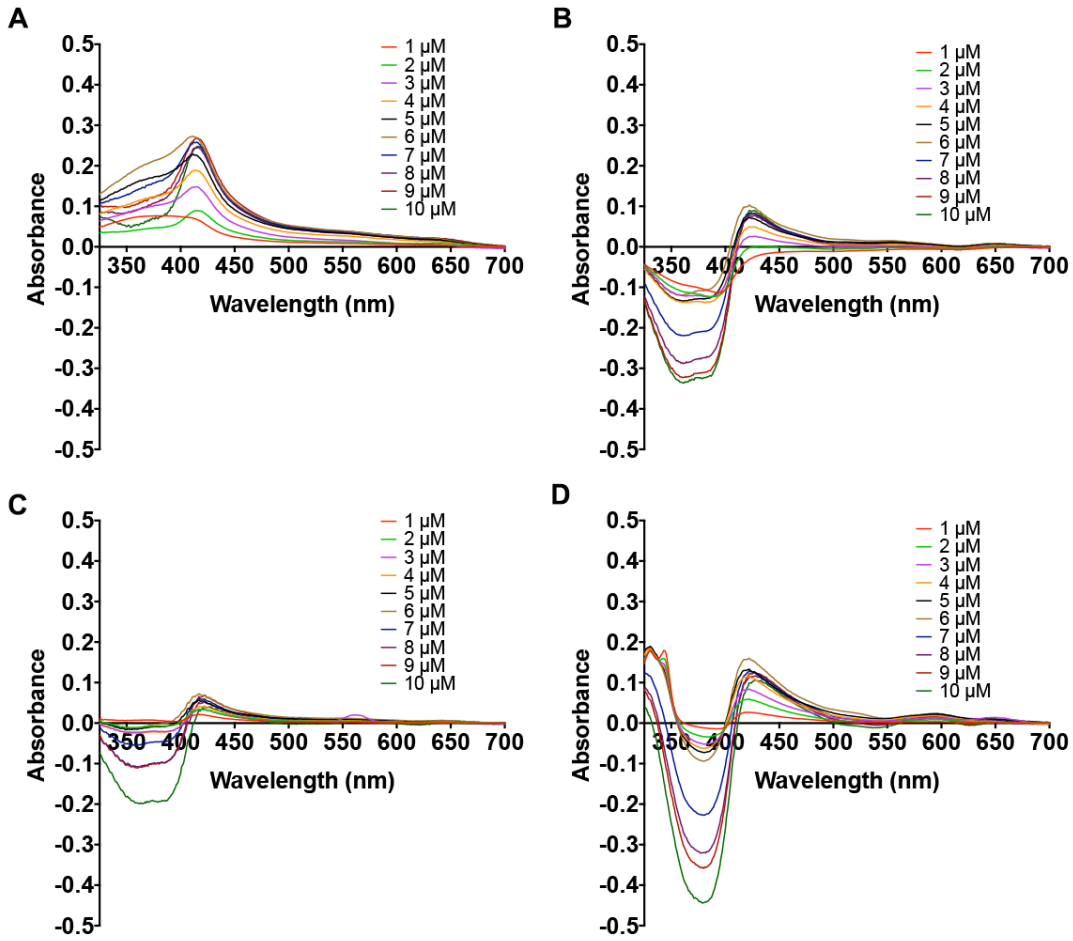

Figure 5-S15. Difference absorption spectra of heme and ligands. Solutions of 10 µM of **L1**, **L2**, **L3**, and **CQ** were titrated individually with 0 to 10 µM of heme on a Cary 300 spectrophotometer. The difference absorption spectra are obtained by {Heme + Ligand} – {Heme} for (A) **L1** (λ_{max} = 414nm), (B) **L2** (λ_{max} = 421nm), (C) **L3** (λ_{max} = 420nm), and (D) **CQ** (λ_{max} = 420nm). All the ligands and CQ show at least weak interaction with heme. **L1** shows the strongest interaction. The absorption data from a dual beam instrument is qualitatively the same as that obtained on a platereader (Figures 3-S9 to 3-S13).

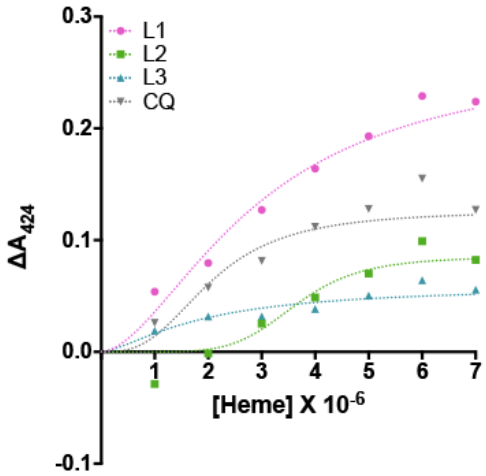

Figure 5-S16. Quantification of ligand interactions with heme. The signal at ΔA_{424} nm was used to compare all heme:ligand interactions. The curves were fit in Prism (one site, specific binding with no constraints on the Hill constant). The apparent strength of the interactions acoss this concentration range is calculated as follows **L3** (EC_{50} = 1.9±1.0 μM, Hill constant = 1.89**)** > **CQ** (EC_{50} = 2.1±0.4 μM, Hill constant = 2.86**)** < **L1** (EC_{50} = 3.0±0.5 μM, Hill constant = 1.72**)** < **L2** (EC_{50} = 3.6±0.4 μM, Hill constant = 3.65**)**.

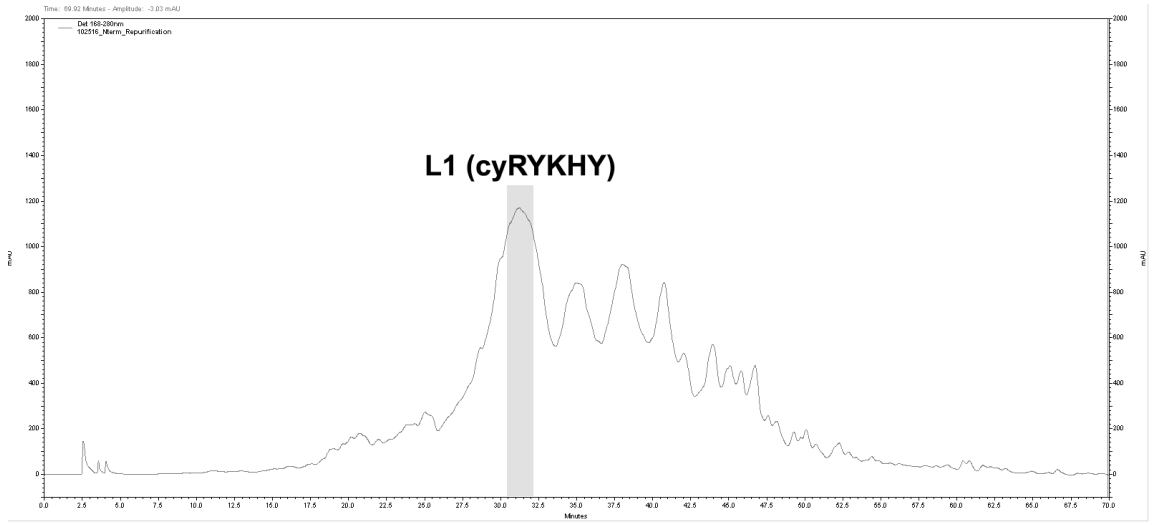

Figure 5-S17. HPLC chromatogram for L1 purification. The UV-Vis chromatogram for the 280 nm channel from the second purification of **L1**. **L1** eluted at 15% acetonitrile in water. All peaks were analyzed via MALDI-TOF MS and fractions containing **L1** were retained and lyophilized in preparation for reconstitution.

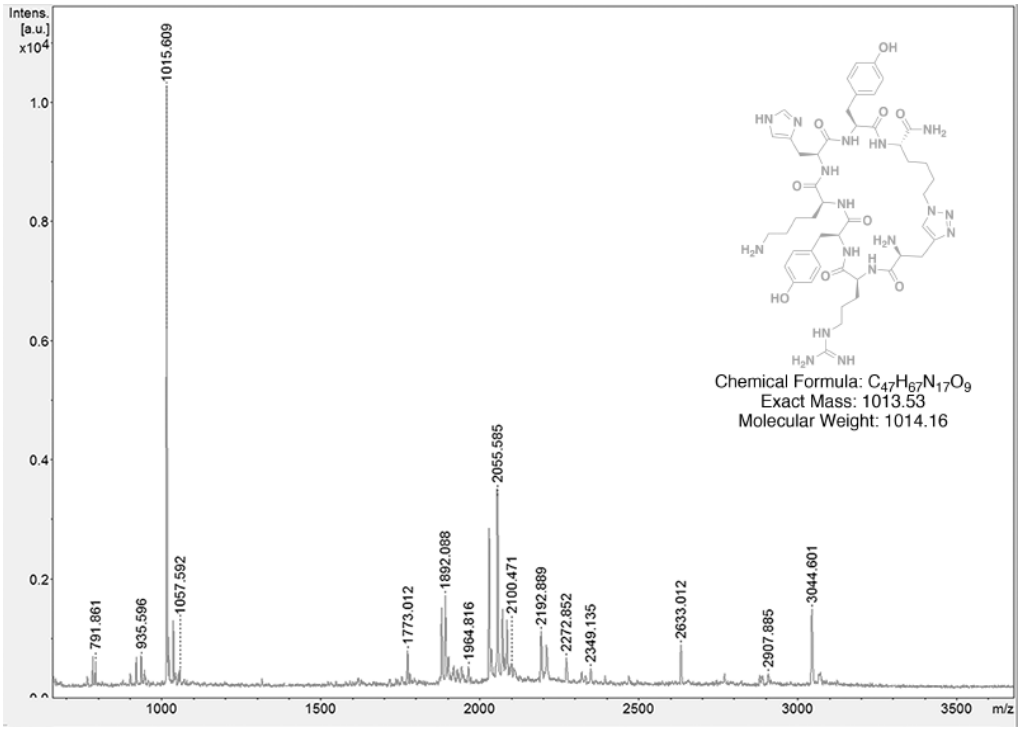

Figure 5-S18. MALDI-TOF mass spectrum of L1 (cyRYKHY). Mass spectrum obtained for **L1** after two purifications via reversed phase HPLC. The prominent peaks are assigned as follows: **L1** monomer 1015.609 [M+H].

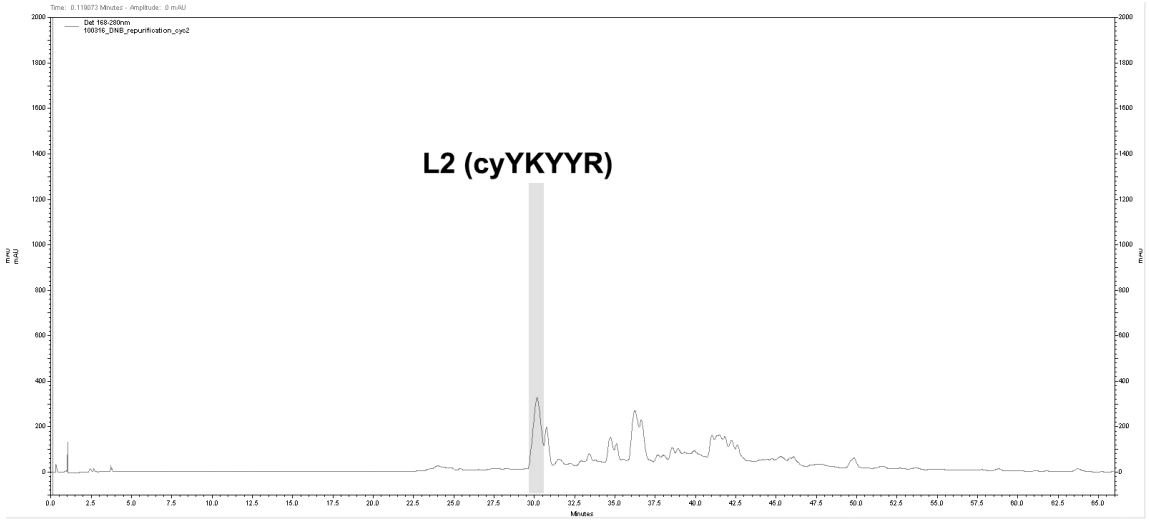

Figure 5-S19. HPLC chromatogram for L2 purification. The UV-Vis chromatogram for the 280 nm channel from the second purification of **L2**. **L2** eluted in 17% acetonitrile in water. All peaks were analyzed via MALDI-TOF MS and fractions containing **L2** were retained and lyophilized in preparation for reconstitution.

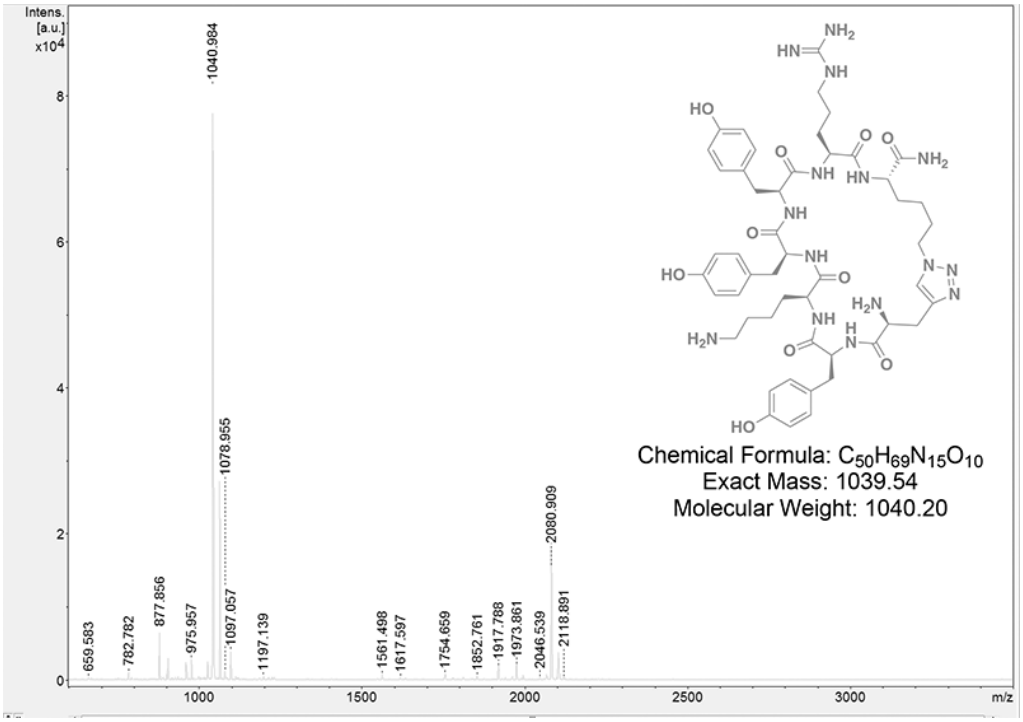

Figure 5-S20. MALDI-TOF mass spectrum of L2 (cyYKYYR). Mass spectrum obtained for **L2** after two rounds of purification via reversed-phase HPLC. The prominent peaks are assigned as follows: **L2** monomer 1040.984 [M+H], dimerization of **L2** with aldehyde addition to the N-terminal amine 2080.909 [M+H].

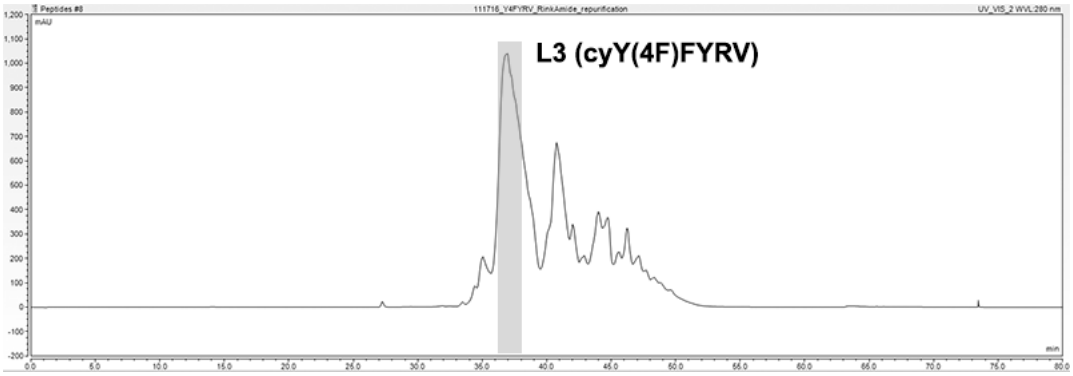

Figure 5-S21. HPLC chromatograms for L3 purification. The UV-Vis chromatogram for the 280 nm channel from the second purification (inset) of **L3** via semi-preparatory scale reversed phase. **L3** eluted at 25% acetonitrile in water. All peaks were analyzed via MALDI-TOF MS and fractions containing **L3** were retained.

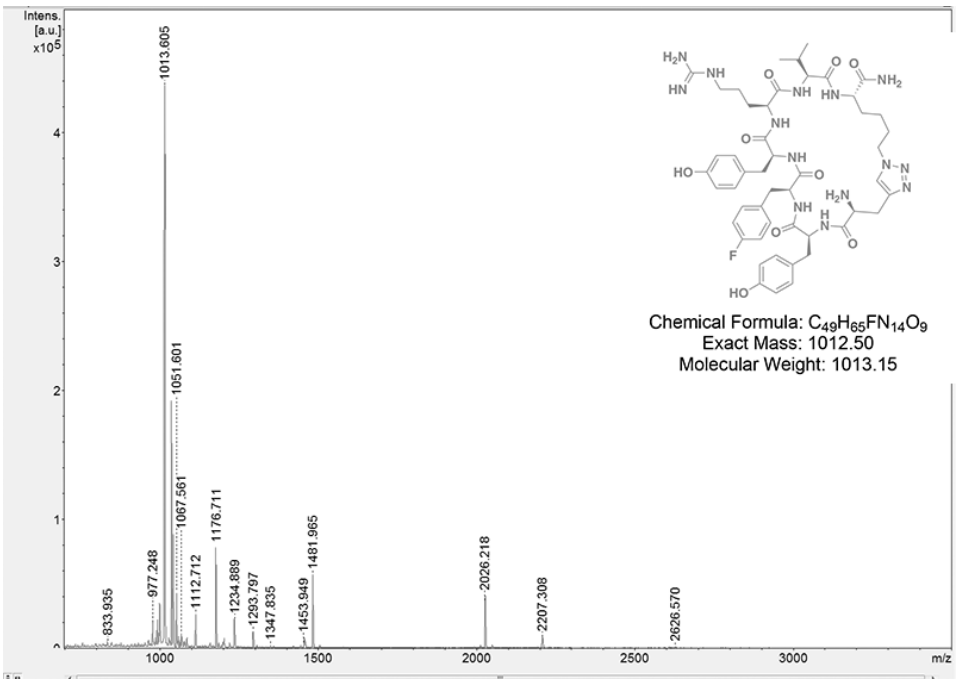

Figure 5-S22. MALDI-TOF mass spectrum of L3 (cyY^{4F}FYRV). Mass spectrum obtained for **L3** after two purifications via reversed-phase HPLC. The prominent peaks are assigned as follows: **L3** monomer 1014.009 [M+H].

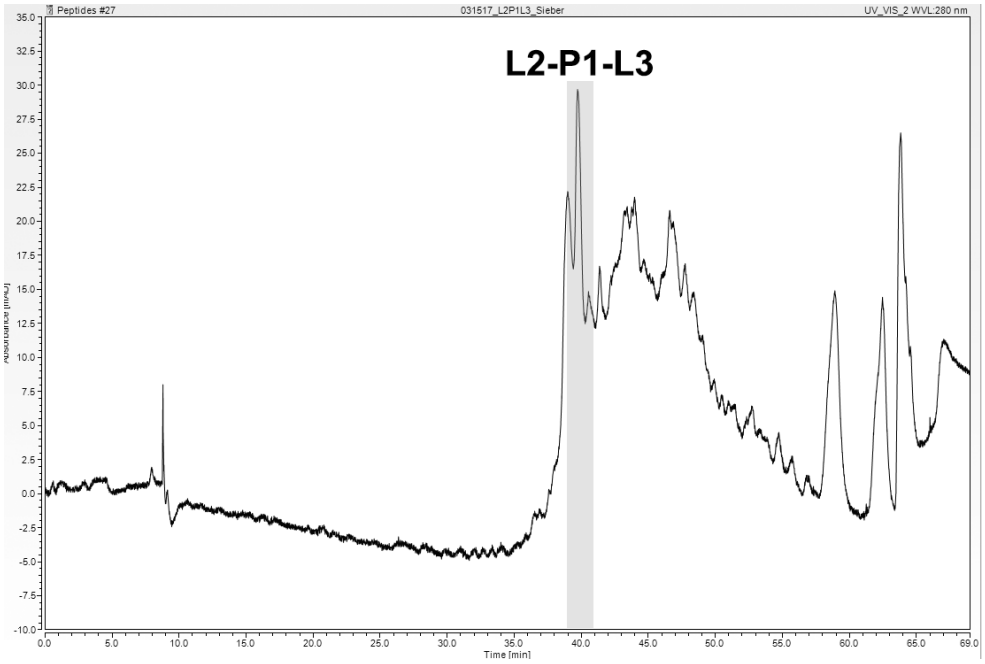

Figure 5-S23. HPLC chromatogram for L2-P1-L3 purification. The UV-Vis chromatograms for the 280 nm channel for the purification of **L2-P1-L3** via preparatory scale reversed phase HPLC is shown. **L2-P1-L3** eluted at 40% acetonitrile in water. All

peaks were analyzed via MALDI-TOF MS and fractions containing **L2-P1-L3** were retained.

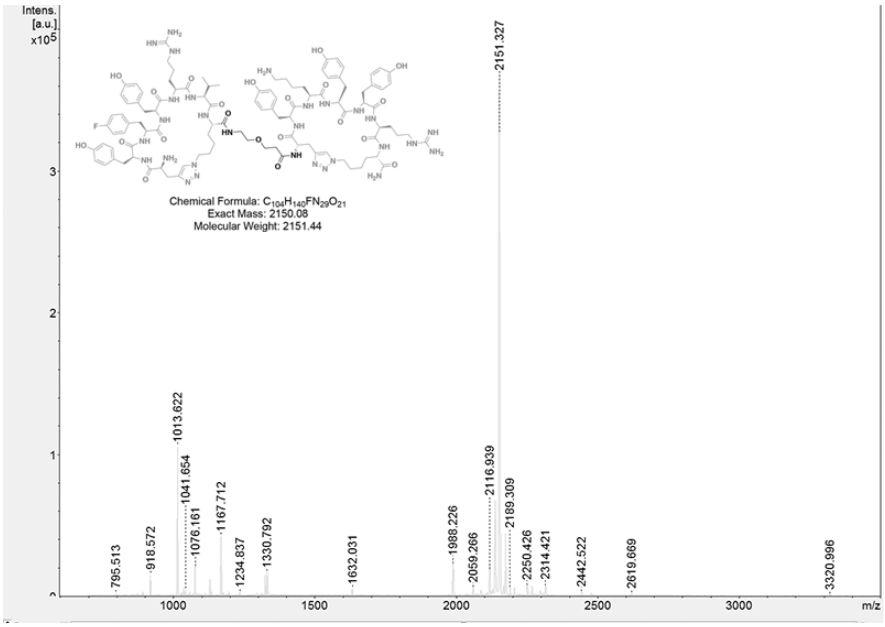

Figure 5-S24. MALDI-TOF mass spectrum for L2-P1-L3. Mass spectrum for **L2-P1-L3** obtained after reversed-phase HPLC purification. The prominent peak is 2151.327 [M+H].

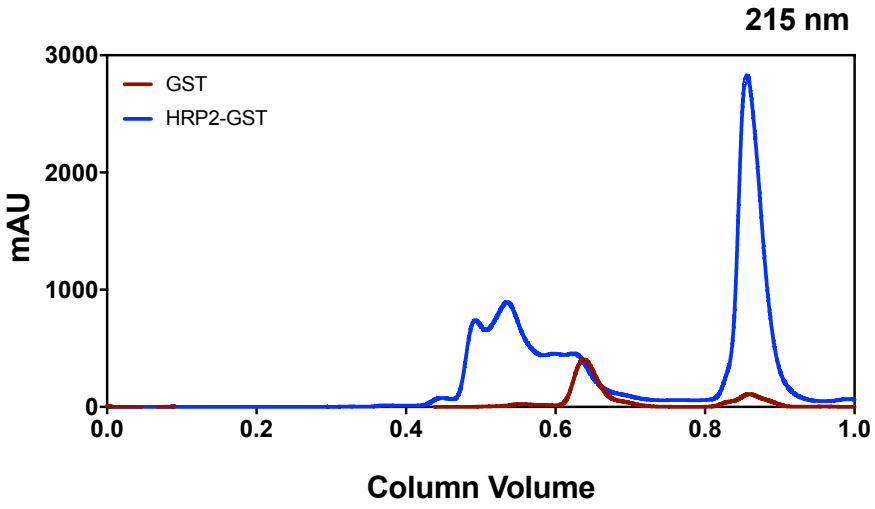

Figure 5-S25. FPLC traces of HRP2-GST and GST. HRP2-GST was analyzed by fast perfomance liquid chromatography (FPLC) at 50 μM. A trace of GST is included for reference.

[HRP2]	A1	A2	A3
1.86E-07	0.1558*	0.1291*	0.2010*
7.23E-08	0.1238	0.1090	0.0806
2.81E-08	0.1040	0.0789	0.1067
1.09E-08	0.0524	0.0465	0.0540
4.25E-09	0.0446	0.0460	0.0457
1.65E-09	0.0353	0.0281	0.0364
6.43E-10	0.0203	0.0169	0.0133
2.50E-10	0.0247	0.0128	0.0134
9.73E-11	0.0175	0.0100	0.0029
3.78E-11	0.0226	0.0075	0.0018
1.47E-11	0.0116	0.0067	0.0152

Table 3-S1. Absorbance data (A450nm) for L2-P1-L3, EC_{50} Binding Curves.

The absorbance values for the **L2-P1-L3** binding assay are shown after background subtraction. The absorbance values were transformed to fraction bound for fitting of the EC_{50} value to fit the two visible isotherms in the binding assay data. Data points excluded from the fits due to nonspecific binding at high [HRP2] are denoted by an asterisk (*).